AGU PUBLICATIONS

Reviews of Geophysics

REVIEW ARTICLE
10.1002/2015RG000481

Key Points:
- Review of methods for measuring snowpack properties
- Advantage of physics-based nondestructive techniques
- Need for automated measurements and onsite feedback to investigators

Correspondence to:
J. W. Pomeroy,
john.pomeroy@usask.ca

Citation:
Kinar, N. J., and J. W. Pomeroy (2015), Measurement of the physical properties of the snowpack, *Rev. Geophys.*, *53*, 481–544, doi:10.1002/2015RG000481.

Received 10 FEB 2015
Accepted 13 MAY 2015
Accepted article online 18 MAY 2015
Published online 30 Jun 2015

Measurement of the physical properties of the snowpack

N. J. Kinar[1] and J. W. Pomeroy[1]

[1]Centre for Hydrology, University of Saskatchewan, Saskatoon, Saskatchewan, Canada

Abstract This paper reviews measurement techniques and corresponding devices used to determine the physical properties of the seasonal snowpack from distances close to the ground surface. The review is placed in the context of the need for scientific observations of snowpack variables that provide inputs for predictive hydrological models that help to advance scientific understanding of geophysical processes related to snow in the near-surface cryosphere. Many of these devices used to measure snow are invasive and require the snowpack to be disrupted, thereby precluding the possibility for multiple measurements to be made at the same sampling location. Moreover, many devices rely on the use of empirical calibration equations that may not be valid at all geographic locations. The spatial density of observations with most snow measurement devices is often inadequate. There is a need for improved automation of snowpack measurement instrumentation with an emphasis on field-based feedback of measurement validity in lieu of postprocessing of samples or data at a lab or office location. The scientific future of snow measurement instrumentation thereby requires a synthesis between science and engineering principles that takes into consideration geophysics and the physics of device operation.

1. Introduction

1.1. The Need for Snowpack Measurements

Snow is a major contribution to the water balance, climate, and economy of many geographic regions. Reviews of the physical processes associated with snow in these environments have been presented by *Gray and Male* [1981], *Marsh*, [1990, 1991], *Oke* [1992], *Pomeroy and Goodison* [1997], *Pomeroy and Brun* [2001], and *Armstrong and Brun* [2008].

Approximately 33% of precipitation in Canada originates as snow [*Brown*, 1995; *Pomeroy and Goodison*, 1997] and "is the primary source of Canadian water supplies" [*McKay and Findlay*, 1971, p. 530]. Snow contributes more than 80% of water to streams located in the Canadian Prairies [*Barnaby*, 1980; *Gray and Landine*, 1988; *McKay and Blackwell*, 1961], Arctic [*Marsh*, 1990], and western United States [*Daly et al.*, 2000; *Marks et al.*, 2001; *Rice et al.*, 2007]. Snow in the mountains of Canada and the western U.S. provides a critical water supply [*Garen and Marks*, 2005], and in the coldest locations, melt does not completely occur in the same year that snow falls, thereby forming glacier firn and eventually ice [*Young and Ommanney*, 1984]. Drought on the North American prairies [*Fang and Pomeroy*, 2008; *Stewart et al.*, 2011] and flooding of the Red River in Manitoba and North Dakota [*Pomeroy et al.*, 2007b] are examples of hydrological processes associated with snowmelt that have wide-ranging social and environmental impacts.

Snow is present in the High Arctic for more than 8 months/yr, and so the hydrology of this region is completely dependent on snow [*Woo*, 1980, 1982]. Climate change in the Arctic will affect vegetation, animals, and biogeochemical cycles, influencing human lifestyles and forestry operations. Because snow-covered area influences energy exchange with the atmosphere, global climates will also be affected by changes in the Arctic snowpack [*Callaghan et al.*, 2011]. Snow falling on sea ice in the Arctic influences formation, growth, and breakup of the ice. A recent trend associated with reduction in the area of the Arctic sea ice will affect biological systems, ocean circulation, and global climates, indicating that snow and snowpack processes have an important role in these cold environments. However, despite the importance of snow on Arctic sea ice, there is currently a lack of snowpack measurements that can be used for monitoring purposes [*Meier et al.*, 2014].

Snow falling on the Greenland [*Chu*, 2014] and Antarctic [*Eisen et al.*, 2008] ice sheets contributes to the mass balance of these regions. Snow is converted to firn, adding to the mass of the ice sheets, whereas snow that melts or sublimates will contribute to a reduction of the mass. Changes in the mass of these ice sheets will affect global climate and ocean levels.

Snowmelt contributes large amounts of water to rivers situated within the United States; examples include rivers in the states of Oregon [*Harr*, 1981], Washington [*Koch and Fisher*, 2000; *Pelto*, 2004], Colorado [*Fassnacht et al.*, 2001], and California [*Davis et al.*, 1999]. Snowfall from the Catskill Mountains provides water to the city of New York [*Matonse et al.*, 2010]; the contribution of snow to the water supply of this city has been monitored for decades [*Porter and Horton*, 2010]. Snowmelt contributions from the San Juan and Sangre de Christo mountains contribute runoff to the Rio Grande Basin of New Mexico that provides water to the city of El Paso, Texas, and parts of northern Mexico [*Rango et al.*, 2010].

Snow provides more than 50% of runoff in California [*Mount*, 1995] and more than 75% of water for agricultural use in this state [*Rosenthal and Dozier*, 1996]. Reservoirs on streams draining from the Sierra Nevada mountains of California do not hold significantly more water than annual snowmelt runoff [*Rittger et al.*, 2011]. Recent drought in California during the 21st century [*Mann and Gleick*, 2015; *Ayars*, 2014] has indicated the need for improved scientific understanding and monitoring of snow in this state. Drought in the Los Angeles region is currently a source of concern for the population in this area since a stable supply of water is required for human use and consumption [*Cousins and Newell*, 2005]. Much of the water supply of agriculture-producing state Idaho is derived from snowmelt, leading *Abramovich* [2007] to refer to snow as "Idaho's frozen liquid gold." In a similar fashion, snow is considered to be "white gold" in California [*Roos*, 1991] and "houille blanche" (white coal) in France [*Landry*, 2012], respectively, indicating the importance of snow to agriculture and hydroelectric power generation.

Population increase in the western United States will place increasing demands on water use in the near future. Accurate knowledge of the amount of water available from snowmelt and the timing of runoff is required to manage water in this region [*Bryant and Painter*, 2010; *Harshburger et al.*, 2005]. *Barnett et al.* [2008] have indicated that due to a reduction in snowfall, an increase in precipitation falling as rain, and snowmelt occurring earlier in the spring, smaller amounts of water will be available during the summer in the western United States. This foretells water shortages for the region and implies that careful planning is necessary to mitigate the effects of these changes.

Snowmelt from the Himalayan mountains provides a majority of fresh water to rivers in Asia. Measurement and modeling of snow in the Himalayas is important since ongoing climate change will alter the hydrology of this region [*Shrestha*, 2015]. Drought and flooding associated with water transported by the Yangtze and Yellow Rivers of China is dependent on snowmelt processes. The failure of crops due to drought and the effect of snowstorms on animal husbandry in China indicates the importance of snow to this region [*Dahe et al.*, 2006]. Snowfall comprises more than half of all precipitation that falls in the coastal plains of central Japan. Snowfall in the mountains of Japan influences local climate and is important to consider for the assessment of hydroelectric power generation [*Watanabe*, 1988].

Snowmelt affects the timing and magnitude of river flow in Britain. The presence of snow also influences climate in this region [*Kay and Crooks*, 2014; *Charlton and Arnell*, 2014]. Although flooding due to snowmelt is more pronounced in northern Britain due to a greater amount of precipitation received as snow, extensive flooding in both southern and northern Britain has been caused by rain-on-snow events [*Marsh et al.*, 2000].

In a similar fashion to snow on the North American tundra, snow cover in Russia influences the magnitude and timing of streamflow and also controls the presence of frozen ground since snow is a thermal insulator [*Dvornikov et al.*, 2015]. High river flows in Russia between the months of April to June 2013 occurred due to snowmelt associated with large amounts of snow accumulation. Similar amounts of snowfall had not been observed since 1967 [*Zotov et al.*, 2015].

The Alps are considered to be the "water towers of Europe" [*European Environment Agency*, 2009, p. 30] and thereby provide much of the water from snowmelt to surrounding European countries. Research in this mountain chain has been conducted to determine how snowpack response to climate change [*Amanzio et al.*, 2015] will influence water availability, flooding, and hydroelectric power generation. Since the presence of snow influences skiing and winter recreation in this region, changes in the snowpack will affect the duration of time that ski resorts can remain open during the winter season [*Gobiet et al.*, 2014]. Changes in snowpack properties also influence the development of avalanches in the Alps [*Castebrunet et al.*, 2014]. Studies to assess snowpack changes in relation to environmental impacts have also been conducted for other mountain chains such as the Australian Alps [*Whetton et al.*, 1996] and New Zealand's Southern Alps [*Kerr et al.*, 2013].

Snowmelt from the Andes of Argentina and Chile provides much of the water to major rivers in the area. Irrigation for agricultural use, water consumption, and hydroelectric power generation are influenced by the variability of snow in the Andes. A major road linking Santiago in Chile and Buenos Aires in Argentina crosses the Andes. The movement of traffic along this road and thereby winter tourism are influenced by the presence or absence of snow in this area [*Masiokas et al.*, 2006].

Scientific instrumentation provides measurements used to investigate, understand, and predict snow processes. These measurements can provide inputs to mathematical models of climate [*Dutra et al.*, 2012], hydrology [*Ellis et al.*, 2011; *Pomeroy and Li*, 2000; *Pomeroy et al.*, 2007a; *Shook and Pomeroy*, 2011; *Helgason and Pomeroy*, 2012b], snowpack evolution [*Marks et al.*, 1998; *Essery et al.*, 2009], and avalanche prediction [*Lehning et al.*, 1999]. The models are sophisticated computer programs used to predict runoff, water availability, natural disasters, drought, flooding, and environmental change. If snowpack measurements are collected for a scientific purpose outside of data collection for mathematical modeling purposes, these snow measurements are often used to observe and understand snow processes. The measurements thereby provide a better understanding of the environmental physics associated with snow and thereby enable the creation of more accurate mathematical models.

This paper reviews near-surface-based snowpack measurement instrumentation and techniques to provide an overview of the literature and an understanding of how observations of snow are made in the field. The operating principle of each type of instrument or technique is described, and the scientific benefit of its use is identified. The purpose of the review is not intended to be entirely exhaustive but to serve as a point of entry for the reader.

Snowpack properties have also been measured by sensors mounted on satellites and airplanes which provide substantially greater spatial coverage than near-surface-based measurements but also have great uncertainty in estimating snowpack properties at the relatively fine spatial and temporal scales by which they vary. Remotely sensed snow properties are very reliant on near-surface-based validation measurements and have been comprehensively reviewed by *Lucas and Harrison* [1990], *König et al.* [2001], *Rees* [2006], *Brown and Armstrong* [2008], and *Frei et al.* [2012]. These applications are outside of the scope of this review which focuses on measurement instrumentation of the seasonal snowpack in the near-surface cryosphere. Moreover, snow chemistry measurement procedures are not discussed in this paper since the focus is on physical hydrology and how data are obtained to provide inputs for physical hydrological models. The in situ measurement of snow physical properties will be relevant for both verifying remote sensing observations of snow-covered surface and for the physical medium that is the basis for snow chemistry.

Moreover, the snow hydrology and glacier scientific communities are often considered to be distinct. Therefore, this paper deals with snowpack measurements that are made on seasonal snow with respect to hydrological observations. Measurements of snow on top of sea ice [*Meier et al.*, 2014], ice sheets [*Eisen et al.*, 2008], and glaciers [*Hubbard and Glasser*, 2005] are often made using snow pits or surface elevation measurements due to a lack of a clear distinction of the recent snowpack from snow accumulation from previous years. At locations where seasonal snow of a bulk density less than ice is present, the measurement instruments and techniques as discussed in this paper can be used.

1.2. Snow Measurement Variables

Snow measurement instrumentation is commonly used to measure physical quantities: snow depth $\overline{d}$, density ρ, snow water equivalent (SWE), porosity ϕ, liquid water content θ_w, permeability k, specific surface area (SSA), thermal conductivity κ, and temperature T.

The snow depth $\overline{d}$ is a measure of the vertical length of snow determined with respect to a reference datum normally taken as the ground. The origin of the measurement is an approximation of the ground surface. This is because the ground can have a vertical scale of roughness that is significant with respect to snow depth.

The density ρ of snow is the mass of snow m_s in a reference volume V_T. The reference volume is often referred to as a "control volume." This is an arbitrary volume for which the mass of snow is measured. Together these variables are used to define snow water equivalent (SWE), a point measurement of the depth of water created by the melting of the snow.

Assuming that water spread over an area of 1 m^2 has a depth of 1 mm and a mass of 1 kg (so the density of water is 1000 kg m^{-3}) and that snow depth $\overline{d}$ has a depth-averaged snow density $\bar{\rho}$, snow density and SWE are defined by [*Pomeroy and Gray*, 1995]

$$\rho = m_s / V_T \text{ and}$$

$$\text{SWE} = \bar{d}\bar{\rho}. \quad (1)$$

SWE is the mathematical product of snow depth and density and is commonly reported in units of mm or kg m^{-2}. The measurement of depth alone is not sufficient to obtain SWE since density can vary over an area [*Gray et al.*, 1970a] and must be measured rather than being assumed to be a particular value such as 100 kg m^{-3} for freshly fallen snow [*Pomeroy and Gray*, 1995]. *Judson and Doesken* [2000] found that new snow density ranges between 10 kg m^{-3} and 350 kg m^{-3} at sites in the United States. Nominal snowpack densities are between 80 kg m^{-3} and 600 kg m^{-3} [*Pomeroy and Gray*, 1995].

A "snow particle" (also referred to as a "snow crystal") is often defined as the smallest constituent element that comprises the snowpack. The particle description of a snowpack is not satisfactory. This is because the snowpack is a porous medium consisting of pore spaces of air and a frame composed of an ice material from snow particles sintered together by metamorphic processes [*Buser and Good*, 1986]. The metamorphic processes occur due to mechanical compression, thermal gradients in the snowpack created due to mass and energy fluxes, and the production of water by melting snow [*Colbeck*, 1997, 1975, 1986a; *Arons and Colbeck*, 1995; *Colbeck*, 1989a, 1986b, 1991; *Colbeck and Anderson*, 1982; *Male*, 1980]. A snowpack is therefore an uneven mixture of air, ice, and water [*Colbeck*, 1976a]. "Layers" in the snowpack are created due to deposition events and metamorphic processes [*Pielmeier and Schneebeli*, 2003b]. Metamorphic processes are responsible for creating and destroying layers in the snowpack and changing the morphology of snow particles over time [*Colbeck*, 1991].

Assuming that the volumes of air (V_a), ice (V_i), and water (V_w) are fractional constituents of a medium with a total control volume V_T, the air porosity θ_a, liquid water content θ_w, and the ice fraction θ_i are given by [*Bartelt and Lehning*, 2002]

$$\theta_a = \frac{V_a}{V_T},\ \theta_w = \frac{V_w}{V_T},\ \theta_i = \frac{V_i}{V_T}, \text{ and} \quad (2)$$

$$\theta_a + \theta_w + \theta_i = 1.$$

Equation (2) is subjected to a continuity constraint since the fractional constituents of the medium cannot exceed unity. Liquid water content θ_w is a measure of the fractional amount of liquid water in the pore spaces of the snowpack. This is distinct from SWE, which is the resulting depth of water if the snowpack was completely converted to liquid.

The density of snow is related to the density of air ρ_a, the density of water ρ_w, and the density of the ice medium ρ_i by [*Bartelt and Lehning*, 2002]:

$$\rho = \rho_a\theta_a + \rho_w\theta_w + \rho_i\theta_i.$$

The porosity ϕ is the volume fraction of pore spaces in the medium:

$$\phi = \frac{V_a + V_w}{V_T}.$$

Assuming that $V_w \approx 0$ or if the liquid water content in snow is not measured, the following equation can be used to calculate porosity. Neglecting the density of air,

$$\phi = 1 - \frac{\rho}{\rho_i}.$$

The liquid water content θ_w and liquid water saturation S_w are two different measurements of snow wetness and are often reported as a percentage calculated from a volume fraction. Whereas the water content θ_w is the volume fraction of water with respect to total volume V_T, the water saturation S_w as used by authors such as *Colbeck*, [1976a, 1976b] is the volume fraction of water in the pore space of the snowpack [*Marsh*, 1991]:

$$S_w = \frac{\theta_w}{\phi}.$$

The irreducible water content θ_e is the residual fraction of liquid water that cannot be removed from the pore spaces of the snowpack due to a quasi-liquid layer surrounding snow particles that comprise the snowpack [*Marsh*, 1991]. This is also expressed as the irreducible water saturation S_e [*Colbeck*, 1976a].

Moreover, the presence of liquid water in the snowpack changes over time during the period of melt. Snowmelt is considered to have three separate time periods: (1) the warming phase, (2) the ripening phase, and (3) the output phase. During the warming phase, the snowpack temperature increases and an isothermal temperature is reached at 0°C. The ripening phase occurs when water is held within the snowpack, but the water does not exit the snowpack as runoff. When the snowpack cannot hold liquid water, the output stage of snowmelt occurs. At the transition point between the ripening and output stages of snowmelt, the snowpack is said to be "ripe" [*Dingman*, 2015, p. 223].

Let V_e be the volume of irreducible water in a control volume. Then,

$$\theta_e = \frac{V_e}{V_T} \text{ and}$$

$$S_e = \frac{\theta_e}{\phi}.$$

From the definition of irreducible water saturation S_e, the effective water saturation S^* as the total amount of water held by the pore spaces of the snowpack and the effective porosity ϕ_e is defined as [*Colbeck and Anderson*, 1982]

$$S^* = \frac{S_w - S_e}{1 - S_e} \text{ and}$$

$$\phi_e = \phi\left(1 - S_e\right).$$

Colbeck and Anderson [1982] state that the irreducible water saturation S_e of snow is approximately 7% ($S_e = 0.07$). However, values of S_e measured from a ripe snowpack have been reported between 2% and 4%, which corresponds to an irreducible water content θ_e of 1% to 2% [*Marsh*, 1991].

Dielectric measurements of snow have shown that liquid water content θ_w can range from ~0% for dry snow to ~10% for a wet snowpack [*Denoth and Wilhelmy*, 1988; *Denoth*, 1994; *Denoth et al.*, 1984; *Sihvola and Tiuri*, 1986]. For dielectric measurements, *Techel and Pielmeier* [2011] proposed a wetness classification scheme. In the context of this classification scheme, a water content θ_w of $< 1.3\%$ by volume is dry or "barely moist" snow and $> 1.3\%$ by volume is wet snow. Another alternate classification scheme is given by *Techel and Pielmeier* [2011] and referred to as the "Martinec" classification scheme after the author of an unpublished report from the Swiss Institute for Snow and Avalanche Research. The scheme shows a liquid water content of $< 0.5\%$ as corresponding to dry snow, 0.5% to 2% as corresponding to moist snow, 2% to 4% as corresponding to wet snow, 4% to 5% as corresponding to very wet snow, and $> 5\%$ as slush snow. The classification scheme proposed by *Fierz et al.* [1999] defines dry snow corresponding to a liquid water content of ~0%, moist snow corresponding to 0% to 3%, wet snow corresponding to 3% to 8%, very wet snow corresponding to 8% to 15%, and soaked snow having a liquid water content of $> 15\%$.

Using the *Colbeck* [1982] classification scheme, the degree of water saturation S_w in the snowpack is classified by two different stages: the pendular and funicular regimes. In the pendular regime of saturation ($< 7\%$ to 14% of water saturation S_w), air has a continuous pathway through the pore space surrounding the snow particles. The water is contained in a film around each particle [*Denoth*, 1982]. The transition between the pendular and funicular regimes of saturation S_w was measured using dielectric techniques as occurring from 11% to 15% [*Denoth*, 1980]. The funicular regime of saturation is from 14% to 25% of water saturation S_w, where the water is continuous throughout the pore spaces of the snowpack and the air is only found as bubbles in localized areas of the liquid [*Colbeck*, 1982].

The saturated permeability k_s of snow is used to model the propagation of air or water through a snowpack when the pore spaces of the medium are assumed to be completely filled with one of these constituents. This is only an approximation that is sometimes useful when modeling air [*Jordan et al.*, 1999] or water [*Colbeck*,

1974] transport through snow. When the pore spaces of the snowpack contain a mixture of air and water, the permeability can be referred to as the unsaturated permeability k_u [*Colbeck*, 1977; *Marsh*, 1991]. Alternately, a saturated permeability can be applied separately to the air or water phase [*Colbeck*, 1972]. The water saturation and permeability is also related to the pressure (p_p) of the liquid water in the pore spaces of the medium. The pressure (p_p) affects the movement of meltwater wetting fronts through snow [*Marsh*, 1991].

The permeability governs the rate at which air or water will move through snow. Higher-magnitude permeability values indicate higher speeds of air or water transport. Permeability is related to the size of snow particles [*Colbeck*, 1977], as well as snow morphological properties [*Albert et al.*, 2000], and therefore changes over the snow accumulation and ablation season due to metamorphic processes driven by mass and energy fluxes.

Permeability is mathematically defined by Darcy's law. Assuming that the flow is laminar, the speed c of air or water moving through a saturated snowpack (c_s) or incompletely saturated snowpack (c_u) is given by

$$c_s = -\frac{k_s}{\mu_s}\frac{\partial p}{\partial y} \text{ and}$$

$$c_u = -\frac{k_u}{\mu_u}\frac{\partial p}{\partial y}.$$

The viscosity of the fluid is μ_s or μ_u, and the pressure gradient is $\partial p/\partial y$.

The diffusion of a gas into a snow cover in the absence of wind is dependent on the tortuosity α, which is a dimensionless number quantifying the straight-line deviation of the pore spaces in a medium. The tortuosity is a measure of the convoluted nature of the pore spaces. The tortuosity is always $\alpha \geq 1$, with $\alpha = 1$ for cylindrical pores oriented parallel to the direction of fluid motion [*Stoll*, 1989]. The assertion that $\alpha < 1$ is incorrect since this neglects the effect of tortuosity on the speed of flow through the porous medium [*Bear*, 1972, p. 111]. Tortuosity is one of the variables used to model gas diffusion in snow using Fick's law [*Jones et al.*, 1999].

The specific surface area of snow in a control volume of the snowpack is defined as $\text{SSA} = A_s/m_s$, where A_s is the snow area and m_s is the mass of snow. A_s is the internal area of the ice surfaces in the snow and is not the same as snow-covered area. Snow-covered area is the area of a landscape that is covered by snow.

The SSA is related to the effective diameter d_p of the snow particles and the density of the ice ρ_{ice} comprising the particles and is therefore dependent on snow metamorphism [*Gallet et al.*, 2009]:

$$\text{SSA} = \frac{6}{\rho_{\text{ice}} d_p}.$$

The effective diameter d_p is the diameter of equivalent spheres in the snowpack with the same SSA. In this regard the snow particles are assumed to have an equivalent spherical diameter.

The SSA is used to model the reflection of light from snow and is an important parameter that can be used in snowpack evolution models. The SSA also governs the absorption of chemical species by snow and affects chemical reactions that occur within the snowpack [*Gallet et al.*, 2009].

Temperature T is a measure of heat present in a substance. For a snowpack, temperature measures the effective heat of the air, ice, and water that comprises the porous medium. Assuming that the effective thermal conductivity of the porous snow medium is κ and the temperature gradient over a depth of snow is $\partial T/\partial y$, the heat flux q_F for steady state heat flow is given by Fourier's law [*Langham*, 1981; *Powers et al.*, 1985]:

$$q_F = -\kappa\frac{\partial T}{\partial y}.$$

Snow density is related to the effective thermal conductivity by empirical equations developed from gravimetric and heat pulse probe measurements of snow [*Sturm et al.*, 1997; *Usowicz et al.*, 2008]. By the Stefan-Boltzmann law, the temperature of the snow surface can be determined from measurements of longwave radiation (with wavelengths between 4 μm and 100 μm) emitted from the snowpack. This is the principle of operation of an IR thermometer (section 2.17).

Irradiance is a measure of the radiation flux incident on a surface at a given wavelength for light that has been transmitted or reflected from the snowpack [*Bryant and Painter*, 2010]. Related to irradiance is albedo, measured as a function $a(\lambda)$ of wavelength λ [*Warren*, 1982]. The albedo is often reported as a single-value a that is averaged over wavelength. Albedo is the ratio of the magnitude of shortwave radiation (with wavelengths between 0.1 μm and 4 μm) that has been reflected from the snowpack to the magnitude of the shortwave radiation that is incident on the snowpack [*Oke*, 1992]. In this regard, albedo is a reflection coefficient of electromagnetic energy that is an important variable in snowpack evolution and snowmelt models [*Granger and Gray*, 1990].

The hemispherical-directional reflectance factor is a measure of the reflection of light from snow at a hemispherical angle to the snow surface and thereby influences the energy balance and metamorphic processes occurring within the snowpack [*Painter et al.*, 2003]. *Warren* [1982] presents a review of snow optical quantities. *Pomeroy and Male* [1985] review the optical properties of blowing snow.

The energy and heat balances of the snowpack are determined for input into models of snowpack evolution such as SNTHERM (SNow THERmal Model) [*Jordan*, 1991; *Koivusalo and Heikinheimo*, 1999; *Frankenstein et al.*, 2008], SNOBAL (Energy-BALance SNOw Model) [*Link and Marks*, 1999; *Marks and Winstral*, 2001; *Marks et al.*, 2002], SnowMODEL (Snow-Evolution MODELing System) [*Liston and Elder*, 2006; *Liston et al.*, 2007], and CROCUS [*Brun et al.*, 1992, 1989; *Carmagnola et al.*, 2014]. Radiation balance measurements over snow and applications of snow models are discussed in detail by *Essery and Pomeroy* [2004], *Bewley et al.* [2010], *Pomeroy et al.* [2009a], *Essery et al.* [2008a], *Bewley et al.* [2007], *Essery et al.* [2008b], *Pomeroy et al.* [2008], *Harding and Pomeroy* [1996], *Pomeroy and Essery* [1999], *Pomeroy et al.* [2003], and *Pomeroy and Dion* [1996]. Snow observation sites are often used to provide data for model calibration and validation. Stationary instrumentation is deployed at these sites, and observations of snow by a human observer are also periodically made [*Morin et al.*, 2012; *Marks et al.*, 2001].

1.3. Online Snow Data Repositories

Over the past decade, the geoscience community has placed an increased emphasis on the need for community repositories of data where scientific measurements are archived to serve as records of observation and as sources of information for numerical analysis after the data have been collected. These repositories serve to document observations that have been made and also to provide data that can be used for educational and research purposes. Data repositories are a good idea since data collected during the previous and current centuries are often stored as digital files and can be made available for expeditious electronic download. Because computing storage media and file formats drastically change over periods of decades and physical media is often subjected to data degradation, the history of recent scientific experimentation is jeopardized by researchers independently keeping observations of scientific importance on local storage media. These and additional issues with data archives — including which data sets should be selected for preservation — are discussed by *Palmer et al.* [2011].

The National Snow and Ice Data Centre (http://nsidc.org/) serves as an online data repository for snow science data. Some snow data, particularly collected for the extensive Boreal Ecosystem-Atmosphere Study experiment during the 1990s [*Sellers et al.*, 1997], can be found in the Oak Ridge National Laboratory Distributed Active Archive Center for Biogeochemical Dynamics (http://daac.ornl.gov). The PANGAEA® data repository (http://www.pangaea.de) has also been used to store data from snow science experiments.

Data sets submitted to these online repositories have been fully documented and carefully prepared for online distribution. An example of a journal used to publish data documentation is Earth Systems Science Data (Copernicus Publications, http://www.earth-syst-sci-data.net). An exemplary publication of a snow measurement data set is that describing the long-term measurements at Col de Porte in the French Alps [*Morin et al.*, 2012].

Generally, the file formats used for data are standardized and should be readable by commonly available software. Moreover, the data should be available under a permissive license that freely encourages the data to be used.

However, although most data sets are associated with published scientific research, there is often a lack of digital photographic images available of the research instrumentation used to collect the data. Although this paper provides some unpublished images of snow measurement instrumentation, there is a need for systematic preservation of these images.

Digital photographic images of snow measurement instrumentation contribute to documentation of an experimental observation, and along with verbal descriptions and diagrams of an experimental apparatus, can help to interpret published results. Therefore, there is a need to provide extensive visual documentation of snow measurement experiments. Although a published paper might have space only for a diagram and a few pictures of field measurement experiments, an online archive can be used to hold extensive pictures of field site conditions, steps involved in instrumentation deployment, and images of how data are collected. Supplemented with video, such a visual archive would present an unprecedented opportunity for documentation and postcollection evaluation of snow science data. If photographs are available under a permissive license, the photographs can be reused in textbooks and for training of students and researchers in the use of snow measurement observation instruments and techniques. Such data can be easily collected using ubiquitous mobile devices such as smartphones and quickly submitted for upload consideration using a custom-made software application.

2. Instrumentation and Techniques

2.1. Classification of Snowpack Measurements

Instrumentation used to collect snow measurements can be "portable" or "stationary." Portable devices are taken to different locations, whereas stationary devices are attached to a fixed location. Portable devices are used to obtain a data set that is spatially representative of snowpack properties, whereas stationary devices are used to monitor temporal changes in the snowpack at a fixed location.

Snowpack measurements can be considered as "invasive" or "noninvasive." Within these two categories, measurements can rely on "empirical" or "nonempirical" relationships between snow properties. Invasive measurements disrupt the snowpack by the extraction of a snow sample. In a similar fashion to the excavation of an archeological site, the invasive measurement irrevocably changes the snowpack. Noninvasive instruments do not modify the snowpack. This allows for snow measurements to be made at the same location without having to disturb the snowpack. Noninvasive measurements can be more easily automated than invasive measurements that often require the presence of a human observer. Empirical relationships are often specific to an observation site and have been developed from a necessarily finite set of measurements that may not always be valid at all geographic locations or for all data sets.

These classification categories can be further refined by the type of measurement that is being made. Using terminology from sonar and radar sensing systems, the snow measurement can be "active" or "passive." Active measurement techniques require an action such as the sending of an electromagnetic wave or charged particle. The wave or charged particle is detected using a sensor. Passive measurement techniques rely on visual observations or the detection of an electromagnetic wave or particle that is already naturally present in the environment and not produced during the measurement procedure by the measurement device.

2.2. Depth Measurement Rods and Rulers

Measurements of total snow depth along a transect are commonly made using a portable depth rod. The rod is inserted through the snow surface and used to determine the distance to the ground surface. The measurement is destructive and invasive in that another measurement cannot be made at the same location.

Snow depth measurement along with snow density measurements are used to determine SWE as an input into hydrological models used to compute runoff or as a comparison measurement used to validate model inputs [*DeBeer and Pomeroy*, 2010]. Moreover, snow depth measurements can be used for civil planning [*Goodison et al.*, 1981] or to understand the geographic distribution of animals [*Halpin and Bissonette*, 1988; *Schwab and Pitt*, 1991].

Snow interception refers to physical processes associated with the trapping of snow by vegetation, either in the canopy of a forest or on the land surface. Measurements of snow depth by the instruments discussed in this section have enabled a greater scientific understanding of the processes by which snow accumulates in a forest, the transport of snow by wind, and the spatial distribution of snow over arctic, prairie, and alpine landscapes [*Pomeroy and Gray*, 1995].

The rod is generally a graduated metal stick with markings indicating a measurement scale used to determine the location of the snow surface [*Goodison et al.*, 1981]. Screw threads on each rod permit multiple sections to be coupled together so that deep snow can be measured. The rod section is designed to ensure that the

Figure 1. Snow depth rod measurement of snow depth. The investigator in the background is recording a measurement of snow depth read by the observer in the foreground.

ground surface can be contacted, and the measurement rod remains upright when snow depth is determined [*Woo*, 1997]. Figure 1 shows a measurement rod being utilized to determine snow depth along a transect.

Because measurement of snow depth is time consuming, *Sturm* [1999] devised a self-recording snow depth probe (MagnaProbe). Similar to a ski pole, the device uses a sliding electromechanical basket that coincides with the snow surface when the tip of the pole contacts the ground surface. A switch is closed when a depth measurement is made, and a circuit logs the distance between the tip of the pole and the ground surface. A GPS system provides the geographic location of each point. Time, location, and snow depth can be recorded electronically using standard data loggers.

Snow rulers can be classified as being either portable or stationary. Portable snow rulers are commercially available rectangular rulers or a carpenter's folding ruler. The portable snow ruler is used to measure the depth of snow and the position of layers in a snowpit (section 2.4).

The snow ruler is often used with a snow board, which is a piece of metal or wood with dimensions spanning at least 40 cm by 40 cm that serves as a known reference datum. The snow ruler is used to measure the depth of snow that has accumulated on top of the board. The snow is cleared from the board after each measurement to provide a daily estimate of snowfall [*Goodison et al.*, 1981].

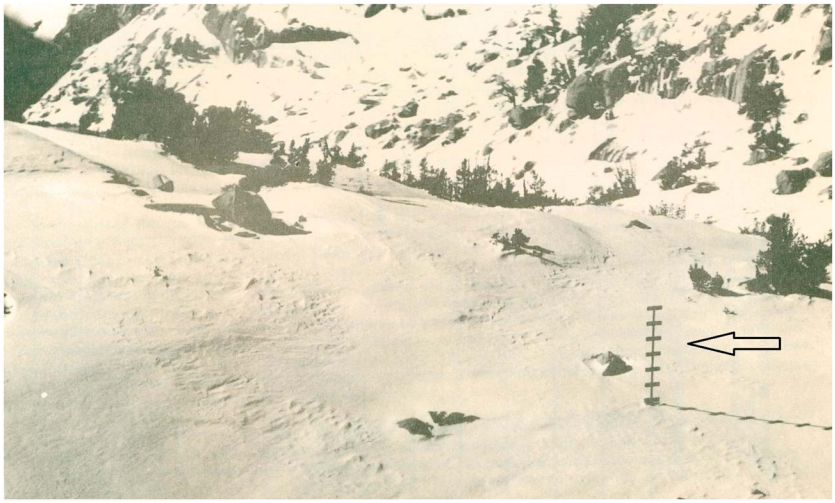

Figure 2. Stationary version of the snow ruler [from *Henderson* [1953]]. The position of the marker in the foreground of the picture is shown by a left-facing arrow.

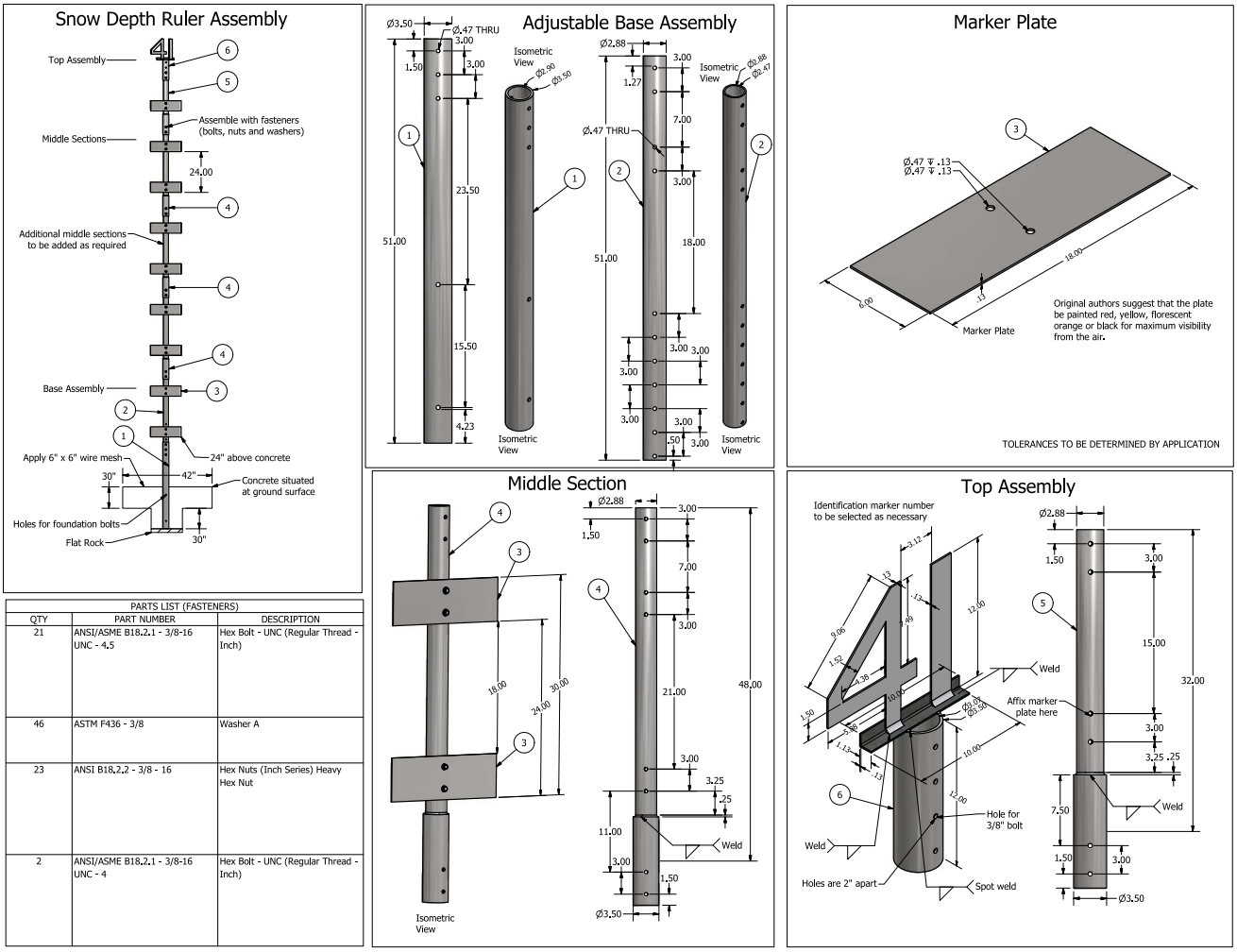

PARTS LIST (FASTENERS)		
QTY	PART NUMBER	DESCRIPTION
21	ANSI/ASME B18.2.1 - 3/8-16 UNC - 4.5	Hex Bolt - UNC (Regular Thread - Inch)
46	ASTM F436 - 3/8	Washer A
23	ANSI B18.2.2 - 3/8 - 16	Hex Nuts (Inch Series) Heavy Hex Nut
2	ANSI/ASME B18.2.1 - 3/8-16 UNC - 4	Hex Bolt - UNC (Regular Thread - Inch)

Figure 3. Snow ruler with vertical cross arms redrafted from *Miller* [1962]. Dimensions given in inches.

Similar to the depth rod, the numbers on the ruler are large enough to be manually read by snow surveyors. The main difference between a snow rod and a snow ruler is that the snow rod is used to create a hole in the snowpack for more rapid sampling of snow depth, whereas the snow ruler is either temporarily installed against the wall of a snowpit (section 2.4) or used to measure snow depth over the winter season.

In geographic areas that are not easily accessible during the winter, the markers on the stationary version of the snow ruler can be read from the ground but are also large enough to be recognized from a low-flying airplane (Figures 2 and 3). This is a passive type of measurement that is dependent on human observation. Snowmelt around the base of the ruler can cause inaccuracies in the measured snow depth [*Goodison et al.*, 1981; *Pomeroy and Gray*, 1995]. Some stationary versions of the snow ruler have markers spaced every 2 feet (0.6 m) along a 20 foot (6 m) post [*Henderson*, 1953].

Ablation stakes are used to measure relative changes in snow depth [*Jordan*, 1983]. The ablation stake is often deployed on snow that has accumulated on top of glaciers and the exposed length measured with a tape measure [*Karpilo*, 2009]. The ablation stake provides an indication of how quickly mass is being lost from the glacier. This data can be used to validate remote sensing estimates of glacier mass balance or provide a better understanding of how much water is available as runoff from the glacier [*Hopkinson et al.*, 2010].

2.3. Snow Tubes

A snow sampling tube ("snow tube") is used to extract gravimetric samples of snow to measure SWE and depth-averaged snow density [*Goodison et al.*, 1981]. Depth measurements taken with a measurement rod (section 2.2) allow for determination of depth-averaged snow density from SWE measurements made by

Figure 4. (a) Snow tube sampling on a slope using a plastic-body ESC30 snow tube. After a snow sample is extracted, the ESC30 is weighed on a spring scale. (b) Container with 6 inch diameter (15.3 cm) used as gravimetric snow tube sampler [from *Dyck*, 1969].

the snow tube. This is calculated by suitable rearrangement of equation (1). Snow sampling tubes are used along snow courses by snow surveyors to measure areal estimates of SWE, thereby permitting streamflow forecasting and runoff modeling [*Goodison*, 1975; *Tabler*, 1982].

Snow tube use was first popularized by *Church* [1933]. The snow tube used by most snow surveyors is made of metal or nonopaque plastic with a serrated cutting end [*Crook and Freeman*, 1973; *McKay and Blackwell*, 1961]. The plastic tube allows the snow surveyor to visibly see the snow sample after it has been extracted, although metal snow samplers are often designed with slots so that the snow sample can be seen. A sample is extracted by pushing the tube through the snowpack until the serrated cutting end reaches the ground surface. Handles on the topside of the tube allow the sampler to be turned so that the serrated cutting end extracts a plug of soil. The sampler is carefully removed from the snowpack and placed on a calibrated scale to measure SWE [*Goodison et al.*, 1981]. The snow sampling tube accuracy can show high correlations with snowpit measurements of SWE [*Fassnacht et al.*, 2010].

Figure 4 shows a snow tube being used to extract a snow sample from the snowpack. For comparison, some snow tubes used in the past were simply containers that were used to extract a snow sample. A diagram of a snow tube is given in Figure 5.

Farnes et al. [1980, 1982] tested 22 different snow tube designs against gravimetric snowpit measurements of SWE. Ensuring that snow was not lost from the tube, they found that smaller-diameter snow tubes without a sharpened cutting end overestimated SWE by 9% to 10%, whereas snow tubes with sharper cutting ends had an overestimation of 3% to 6%. This finding coincides with *Peterson and Brown* [1975], who compared "Federal" snow sampling tubes to samples of snow carefully extracted from the snowpack, finding that the

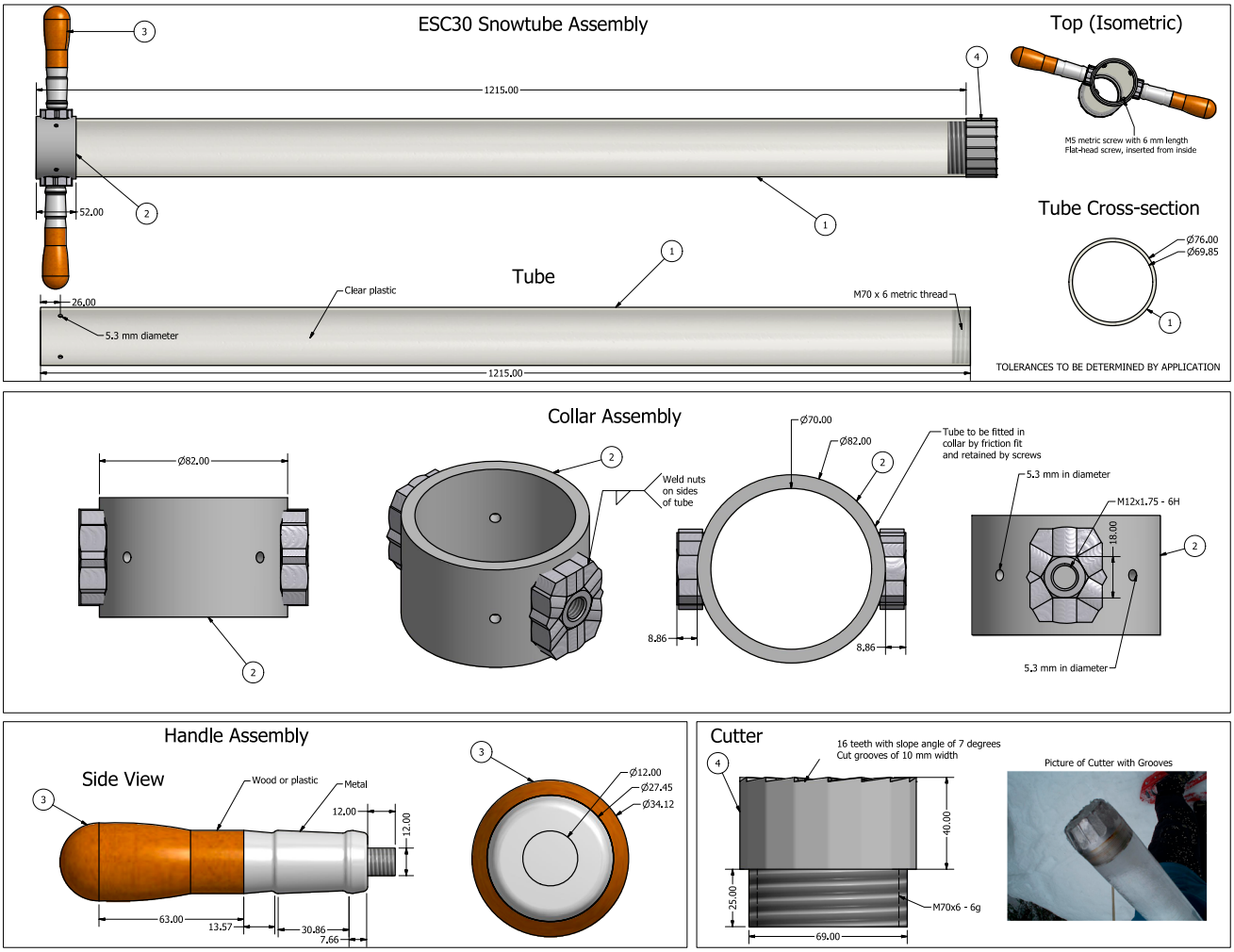

Figure 5. Design of metric ESC30 snow sampling tube based on *Farnes et al.* [1980]. Dimensions given in millimeters.

snow tube overestimated SWE. For shallow snowpacks with less than 1 m depth, the error in measurement was found to be 1% to 3% *Goodison* [1978]. *Farnes et al.* [1980, 1982] found that increasing the snow tube diameter decreased the overestimation of SWE. Snow tubes with a sharpened cutting end area >20 cm^2 had the least error and the ESC-30 snow tube with a cutting end area of 30 cm^2 showed the least measurement error when used to sample snowpacks with a depth of less than 1 m. *Turčan and Loijens* [1975] present a simple model of snow tube insertion into snow, showing that compression of the snow as the snow tube moves through the snowpack can be a source of error in the application of this technique.

The snow sampling tube is invasive since it destroys the snowpack at each sampling location [*Smith et al.*, 1967a]. *Davis* [1973] refers to snow sampling as "archaic, inefficient, and hard work." If a plug of soil is not extracted to cap the bottom of the tube, the extracted snow sample can fall out and the measurement will have to be repeated. When the snow temperature is colder than the air temperature, snow can freeze to the inside of the tube [*Goodison et al.*, 1981]. The snow will have to be extracted before another measurement is made. The presence of buried vegetation and logs beneath the snow surface will often interfere with the collection of a snow sample. Ice crust formation inside of the snowpack can cause difficulties with the extraction of a sample [*Powell*, 1987]. Due to the relative size of the snow tube, it can be difficult to carry over long distances. To allow for easier transportation of the snow tube, *Gluns and Rose* [1992] designed a special backpack referred to as the "Kootenay Cruiser."

2.4. Snowpit Observations

A snowpit is created when measurements of snow stratigraphy are required, invasive instruments (as discussed in the following sections) are used to measure the snowpack, or when visual observations of snowpack

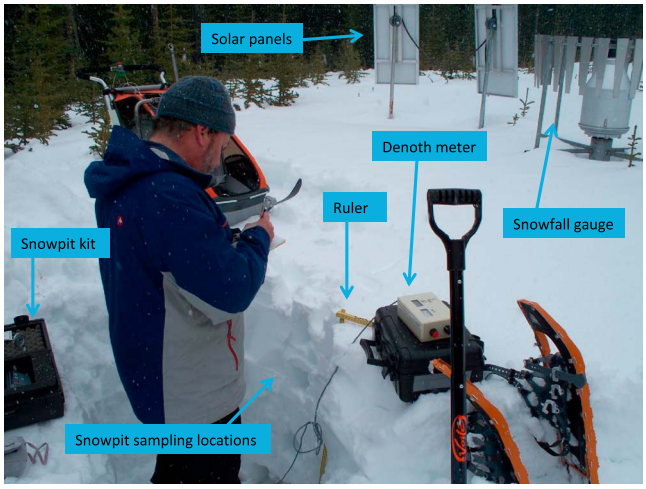

Figure 6. Snowpit being created at a field site in the Rocky Mountains of Alberta, Canada. Visible in the image is a snowpit kit, snowpit sampling locations where snow has been extracted using a gravimetric sampler, a folding ruler, a Denoth capacitance wetness meter (section 2.9), and a Geonor snowfall gauge with an Alter shield. Solar panels are shown in the background. These were used to power a data logger and other associated electronic circuitry at this field site.

properties or processes are being made. The snowpit is simply a hole in the snowpack that is dug using a shovel down to the ground surface. The ground surface is taken as the origin of the depth reference datum, with a ruler used to measure the distance of each layer from the bottom. Layers are classically identified by an observer in the field using visual interpretation [*Fierz et al.*, 1999]. Snowpit measurement and creation techniques are discussed by *Tremper* [2008]. Invasive instruments used to measure properties of snow in a snowpit are often placed in a box (snowpit kit) for transportation to the field site (Figure 6).

The use of the snowpit has allowed investigators to better understand snowpack evolution and metamorphic processes so that snowpack models can be created and landscape-scale snow processes can be better understood [*Williams et al.*, 2010]. Transport of water through snow has been observed by snowpits [*Marsh and Woo*, 1984a] and field observations compared to the outputs of physical models [*Marsh and Woo*, 1984b]. Snowpit observations are often made to assess changes in snow density or mechanical properties so that avalanche predictions can be made [*McClung and Schaerer*, 2006].

To reduce the subjectivity of layer identification, infrared imaging and image processing algorithms have been used to identify layers after the snowpit is created [*Shea et al.*, 2012a; *Tape et al.*, 2010]. Layering can also be easily identified by spraying the side of the snowpit with a blue dye [*Kovacs*, 1993] or by back illuminating the snowpit [*Harper and Bradford*, 2003]. The size of snow particles in the snowpack can be measured by spectroscopy (section 2.13) or microscopy (section 2.5). By photographing the snow surface, the snow surface profile can also be determined [*Fassnacht et al.*, 2009; *Rees*, 1998; *Kinar and Pomeroy*, 2008a]. A uniform cut through the snow surface can be obtained by a "snow blade" with a bubble level [*Albert*, 2002]. To create a flat surface for stratigraphic interpretation, the side of the snowpit can be made flat by the use of a hot slicing wire apparatus situated on a frame installed close to the snowpit wall [*Good and Krusi*, 1992]. Snow extracted from the side of a snowpack and squeezed by hand can be used to provide a semiqualitative indication of liquid water content [*Techel and Pielmeier*, 2011].

Church [1948] reported what may have been the first use of fuchine dye to trace the path of meltwater propagation through snow. The *U.S. Army Corps of Engineers* [1956] also used fuchine dye. *Marsh and Woo* [1984a] measured the propagation of water in a melting snowpack by injecting a red dye tracer into the side of a snowpit. Photographs of the snowpit side revealed preferential flow paths for meltwater (Figure 7). A similar experiment was conducted by *Peitzsch et al.* [2008] at a field site using red food coloring as the dye tracer. The dye tracer technique has been used to show flow paths through snow and between ice layers on a slope [*Langham*, 1973]. The use of these methods led to a better understanding of the physics associated with the rate and timing of meltwater flow through snow. *McGurk and Kattelmann* [1988] and *McGurk and Marsh* [1995]

Figure 7. A dye tracer experiment being used to visualize meltwater flow paths in a snowpack (photograph courtesy of Dr. Phil Marsh).

injected dye into snow and used a "cutter box" to extract horizontal slices out of a snowpit wall. The slices were photographed and then observed for melt channel formation.

Waldner et al. [2004] placed snow inside of a transparent box in a cold room. Infrared lamps were used to heat the snow surface. Thermistors and time domain reflectometry (TDR) probes sampled snow temperature and liquid water content at depths throughout the transparent box. Dye tracer was mixed into snow, and the dye-snow mixture was placed on top of the snow in the transparent box. The transparent box allowed the dye tracer flow paths throughout the transparent box to be photographed in a laboratory setting as the snowpack changed over time and provided insight into how meltwater flow was related to snow structure. The dye tracer was not injected in a similar fashion to Figure 7, but the idea is similar: movement of the dye indicated water flow through snow.

Williams et al. [2010] injected a blue dye tracer into a snowpack and then used a large "snow guillotine" to progressively shave away vertical sections from the snowpit wall. The instrument created by *Williams et al.* [2010] is similar to but much larger than a microtome utilized to prepare biological specimens for mounting on a microscope slide [*Hodge et al.*, 1954]. *Williams et al.* [2010] photographed the side of the snowpit after each snow slice was removed and then used commercial software to recombine the camera images into a 3-D image of meltwater flow in snow. The experiments allowed for spatial statistical analysis to be conducted on the 3-D data associated with the image. The results enabled a better understanding of temporal and spatial meltwater flow transitions throughout the snowpack.

Fortin et al. [2002] injected artificial ice layers with a florescent dye tracer and inserted the ice layers into the side of a snowpit. Interaction of water with the ice layers was revealed by movement of the dye tracer.

Stähli et al. [2004] used dye tracer techniques to study the physics of snow water infiltration into semifrozen soils. The tracer was applied as a powder either to the surface of a shallow snowpack at the beginning of the winter season or to the soil surface which was then covered with snow by the use of shovels.

The density of each layer in the snowpit is normally estimated using a measurement sampler with a known volume. Samples are extracted from a pit wall not facing the Sun to mitigate the effects of solar insolation on changes in snowpack properties. A sample from each snowpack layer is extracted using the measurement sampler if the layer has a vertical dimension large enough to fit the snow sampler. The mass of the measurement sampler is determined using a weight scale and the density of each layer calculated by dividing mass by volume [*Fierz et al.*, 1999].

Gravimetric snowpit sampling has long been practiced in snow science. *Seligman* [1936] recounts the use of a cylindrical measurement container with a volume of 500 cm^3 that was placed on a steelyard measurement balance. Similar balances were used by Russian investigators in the early part of the twentieth century [*Radionov et al.*, 1997].

Triangular measurement samplers (Snowmetrics Inc., Fort Collins, CO) are commonly used to determine snow density (Figure 8). The triangular measurement sampler is ideal for density measurement since a metal cutter fits into a slide on the top of each sampler. The triangular sampler is inserted into a snowpack layer, and the

Figure 8. Photograph of a triangular sampler being used with a scale to determine the mass of snow within the sampler.

cutter is used to extract a snow sample. Two types of triangular samplers have been used: a small sampler with a volume of 250 cm^3 and a large sampler with a volume of 1000 cm^3.

The "CRREL" snow sampler is a 500 cm^3 cylinder with a serrated metal edge that is inserted into the side of the snowpit [*Crook and Freeman*, 1973]. The length of the CRREL sampler is 20 cm long. Alternately, the "Canadian" snow sampling sampler has a volume of 250 cm^3, is only 19 cm in length, and may contain serrated cutting teeth for sampling high-density snow. Both types of snow tubes can be capped for sample extraction. Snow density samples collected using these tubes show high correlations between data sets, indicating that both samplers perform in a similar fashion [*Gary*, 1967].

Granberg and Kingsbury [1984] describe two other snow samplers. A triangular "Swedish" snow sampler has a hinged cutting lip. A metal cutter similar to the triangular sampler fits into a slide at the top of the sampler. The "Granberg-Crocker" (G-C) sampler is a cylindrical tube with a sharpened cutting end similar to the CRREL or Canadian sampler. The G-C sampler is different than these other two samplers since a series of slits in the snow sampler wall at 1 cm increments allow the snow sample to be cut and snow density to be measured at increments into the pit wall.

Perla et al. [1982] used an oval sampler with a 2 cm thickness to extract snow samples from the wall of a snowpit. The sampler had a precision of 1% over 100 measurements and had a 1% error when compared with a 5 cm diameter (25 cm length) snow sampler. The sampler was used to collect data to relate snow particle morphology to the mechanical properties of snow and to provide greater insight into the correlations between snow properties.

Snowpit sampling is time consuming, and the creation of a snowpit is labor intensive [*Pomeroy and Gray*, 1995]. In a similar fashion to the other measurements discussed in this section, the digging of a snowpit is an invasive procedure that destroys the snowpack structure. After the snowpit is created, heat transport from the surrounding landscape and insolation from the Sun will cause melting of the snow. This is the reason why the snowpit is covered with a tarp [*Marsh and Woo*, 1984a] if further experiments are required hours after the snowpit is dug.

2.5. Snow Morphology and Structural Measurements

Snow particles are often removed from a snowpit wall or the snow surface and placed on a plastic card with a graduated black background. The snow particle size and type are recorded by a human observer who makes an observation, often with recourse to snow classification schemes such as *Fierz et al.* [1999]. Although a magnification loupe or portable magnifier can be used, the disadvantage of this method is that the human observer can often be subjective. Snow morphology measurements allow for a better understanding of the physics related to snowpack evolution and how the snow particles change over time.

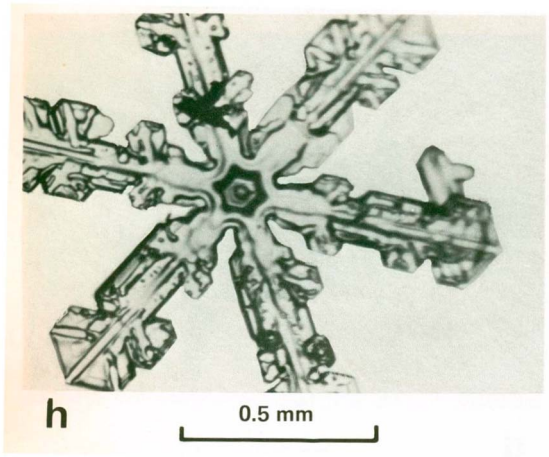

Figure 9. Picture of newly fallen snowflake [from *Perla*, 1978].

Bentley and Humphries [1931] trapped falling snow on a black board and carefully transferred snow particles to a microscope slide. A specially designed microscope fitted with a camera was used to photograph snow particles.

Seligman [1936] used an f/4.5 lens with a focal length of 42 mm attached to a 20 inch (50.8 cm) bellows and a film camera to photograph snow particles. The bellows allowed the lens to be moved in front of the camera so that magnifications between 12X and 2.5X could be obtained. Artificial light was not required due to the f/4.5 aperature and because Seligman took most of his pictures outdoors under direct sunlight using exposure times of 4 s to 15 s. The snow particles were extracted from the snowpack and filmed inside of an aluminum container with a transparent lid; the inside of the container was painted black to provide a contrasting background for observation of snow particles.

Nakaya [1954] utilized a microscope in a cold room with an attached camera. Some of the crystals photographed by *Nakaya* [1954] were artificially grown in a laboratory. *LaChapelle* [1977] distinguished between conventional cameras and cameras attached to microscopes, recognizing that shorter exposure times are required for lenses with larger apertures due to larger amounts of light admitted into the lens. Magnifications of 25X to 40X were recommended by *LaChapelle* [1977] for fine-detailed studies of snow particles, with lower magnifications used as required. From his observations, *LaChapelle* [1977] discovered that most snow particle sizes ranged between 0.5 mm and 5 mm. Reflected, transmitted, and low-oblique illumination of snow particles was attempted using artificial light.

Perla [1978] extracted snow particles from a snowpack and placed the particles in a petri dish under a microscope in a laboratory situated in the Canadian Rockies. *Perla* [1978] used polarized light to photograph the snow particles so that greater detail could be observed. A reference grid of 1 mm to 2 mm was used for reference and photographed. Sometimes this grid was situated outside of the frame. Figure 9 shows a newly fallen snowflake, whereas Figure 10 shows a melt-freeze cluster photographed by *Perla* [1978]. *Fierz et al.* [1999] present a range of snow particle photographs that clearly show snowpack metamorphism and a wide range of snow particles.

Libbrecht and Tanusheva [1998] and *Libbrecht* [2005, 2006] show many photographs of snow particles and discuss the physics of snow particle formation. Some of these particles were artificially grown in a laboratory diffusion chamber. Photographic analysis of particles during particle formation and over time permits a better understanding of the physics related to particle formation, morphology, and the atmospheric conditions required for snow particle growth.

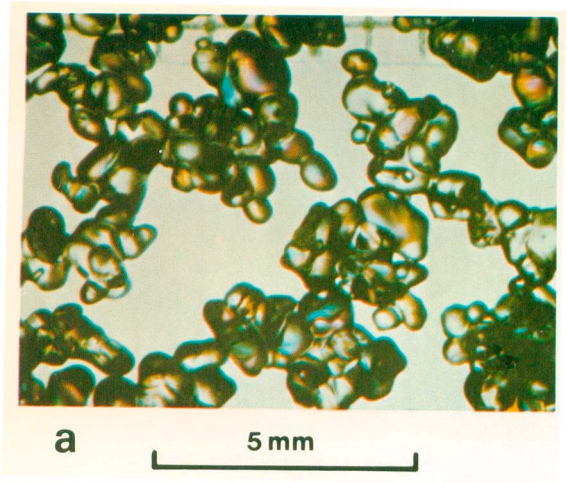

Figure 10. Picture of melt-freeze cluster [from *Perla*, 1978].

After being photographed, snow particles can be subjected to spatial and statistical analysis. *Langlois et al.* [2010] determined snow particle size and geometry from digital images. *Ishizaka* [1993] used stereopairs of images to measure the volume of snow particles and obtain an estimate of individual snow particle densities. The analysis of snow particle morphology and connectivity permits a better understanding of how these properties are related to snow permeability [*Albert and Perron*, 2000; *Albert et al.*, 2000;

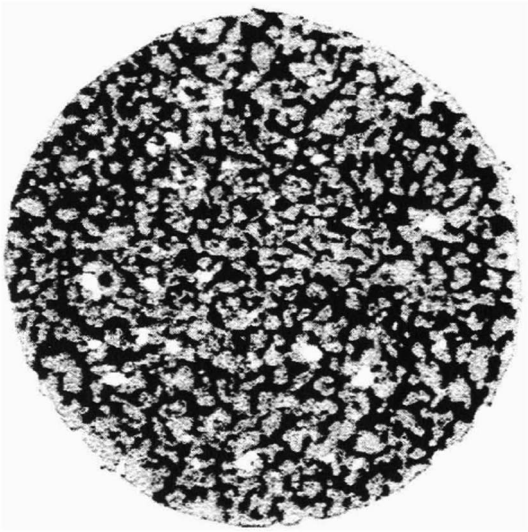

Figure 11. Computed tomography (CT) section of a snow sample [from *Lundy and Adams*, 1998].

Albert, 2002], the evolution of the snowpack, and the movement of air, gas, and water through snow [*Colbeck*, 1986a, 1989b, 1991].

Schaefer [1964] created a replica of a snow particle by encapsulating it in plastic. The ice material comprising the snow crystal was allowed to evaporate, thereby leaving behind a plastic cast. *Brun and Pahut* [1991] found that snow particle metamorphism can be delayed for a timescale on the order of months by extracting snow particles from a snowpack and placing the particles in a solution of trimethyl 2-2-4-pentane kept at temperatures below 0°C. These methods permit the snow particle to be photographed at a later time.

Most photographic measurements of snow particles have been made using snow that has been deposited on the ground or collected from a surface. More recently, the Multi-Angle Snowflake Camera utilized a number of cameras and light sources at multiple angles to a measurement plane to obtain stereographic images of snow particles in free fall. Since the particle is measured in free fall, the fall velocity and particle morphology can be noninvasively measured [*Garrett et al.*, 2012]. The apparatus is now commercially available (Falgatter Technologies, Utah), and research continues on the development of newer prototypes.

Aside from independently photographing snow particles, the porous structure of the snowpack composed of snow particles bonded together by metamorphic processes has been determined by extracting a snow sample from the snowpack and filling the pore spaces with an organic chemical such as diethyl phthalate. A dye can be added for contrast, and the sample is frozen [*Perla*, 1982]. Flash freezing can also be used in lieu of conventional freezing in a cold room [*Brzoska et al.*, 1998]. A microtome is used to cut sections from the sample, and the sections are digitized with areas of 100 mm^2 and 10^5 to 10^{16} pixels for a resolution of $\sim$ 10 μm [*Dozier et al.*, 1987]. Stereological and fractal parameters related to the connectivity of the porous medium can be obtained by computer analysis of the thin-section slices and the results related to metamorphic processes [*Perla*, 1985; *Dozier et al.*, 1987; *Good*, 1987; *Davis and Dozier*, 1987].

Tortuosity can be measured using X-ray tomography [*Kaempfer et al.*, 2005]. In lieu of microtoming a frozen sample, computed tomography (CT) images can be obtained of snow samples (Figure 11). These images are virtual "slices" through the sample created by X-rays and are comparable to sample images prepared by microtome methods. This allows for the structure of the snow sample to be determined without microscopic analysis. A disadvantage of this CT imaging is wet snow. When the pore spaces of the snowpack are filled with water, there is not high contrast between the pore spaces and the porous ice structure. The technique can be used to extract morphological measurements and snow density [*Lundy et al.*, 2002; *Lundy and Adams*, 1998]. X-ray tomographic techniques used to image snow have been reviewed by *Heggli et al.* [2011]. Alternately, magnetic resonance imaging (MRI) of snow has also been used to obtain images of snow samples [*Ozeki et al.*, 2003]. An example image is shown in Figure 12.

The specific surface area (SSA) of snow is a morphological parameter that can be measured by optical devices (section 2.13) or by thin-section analysis with X-ray tomography. For comparison with these optical methods, the absorption of methane gas by a snow sample can be used to determine SSA [*Kerbrat et al.*, 2008]. Absorption of methane gas is not an optical method but is used to obtain comparison data for testing of optical methods. These optical devices allow for measurements to be quickly made along a snowpit wall and has led to an improved understanding of how SSA changes over depth in a snowpack.

2.6. Pressure and Load Cell Sensors

The most common pressure sensor used to measure SWE at a fixed location is a snow pillow. Snow pillow data allows for continuous monitoring of SWE that can be used for water forecasting or flood forecasting applications. The data collected at "SNOTEL" sites throughout the United States includes snow pillow data

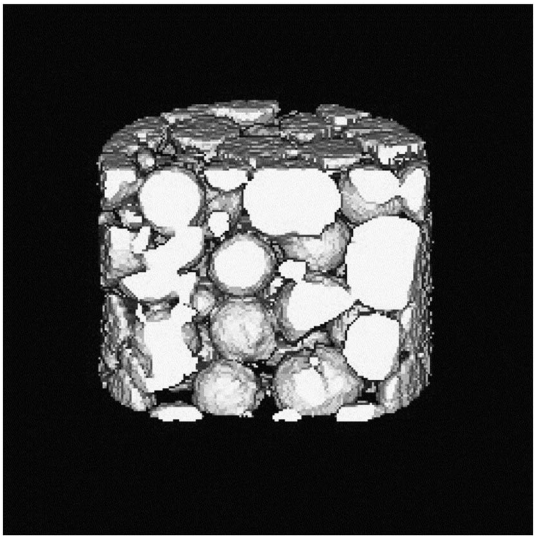

Figure 12. Magnetic resonance imaging (MRI) reconstruction of a snow sample showing snow particles [from *Ozeki et al.*, 2003].

(National Resources Conservation Service, http://www.wcc.nrcs.usda.gov/snow/). This data have been used to provide insight into the spatial distribution and regional climatology of snowfall [*Molotch and Bales*, 2006].

The classic snow pillow (Figure 13) is an oval [*Beaumont*, 1965] or rectangular [*Molnau*, 1971] pressure transducer buried in the ground surface under the snowpack. The pressure transducer is filled with an antifreeze chemical. A manometer senses the mass of snow on top of the pillow by measuring changes in fluid pressure [*Beaumont*, 1965]. The mass of the snow m_s on the pillow and the area of the pillow A_s is related to SWE by

$$\mathrm{SWE} = \frac{m_s}{A_s}. \tag{3}$$

In the above equation (3), A_s is computed using simple geometry. For example, $A_s = \pi r_p^2$, where $\pi \approx 3.14159$ and r_p is the radius of the pillow.

Snow pillows are only suitable for permanent installation at a field site and cannot be moved. This adds logistical and cost considerations to the selection of a snow pillow site [*Farnes*, 1967]. Moreover, because the pressure transducer is filled with a liquid, mechanical abrasion can cause leakage [*Ord*, 1968], damage can be inflicted by animals [*Shannon*, 1968; *Davis*, 1973], and air bubbles can develop in transducer lines [*Cox et al.*, 1978]. Frost-heave processes and the presence of bears in high-latitude environments necessitates the need for snow pillows in Alaska and the Yukon Territory to be installed on top of a specially designed frame [*Clagett and McClure*, 1994]. Because the antifreeze chemical mixture commonly used in the snow pillow is hazardous to animals, some research has been conducted to find suitable mixtures that are less toxic [*McGurk*, 1992].

The size of the pillow is related to the maximum SWE that can be measured. Pillows with larger area are required for sites with greater snow depth and SWE [*Beaumont*, 1965]. A recommended minimum diameter for the snow pillow is 3 m [*Farnes and Rompel*, 1969]. The development of ice layers between the pillow and the ground surface and uneven melt rates between the ground and the top of the snow pillow [*Johnson and Schaefer*, 2002] can cause measurement errors. *Julander* [2007] noted that snow pillows can be manufactured from steel or Hypalon, a black synthetic rubber compound. *Julander* [2007] found that the steel pillows

Figure 13. Classical snow pillow installation on the ground surface at a field site in northern Canada. Snow accumulates on top of this pressure transducer over the winter season. Visible in the background is a small control shed with the manometer and associated apparatus.

Figure 14. Load cell measurement device with rectangular plates buried under a layer of snow. This sensor was installed at a field site in the Rocky Mountains of Canada. Some uneven settling of snow is present around the load cell device.

accumulated more SWE than the Hypalon pillows, suggesting that the black color of the Hypalon rubber influenced snowmelt rates. The snow pillow is often painted white to reduce heating by solar insolation [*Beaumont*, 1965].

Snow pillows are tested in the field by removing all of the snow from the top of the pillow. The mass of removed snow is then carefully determined by bagging and weighing [*Davis*, 1973]. *Smith and Boyne* [1981] installed a snow pillow in a laboratory test chamber, finding that the response of the transducer did not show a linear relationship with applied pressure. They also presented a mathematical model of changes in snow pillow pressure with environmental temperature. *Johnson* [2004] realized that most snow pillow designs rely on "rule-of-thumb" engineering estimates. To quantify errors in snow pillow measurements, *Johnson* [2004] used mathematical modeling to show that SWE pressure sensor errors occur due to (1) a shear stress exerted from the side of the snow pillow caused by a difference in compressibility between the adjacent snow and the pillow, (2) differences between thermal properties of the pillow and the surrounding snowpack causing an uneven melt rate, and (3) sensors with a high compressibility that influence measurement of the snowpack's mass. A mathematical procedure for correction of these errors has been proposed by *Johnson and Marks* [2004].

Modern snow measurement devices that are similar to snow pillows use load cells in lieu of antifreeze. This reduces the possibility of mechanical breakdown. The load cell is a transducer that changes in resistance with a change in applied pressure.

Engman [1966] reported on some preliminary trials of a "diaphragm deflection method" using load cells. At the time, load cell transducers were not accurate enough for operational use in a snow measurement device. Load cells were later installed beneath triangular pieces of plywood. The mass of snow on the triangular piece was related to SWE [*Pangburn and Kim*, 1984; *Pangburn and Pratt*, 1980].

Moffitt [1995] designed a load cell device referred to as a "snow plate." A circular plate with 1.1 m diameter was suspended on three load cells. Due to the smaller area of the sensor relative to most snow pillow designs, ice-bridging effects were observed to be a major influence on sensor results.

Johnson et al. [2007] describe a load cell-based SWE measurement device (Figure 14) that consists of eight aluminum plates with dimensions of 3.2 m by 3.0 m. In a similar fashion to a snow pillow, the plates are installed during the snow-free season in a frame flush with the ground surface to ensure that measurement errors do not occur due to uneven settling of the snow. The plates are perforated with holes to reduce the ponding of meltwater on the surface of the device. Load cells are situated on each corner of the center plate to measure the mass of the snow on each of the surrounding plates. The idea is similar to a much older design that arranges triangular plates around a weighing scale [*Beaumont*, 1966].

Figure 15 shows a picture of a hanging snow lysimeter used to measure unloading of intercepted snow from a forest canopy at the Marmot Creek Research Basin. The "horse feeding trough" has been hung from a load

Figure 15. Hanging lysimeter used to measure unloading of intercepted snow from a forest canopy at the Marmot Creek Research Basin.

cell, and its weight is recorded using a data logger. Load cell sensors have also been utilized to measure the mass of snow accumulated on the branches of a tree due to interception. *Schmidt et al.* [1988] placed the base of a small artificial conifer on a load cell and measured changes in the mass of the tree over time as the intercepted snow sublimated. *Pomeroy and Gray* [1995] and *Hedstrom and Pomeroy* [1998] recount an experiment where a black spruce tree with a height of 9 m was cut down and suspended from a load cell attached to a tower (Figure 16). Changes in the mass of the tree as well as desiccation of the tree were recorded by a data logger over the winter season. The data collected from these experiments provided greater insight into physical processes related to deposition, sublimation, and unloading of snow and allowed for the development of more physically accurate models of these processes [*Hedstrom and Pomeroy*, 1998]. *Storck et al.* [2002] utilized weighing devices to determine the amount of snow intercepted by a tree. Unlike *Hedstrom and Pomeroy* [1998], the tree was not suspended from a tower. The tree was cut down and placed in a bolted mechanical assembly. A weighing platform was used to determine the amount of snow intercepted by the tree, whereas another weighing platform was used to determine the amount of snow deposited on the ground surface.

2.7. Snowmelt Lysimeters

A snowmelt lysimeter is an apparatus used to determine SWE as depth of water that results from the melting of a snowpack. Water from melting snow that reaches a collection pan is admitted into a measurement gauge through a pipe or orifice. This is often a precipitation gauge or a container. The lysimeter is often used to determine the amount of water available from snowmelt as runoff (Figure 17).

Kattelmann [1984] reviewed and classified snowmelt lysimeters. The lysimeter can be "enclosed" around a column of snow using an isolation barrier. Alternately, an "unenclosed" lysimeter consists of a metal collection pan that does not isolate the snowpack. A "zero-tension" lysimeter has a collection container that is under atmospheric pressure, whereas a "tension" lysimeter has a collection container with a pressure different than atmospheric pressure. As noted by *Kattelmann* [1984], the physics of snowmelt lysimeters was discussed by *Wankiewicz* [1978a] and such devices were first used by *Church* [1948]. *Kattelmann* [2000] later presented another review of snowmelt lysimeters, discussing the applicability of these devices in the evaluation of snowmelt models.

The *U.S. Army Corps of Engineers* [1956] installed 56 m^2 and 120 m^2 lysimeters at a permanent field location, finding that ice layers in the snowpack-diverted flow, thereby causing a 45% error in the observed flow [*Marsh*, 1991]. A portable lysimeter with a collection area of 2 square feet (0.19 m^2) was also created by the *U.S. Army Corps of Engineers* [1956], but the data collected did not provide an accurate assessment of runoff due to its small area.

Haupt [1969] installed an enclosed lysimeter with a 0.25 m^2 area; although the lysimeter enclosure had to be adjusted after every snowfall event, the data collected were deemed to be accurate. *Haupt* [1969] notes that this lysimeter is not suitable for deep snowpacks and that snowmelt had occurred around the edges of the

Figure 16. Conifer tree suspended from a load cell. (a) Side view of apparatus. (b) Underside view of apparatus.

enclosure. *Hermann* [1978] considered a 25 m^2 lysimeter to be the smallest lysimeter that can be constructed to accurately measure runoff from snow. The system described by *Hermann* [1978] had a collection container that was automatically emptied by a magnetic valve.

Marsh and Woo [1985] installed lysimeters with 1 m^2 and 0.25 m^2 areas, finding an agreement of less than 10% error between these two devices. One collector with 0.25 m^2 area was subdivided into 16 subenclosures. The error in determining runoff using these collectors ranged between 0% and 250% [*Kattelmann*, 2000].

Greenan and Anderson [1984] note that mechanical adjustment of the enclosure was a design feature of the enclosed lysimeter described by *Thompson et al.* [1975]. The *Greenan and Anderson* [1984] lysimeter utilized a heated melting bar to separate the snow inside of the lysimeter from the rest of the snowpack.

Dunne et al. [1976] and *Price and Dunne* [1976] describe a lysimeter composed of a 1 m deep trench at the bottom of a slope. An artificial surface channel and subsurface channel created from the trench conveyed water from melting snow. Water in both channels was transported by pipes to a weir where a meltwater hydrograph was obtained.

Jordan [1983] installed a lysimeter into a small hole dug through the side of the snowpit near the ground surface (Figure 17). The lysimeter consisted of a large melting pan with a 1 m^2 area, a funnel, and a tipping bucket precipitation gauge and recorder. Blocks of snow were used to seal up the hole. A source of error in the measurement was due to spatial flow nets of water in the snowpack. The average error was $\pm$ 3 mm of SWE. The data collected provided insight into the physics of meltwater wave propagation in the snowpack.

Figure 17. Picture of snowmelt lysimeter installation at Guzelyayla Station in Turkey [from *Tekeli et al.*, 2003]. Further details on the design of the system are given by *Tekeli et al.* [2003].

Kattelmann [2000] considered that if a snowmelt lysimeter has an area ranging between 1 m^2 and 2 m^2, more than one lysimeter should be deployed per measurement site to obtain an accurate measurement of runoff from snowmelt. For snowmelt lysimeters with areas between 10 m^2 and 20 m^2, at least three lysimeters should be used. To ensure uniformity of water flow through snow over a measured area, *Kattelmann* [2000] cites a rule of thumb proposed by *Male and Gray* [1981] that the measured area of the snowpack A_s should be such that $A_s > d^2$, where d is snow depth. *Tekeli et al.* [2003, 2005] note considerations of *Kattelmann* [2000] in the design of a small 1.53 m^2 snowmelt lysimeter, also presenting the civil engineering aspects of the design.

2.8. Snow Tensiometers

In a similar fashion to the use of tensiometers to measure negative water pressure (tension) in soils, a snow tensiometer measures the pressure p_p of liquid water and air in the pore spaces of the snowpack. However, despite the similarity of operation between tensiometers used in soil and snow science applications, some differences in design are necessary to apply this measurement device to snow. The use of such devices installed in the side of a snowpit enables the observation of diurnal meltwater fluxes through the snowpack and the rate of movement of water in snow [*Colbeck*, 1976b]. Use of the tensiometer in snow science provided data used for inputs into physical models of meltwater propagation through snow [*Wankiewicz*, 1978b; *Colbeck*, 1976b].

The tensiometer is composed of a porous cylinder connected to a flexible tube at the end of which is a manometer (Figure 18). A support clamp allows for the manometer to be attached to the tube when the tube is inserted vertically into the side of a snowpit [*Jordan*, 1983]. The accuracy of pressure measurement is within ±80 Pa, with a precision of ±20 Pa between measurements taken at different times [*Wankiewicz*, 1978b].

An electronic tensiometer is composed of a porous cylinder at the end of which is an electronic pressure sensor. The pressure sensor is attached to a bridge circuit. The voltage difference across the bridge is then amplified and recorded [*Colbeck*, 1976b]. The sensor electronics described by *Colbeck* [1976b] can be packaged into a small box with a battery power supply for deployment at a field site. To measure high liquid water content pressures, wet cotton can be wrapped around the porous cylinder and the end placed into packed snow. The electronic version developed by *Colbeck* [1976b] was able to measure up to 8.8 kPa of pore space pressure.

2.9. Dielectric Sensors

Dielectric measurement techniques relate the relative permittivity (complex dielectric constant) of snow to the porosity and/or volumetric water content. For most of these techniques, the relationship between the quantities is empirical. Dielectric instruments generally measure snowpack wetness as liquid water content θ_w instead of water saturation S_w. The use of dielectric methods enable liquid water content to be rapidly determined in the field without chemical analysis (section 2.20) or centrifugal techniques (section 2.22), active methods of observation that rely on extraction of a snow sample from the snowpack. Similar to snow tensiometers (section 2.8), this has led to a better understanding of the rate and timing of meltwater propagation through snow [*Techel and Pielmeier*, 2011; *Denoth et al.*, 1984; *Denoth and Wilhelmy*, 1988; *Denoth*, 1989, 1994]. Moreover, density measurements using dielectric techniques can be quicker than gravimetric measurements

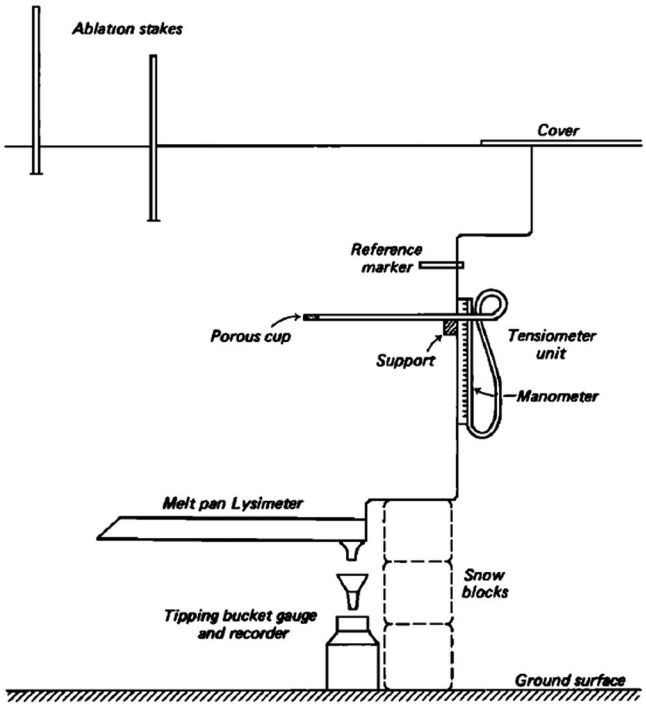

Figure 18. Installation of a tensiometer in the side of a snowpit wall. Also visible in the diagram are ablation stakes and a snowmelt lysimeter [from *Jordan*, 1983].

(section 2.4). Dielectic devices buried in the snowpack can report changes in the density or liquid water content of snow at smaller temporal time scales than other invasive measurements, thereby enabling a better understanding of diurnal snowpack changes in density and liquid water content.

The Finnish snow fork (Figure 19) consists of two parallel stainless steel prongs with sharpened ends that act as a transmission line [*Sihvola and Tiuri*, 1986; *Tiuri and Sihvola*, 1986; *Toikka*, 1992; *Tiuri et al.*, 1984]. Although popularized by Finnish investigators, similar methods involving three prongs [*Gerdel*, 1954] and four prongs [*Kendra et al.*, 1994] have also been devised. These are invasive snowpack measurement instruments.

The Finnish snow fork is normally used in a sampling configuration where the prongs are inserted horizontally into the side of a snowpit. The prongs can also be placed on the snow surface for a dielectric half-space

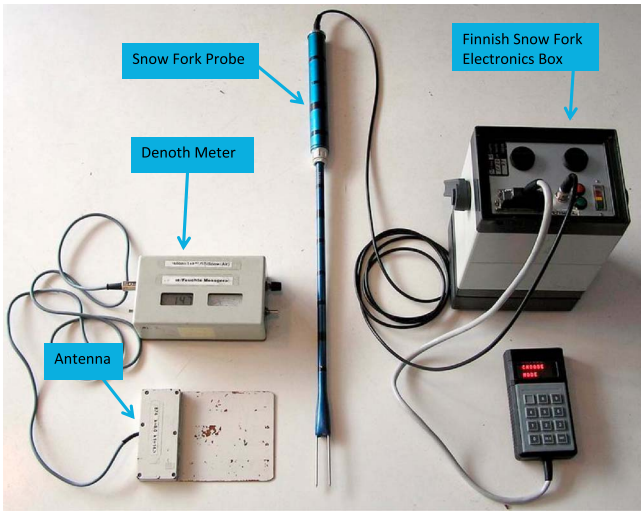

Figure 19. Picture showing two common dielectric measurement devices: the Denoth Meter and the Finnish Snow Fork (image from *Techel and Pielmeier* [2011], modified in this paper with labels pointing to the different devices).

measurement or inserted into the snow surface at a 30° or 45° angle. This requires the snow fork measurements to be multiplied by a correction factor [*Moldestad*, 2005]. Using snow fork measurements, *Moldestad* [2005] was able to relate changes in snow density to liquid water content, snow temperature, and snow particle morphology on a cross-country ski track.

The effective measurement volume of the Finnish snow fork has been estimated as 47 cm^2 [*Techel and Pielmeier*, 2011]. Alternately, assuming that the volume of measurement is composed of a cylinder with 1 cm radius and 7.5 cm height, the volume has been estimated as 24 cm^2 [*Moldestad*, 2005]. The effective sampling area has been estimated as 15 cm^2 [*Techel and Pielmeier*, 2011].

The Finnish snow fork can measure snow with a maximum liquid water content of 10% and a maximum snow density of 600 kg m^{-3}. The water content measurement error of the Finnish snow fork is reported as ±0.5% [*Sihvola and Tiuri*, 1986] but has been claimed to be as low as ±0.3% [*Moldestad*, 2005]. Mechanical compression of the snow as the snowfork is inserted into the snowpack will cause snow density to increase by 1% to 2%, adding another source of error to the measurement [*Techel and Pielmeier*, 2011]. The error in determination of density is ±5 kg m^3 [*Moldestad*, 2005]. The Finnish snow fork was estimated by *Harper and Bradford* [2003] to have a density measurement error of 5%. *Techel and Pielmeier* [2011] used the snow fork to measure snowpack liquid water content and density, thereby gaining insight into the spatial and temporal changes of snow at a number of field sites in the Swiss Alps.

Two other resonant-frequency sensors have been designed [*Denoth et al.*, 1984]. The saw resonator consists of a saw blade with a parallel wire. Designed for hard snow such as melt crusts and ice layers, the sensor operates using a sensing principle where the RF (radio frequency) wave creates a mirror image of the saw blade in the snowpack. In a similar fashion to the snow fork, the ratio of resonant frequencies is used to calculate the dielectric constant. The coaxial resonator sensor is placed on the snow surface. The sensor is pushed slightly into the snow surface to ensure proper coupling of the sensor to the snow medium. A dielectric half-space calculation is used to determine the complex dielectric constant of the snow surface layer.

Free-space measurement sensors require the extraction of a snow sample from the snowpack [*Denoth*, 1989]. The sample is placed in a styrofoam holder between a transmitting and a receiving horn antenna. An electromagnetic wave at a frequency in the GHz range is sent between the two horns. Measurements made in the air medium without a sample present allow for determination of the complex transmission and reflection coefficients of the snow sample. The reflection coefficients are related to the dielectric constant of the snow [*Hallikainen et al.*, 1986]. An alternate "ellipsometric" measurement places the two horns at an angle to the surface of the snow sample. Measurement of the reflection coefficient is related to the dielectric constant by an empirical relationship. These measurements have been used to better understand how liquid water content in snow influences wet snow metamorphism [*Denoth*, 1999].

Capacitor cell sensors are composed of two parallel metal plates, between which is placed a snow sample. Similar to the measurement of an unknown capacitor on a circuit board, an impedance bridge is used to measure the capacitance of the snow using frequencies in the 10 kHz to 10 MHz range. The ratio of snow capacitance to the empty cell capacitance is used to calculate the dielectric constant of the snow [*Perla*, 1991]. An alternate design uses an aluminum pipe. The snow sample is placed inside of the pipe [*Camp and LaBrecque*, 1992; *Perla and Banner*, 1988]. A parallel plate capacitor sensor can be placed on the end of a rod, and the rod used to penetrate the snow surface to obtain snow profile measurements [*Louge et al.*, 1998]. Capacitor probes ordinarily used for measuring soil water content have been buried in the snowpack and utilized for temporal measurements of snow [*Avanzi et al.*, 2014].

The Denoth capacitive sensor (referred to as a "Denoth meter" and shown in Figure 19) consists of a flat plate antenna that is inserted into the snowpack [*Denoth*, 1994]. The volume of measurement of a flat plate antenna sensor is 900 cm^2 corresponding to a 4 cm by 15 cm by 15 cm cuboid [*Boyne and Fisk*, 1990]. The area of measurement has been estimated as 176 cm^2 [*Techel and Pielmeier*, 2011]. This is a larger measurement area than the Finnish snow fork. A flat plate antenna design was used by *Ambach and Mayr* [1981] to measure the liquid water content on the bottom of a ski and provide greater insight into the physics of skiing. The flat plate sensor can be buried in the snowpack and used to measure diurnal cycles in snowpack wetness [*Denoth*, 1994]. *Techel and Pielmeier* [2011] have shown that when compared to snow wetness measurements made with the Denoth capacitive sensor, the Finnish snow fork overpredicted water content by 1%. Although *Denoth et al.* [1984] found that the Finnish snow fork had a slightly higher standard deviation of measurements as compared

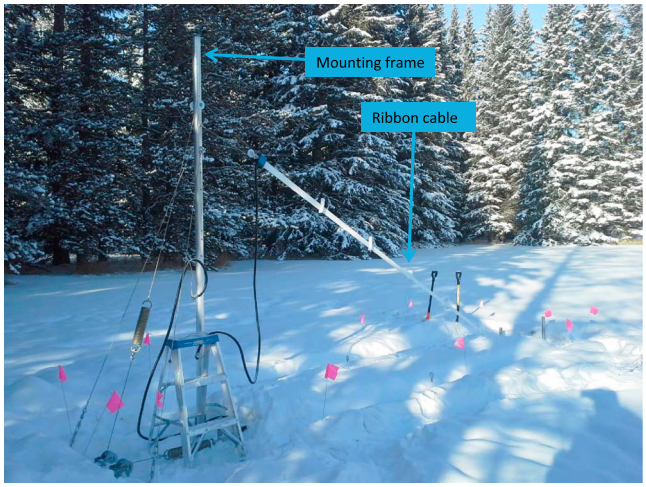

Figure 20. Picture showing installation of a dielectric ribbon cable sensor in the snowpack for the SNOWPOWER sensor, now sold as the Snowpack Analyzer (SPA). The ribbon cable sensor and the mounting frame for the ribbon cable are shown in the image.

to Denoth meter measurements, *Williams et al.* [1999] showed that there is no statistically significant difference between Denoth meter and Finnish snow fork measurements.

The SNOWPOWER system is commercially available as the SPA (Snowpack Analyzer) from Sommer Messtechnik, Koblach, Austria. The system is described by *Niang et al.* [2003]. SNOWPOWER uses a flat coaxial cable antenna (Figure 20) installed at an angle to the ground surface. The antenna is used by the system to measure density and liquid water content of snow. A measurement of snow depth using an acoustic ranging sensor permits the calculation of SWE. A number of ribbon sensors situated parallel to the ground surface can be used to measure snow densities and liquid water contents throughout the snowpack. The sensor assembly needs to be installed during the snow-free season so that snowfall can accumulate over the antenna, which is buried in the snowpack in a similar fashion to a thermocouple assembly. Contact between the cable and snow is critical to the SPA performance and can be lost due to cable vibration in wind and preferential melt around the cable where it emerges from the snowpack.

The SNOWPOWER sensor measures the dielectric constant of snow using time domain reflectometry (TDR). This relates a reflected electromagnetic pulse from the snowpack to the snow dielectric constant [*Jones et al.*, 2002]. A similar procedure was utilized by *Waldner et al.* [2004] using a commercially available TDR probe to measure liquid water content of snow in a cold room.

Kitahara et al. [1993] describe a dielectric sensor to measure the fraction of snow in a snow-water mixture. The purpose of developing this sensor was for process control of snow removal operations where snow is transported through pipes. The sensor consists of two parallel plates through which is passed the snow-water mixture. Maxwell's equation for the resistivity of a two-phase mixture was used to determine the snow fraction of the mixture without the use of empirical equations.

Kulessa et al. [2012] adapted the electrical self-potential (SP) method from geophysics to measure unsaturated flow in snow. This is a passive sensor application that utilizes the voltage difference between two sensors and a semiempirical model to measure the chemical and physical properties of the snowpack.

2.10. Radar Devices

Radar snow measurement systems operate by sending electromagnetic waves into snow and receiving the reflections. Radar sensors have provided a noninvasive method of measuring snowpack layering. When radar is used to measure snow over a transect, this has led to a better understanding of the spatial relationships between snowpack layers [*Harper and Bradford*, 2003]. Stationary deployments of radar devices [*Gubler and Hiller*, 1984] can noninvasively indicate the formation of snowpack layers without the need to create a snowpit, thereby providing better insight into the physics of snowpack evolution.

Two different types of radar measurements have been used for snowpack sensing applications. Pulse radar sends a short impulse into the snowpack, and the time difference between the sent and received pulses is

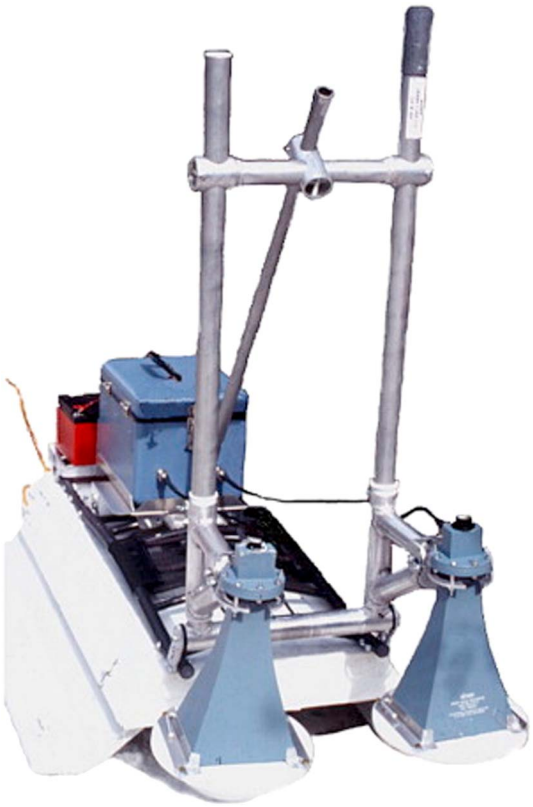

Figure 21. FMCW radar device used by researchers at the National Hydrology Research Institute of Environment Canada in the early 1990s, photograph courtesy of Mike Demuth [*Pomeroy and Gray*, 1995] and color image from *Marshall and Koh* [2008].

used to determine snowpack stratigraphy [*Harper and Bradford*, 2003]. The disadvantage of pulse radar is that the resolution is limited by the duration of the pulse. Pulses of smaller duration will give better resolution of layered media [*Klauder et al.*, 1960; *Lalumiere*, 2006]. However, the minimum pulse duration is limited by the transmitter, and receiver circuits since the transistors as switches or amplifiers used to create and detect the pulse have a response time limited by the physics of transistor operation [*Protiva et al.*, 2009; *Xia et al.*, 2014; *Yi and Hong*, 2008]. This in turn limits the operating resolution of pulse radars [*Meikle*, 2008]. A unique application of pulse-based radars is tomographic imaging of a snowpack [*Fortin and Fortier*, 2001].

Frequency-Modulated Continuous Wave (FMCW) radar uses a frequency-swept pulse (chirp) to determine the distance to a reflector. Two horn antennas are situated at an offset distance (Figure 21). One horn produces an electromagnetic wave, whereas the other receives reflections [*Stove*, 1992]. This is a bistatic radar system [*Willis*, 1991]. The sent and received waves are homodyned by a time domain analog mixer, creating a sum and difference waveform that is low pass filtered and digitized by an Analog-to-Digital Converter (ADC). The output of the low-pass filter is a difference waveform. The difference waveform frequency spectrum is related to the snowpack layer distances and snow stratigraphy using an assumed snow density or dielectric constant of snow [*Yankielun et al.*, 2004]. The bandwidth of the chirp is commonly situated in the 2–6 GHz, 8–12 GHz, and 14–18 GHz ranges. Higher frequencies have better ability to resolve layers in the snowpack, but greater attenuation and less depth penetration [*Koh et al.*, 2002]. Lower frequencies are more appropriate for wet snowpacks due to attenuation created by high liquid water contents [*Marshall et al.*, 2004].

FMCW radars are deployed above the snow surface. Using a sliding assembly, the antennas are moved over a short distance (less than 3 m) to obtain images of snowpack stratigraphy [*Marshall et al.*, 2004]. Movement of the radar system enables a measurement of SWE to be made over a large area [*Marshall et al.*, 2005]. The FMCW radar can also be set up to measure snowpack stratigraphy at a point location [*Ellerbruch and Boyne*, 1980]. FMCW radars have been mounted on a sled towed behind a snow machine to measure snowpack stratigraphy along a transect [*Gubler and Hiller*, 1984; *Holmgren et al.*, 1998; *Pomeroy and Gray*, 1995]. Mounted on a gondola situated ~30 m above the snow surface, the FMCW system has measured snowpack stratigraphy along a transect ranging over ~500 m [*Yankielun et al.*, 2004]. Upward looking FMCW radar has been used to measure snowpack stratigraphy in avalanche-prone areas by burying the system in the ground [*Gubler and Hiller*, 1984]. Snowpack density and SWE can be determined from FMCW radar using an empirical relationship between the radar-measured dielectric constant of snow and these two parameters [*Lundberg et al.*, 2006]. Further applications and a review of FMCW radars are given by *Marshall and Koh* [2008].

Using radar, overestimation of SWE by 20% can occur if the liquid water content of the snowpack is 5% by volume [*Granlund et al.*, 2007]. An upward looking FMCW radar system can be used to determine liquid water content by measuring the attenuation of radar waves in snow and using an empirical relationship to relate attenuation to water content [*Mitterer et al.*, 2011]. The attenuation of electromagnetic radiation in snow was recently investigated by *Sundström et al.* [2013] using Ground-Penetrating Radar (GPR) and a path-dependent attenuation function. *Sundström et al.* [2013] found that liquid water content was underestimated by ~50%,

but the mean error in determining SWE was reduced from 34% for a dry snowpack to 16% when the snowpack was wet.

Williams and Knoll [2002] used tomographic imaging of radar waves sent between two antennas to determine the dielectric constant of snow and measure snow wetness. One antenna was placed at the bottom of the snowpack, whereas the other antenna was placed at the top. Assuming that the snowpack had a constant density, a mixture theory equation was used to determine liquid water content. The 250 MHz frequency used for the radar waves enabled penetration of a snowpack with a depth of 1.5 m.

2.11. GPS Devices

The Global Positioning System (GPS) is composed of a constellation of satellites in orbit around the Earth. A receiver situated near the ground surface detects signals from the satellites and uses triangulation along with the time of arrival of each signal to determine the geographic position and elevation relative to a reference geoid. A survey-grade differential GPS receiver can use signals from a ground-based reference station to provide higher-accuracy measurements of geographic position [*Xu*, 2007].

Elder et al. [1999] placed a survey grade differential GPS receiver on the snow surface before and after snow deposition events. Changes in GPS-determined elevation were then related to changes in snow depth between successive measurements. A GPS device was also placed on a snow machine and changes in snow depth determined along a transect. The snow depth sensing system was designed to have a precision of 15 cm, despite changes in weather conditions and satellite visibility affecting measurement precision. The *Elder et al.* [1999] paper was an application of available GPS technology to determine snow depth by detection of changes in surface height with reference to a digital elevation model (DEM) of a geographic area.

Using multipath attenuation measurements of signals from GPS satellites detected by ground-based receivers, *Larson et al.* [2009] obtained noninvasive measurements of snow depth on the ground surface. This is a "GPS Interferometric Reflectometry Method" (GPS-IR) [*McCreight et al.*, 2014a]. A geodetic quality GPS system was used. The physical model used to determine snow depth was a two-layer model composed of a layer of soil underneath a layer of snow. Electromagnetic signals from GPS satellites were treated as plane waves incident on the soil and snow layers. Multiple reflections of electromagnetic waves from the soil and snow will affect the signal-to-noise ratio (SNR) at a GPS receiver antenna, and changes in the SNR were related to snow depth. The SNR is a measure of the GPS signal amplitude from the satellites relative to atmospheric attenuation and additional reflections from snow, soil, and the surrounding landscape considered to be "noise." An assumed snow density and temperature were used as model inputs, and a model of the dielectric constant of the soil was also required. The soil and snow layers were taken to be planar. Changes in snow density due to layers in the snowpack were not considered in this model [*Larson et al.*, 2009].

Using a similar model of electromagnetic wave propagation through snow and a nonlinear least squares inverse algorithm, *Jacobson* [2010] measured snow depth, density, and SWE using GPS signals. An assumed snow temperature was used, and measured snow depth estimates were used as starting values for the least squares inverse algorithm. The precision of the measurements was not characterized, yet the results were deemed to be physically reasonable.

The measurement footprint for the GPS-IR method was determined to be ~1000 m^2 for a snow-free land surface. This is the area over which snow depth is being determined due to the geometric radiation pattern response of the GPS receiving antennas (referred to as "beam lobes"). However, as the snow depth on the ground increased, the distance from the snow surface to the antenna decreased, and this decreased the measurement footprint. The GPR-IR method was not accurate when the snow surface was closer than 50 cm to the antenna. Using measurements from ~100 geodetic quality GPS sites comprising the Plate Boundary Observatory (http://pbo.unavco.org/), snow depth could be determined with an RMSD (Root-Mean Squared Difference) of 15 cm [*Boniface et al.*, 2014].

McCreight et al. [2014a] determined snow depth at 18 sites situated in the western United States. The GPS receiver antenna was situated 2 m above the ground surface. Snow depth was measured using a rod at multiple points surrounding the measurement antenna, showing that within a 25 m radius of the antenna, snow depth could be accurately determined within an RMSD of 10.3 cm. A spatial bias occurred over the measurement footprint due to the difference in orbits associated with GPS satellites visible at the field sites. Removing a bias of −5.7 cm decreased the RMSD between GPS and rod measurements of snow depth to 8.7 cm.

An empirical model [*McCreight and Small*, 2014b] was used to compute snow density as a function of snow depth so that SWE could be estimated.

Koch et al. [2014] buried two GPS antennas beneath the snowpack and mounted another GPS antenna at a height of 4 m above the snow surface. Unlike the use of survey grade GPS by other investigators, the receivers were low-cost Fastrax IT430 GPS receivers. *Koch et al.* [2014] used a model of electromagnetic wave transmission through snow to estimate snow liquid water content from GPS satellite signals received by the three antennas. The model assumed planar wave propagation and did not take into consideration the effects of multiple reflections. Similar to other investigators, the SNR was used in the calculation. A semiempirical model was used to relate the dielectric constant to the snow density and liquid water content. This model is similar to the model used for the Finnish snow fork (section 2.9). The snow depth was measured using an ultrasonic sensor (section 2.23). The data collected from the GPS system were deemed to be physically reasonable and of the same order of magnitude as comparison measurements of snow density and liquid water content made using dielectric devices.

Applications of GPS snow measurement technology involve the use of preexisting GPS networks to measure snow. This reduces the cost of instrument network deployment and enables the collection of large amounts of data to provide insight into the climatology and distribution of snow [*Jacobson*, 2010; *McCreight et al.*, 2014a]. A disadvantage of this method is that only bulk depth, density, and liquid water content estimates of snow are available over a reasonably large sampling area. In addition, measurements have not been made using a multilayer snow model.

2.12. Laser Ranging Devices

The use of terrestrial laser ranging equipment to measure snow depth relies on two observations. One observation is made during the snow-free season, whereas the other observation is made when snow cover is present. The laser rangefinder is placed at a fixed location that is the same for all measurements, and it is necessary to have precise reference points at several distances in the resulting image to cross-reference snow and nonsnow imagery. An observation is made by sending a short laser pulse toward the ground or snow surface. The pulse is reflected, and the time of flight between the sent and received pulse is used to measure distance from the range finder to the ground or snow surface. The difference between the snow-free and snow-covered measurements is used to determine snow depth. The laser can be turned by rotating the device manually or by a mechanical assembly inside of the device.

Hood and Hayashi [2010] used a handheld laser rangefinder with a 0.905 μm wavelength, finding that snow depth in complex mountain terrain could be measured with an accuracy of 12% compared to manual depth measurements. Due to the similarity of laser ranging to monopulse sonar and radar, the same limitations related to pulse width is also present in the application of this method. The use of a laser rangefinder allowed *Hood and Hayashi* [2010] to measure the rate of snow ablation at a site where manual snow depth measurements could not be made, thereby gaining insight into the hydrologic response of an alpine watershed.

Terrestrial lidar systems (TLS) have been deployed on the ground to measure snow depth. *Osterhuber et al.* [2008] used a TLS with a depth measurement accuracy of ±4 mm to determine snow depth at the Central Sierra Snow Laboratory in California. The TLS was able to obtain a three-dimensional volume of the snow cover by moving the laser beam over the snow surface using a computer-controlled mirror. Gravimetric measurement of snow density permitted computation of SWE. A laser light source with 1.5 μm wavelength did not appreciably penetrate the snowpack and was suitable for use with wet snow. *Deems et al.* [2013] provide a comprehensive review of snow depth lidar measurements, identifying the physics of operation and suggestions for further research.

Musselman et al. [2015] used ground-based lidar situated at a fixed location in a forest clearing to demarcate the fractional amount of forest cover in the surrounding forest and to identify the forest and clearing edge so that a ray tracing model of light propagation through the forest canopy could be applied. This ray tracing model provided insight into the amount of solar radiation received on the snow surface in relation to forest gaps, thereby leading to a better understanding of the physics of radiation and snowmelt under forest canopies.

2.13. Optical Property Measurement Devices

Optical property measurement devices often involve spectral measurements of snow cover. Light reflected or transmitted through snow is measured at one or more optical wavelengths. Light entering through an optical assembly can either pass through a series of filters (monochromator) or pass through a prism (spectrometer).

O'Neill and Gray [1973] extracted a snow sample from a snowpack and placed the sample in a holder above a photodiode to measure light extinction through snow. The photodiode had a response ranging between 300 nm and 1200 nm. *O'Neill and Gray* [1973] also coupled photodiodes to fiber optic cables so that light extinction through a snowpack could be measured without extraction of a snow sample. *O'Neill and Gray* [1973] were able to better understand how albedo influences the reflection of light from snow. This research influenced later model development of snowpack evolution [*Gray and Landine*, 1988].

Roulet et al. [1974] designed a profiling spectrometer that could be inserted through a hole in the snowpack. The instrument was used to measure the intensity distribution of light in the range of 400 nm to 1000 nm.

Richardson and Salisbury [1977] used a monochrometer to measure wavelengths of light between 400 nm and 730 nm. The monochrometer was situated in a permanent laboratory installed in the ground beneath the snowpack and was used to measure light extinction through snow at different wavelengths so that plant growth beneath snowpacks could be related to light spectra. *Richardson and Salisbury* [1977] also provide a brief review of light extinction measurements through snow made using similar techniques.

O'Brien [1977] measured the ultraviolet reflectance of snow in the 200 nm to 400 nm range by placing a snow sample in a cold room and using a monochometer situated at an adjustable offset angle to the snow surface. *O'Brien and Koh* [1981] placed a monochometer above the snow surface and measured snow reflectance in the near infrared from 800 nm to 1800 nm. The data from these experiments provided an understanding of the wavelength distribution of light reflection from snow, since changes in snow reflectance were related to snow microstructure, albedo, and the timing of snowmelt. Reflection of light from snow is thereby important to understand since much of the light that is not reflected transfers energy to snow, thereby resulting in the heating of the snowpack.

Grenfell [1983] designed a monochromator specifically for measuring snow albedo and irradiance. The device was situated on a mounting stand at a distance of 0.8 m above the snow surface to reduce instrument shading effects. A battery pack and electronics allowed for mobile deployment in cold weather conditions. The system measured wavelengths of light between 400 nm and 2450 nm. *Grenfell et al.* [1994] mentioned that the measurement range was later extended into the ultraviolet by using a gallium arsenide phosphide photodetector. *Grenfell et al.* [1994] made measurements between 300 nm and 3000 nm.

Measurements made using optical property measurement devices have been reviewed by *Wiscombe and Warren* [1981], *Warren and Wiscombe* [1981], and *Warren* [1982]. These investigators used the collected data to better understand the physics of light reflection and propagation through snow, thereby establishing one of the first accurate models of snow optics.

Painter et al. [2003] placed a commercially available spectroradiometer on the end of a robotic arm and used the system to determine the snow reflection spectra over a hemisphere situated above the snow surface. Software running on a laptop computer enabled the automatic collection and processing of data. Measurements from the device were reported by *Painter and Dozier* [2004]. Measured light wavelengths were between 400 nm and 2500 nm. The data collected by the system had unprecedented spatial resolution compared with other previous measurements and were used to validate optical models of snow.

Perovich [2007] placed a black piece of plywood on the ground surface and installed upward and downward facing monochrometers above the plywood. Changes in light reflection and transmission during a snowfall was recorded from 400 nm to 1000 nm. The black plywood was intended to reduce reflected light from the bottom of the snowpack that had accumulated on the plywood.

Domine et al. [2006] and *Painter et al.* [2007] used a commercially available spectroradiometer operating at wavelengths between 350 nm and 2500 nm to relate snow spectral radiance to optical snow particle size. The spectroradiometer probe was placed in contact with the side of a snowpit. The radiance output at different wavelengths was related to optical snow particle size by a mathematical model. *Painter et al.* [2007] found that for snow particle sizes ranging between 50 μm and 100 μm, the accuracy was within ±10 μm and ±50 μm.

Figure 22. Measurement of SSA using an integrating sphere [from *Montpetit et al.*, 2011].

Gallet et al. [2009] determined the SSA of snow using an integrating sphere manufactured from a polymer with a known optical reflection coefficient. The sphere was placed in contact with a snow sample extracted from the snowpack. An IR laser diode illuminated the sphere and the snow sample. Reflections from the sides of the sphere and the snow sample were detected by a photodiode. The current output of the photodiode was converted to a voltage by a tranimpedance amplifier and the resulting voltage amplified. The voltage was related to the snow SSA by a semiempirical calibration curve. The error in determination of SSA was 12%. Wavelengths of infrared light used in the experiments were 1310 nm and 1550 nm.

Montpetit et al. [2011] adapted the *Gallet et al.* [2009] system so that the integrating sphere could be used to determine SSA and albedo along the side of a snowpit wall (Figure 22). Calibration curves were used to relate the output voltage to both SSA and albedo.

Arnaud et al. [2011] created a sensor to measure SSA that could be lowered down a hole created in the snowpack. The sensor was composed of two IR lasers that illuminated a mirror facing the side of the hole. One laser was used to measure the distance of the sensor to the snow surface in a similar fashion to a laser ranging (lidar) device, whereas the other laser was used to illuminate the snow surface. Six photodiodes situated at different angles to the snow surface sensed the reflected laser light. A mathematical model related the backscattered light intensity to the SSA of snow with a measurement error in the range of 10% to 15%.

Using modified digital cameras with near-infrared filters placed over the CCD sensors, *Matzl and Schneebeli* [2006] and *Langlois et al.* [2010] measured SSA and albedo using a theoretical model of light reflection from snow. The cameras had to be empirically calibrated in the field for accurate illumination and reflectance. This measurement technique eliminated the need for custom and expensive electronic devices to measure the SSA of snow.

Kasurak et al. [2012] describe a sensor using visible green, red, blue, and white light-emitting diodes (LEDs), as well as an infrared LED. An LED was situated at an offset distance to a photoresistor. Both the LED and the photoresistor were placed inside of a container used to extract a snow sample from the side of a snowpit. This was a snow sampler with LEDs. The extinction of light by the snow sample was related to snow particle size and shape using a completely empirical relationship developed from microscopic observations of snow particles made by a human observer.

2.14. Mechanical Trap Blowing Snow Measurement

The mechanical trap is a device used to measure blowing snow mass flux (Figure 23). The trap consists of a collection container or a fabric bag with an open orifice. The container is oriented toward the wind, and snow particles are collected in the container. Often, the container is mounted on a turntable device so that the gauge can be turned toward the wind. A major disadvantage of the mechanical trap is that the container must be periodically emptied by a human observer. Mechanical trap measurements of blowing snow have enabled the validation and calibration of the physics associated with blowing snow models and provided insight into the amount of snow distributed by the wind at various geographic locations.

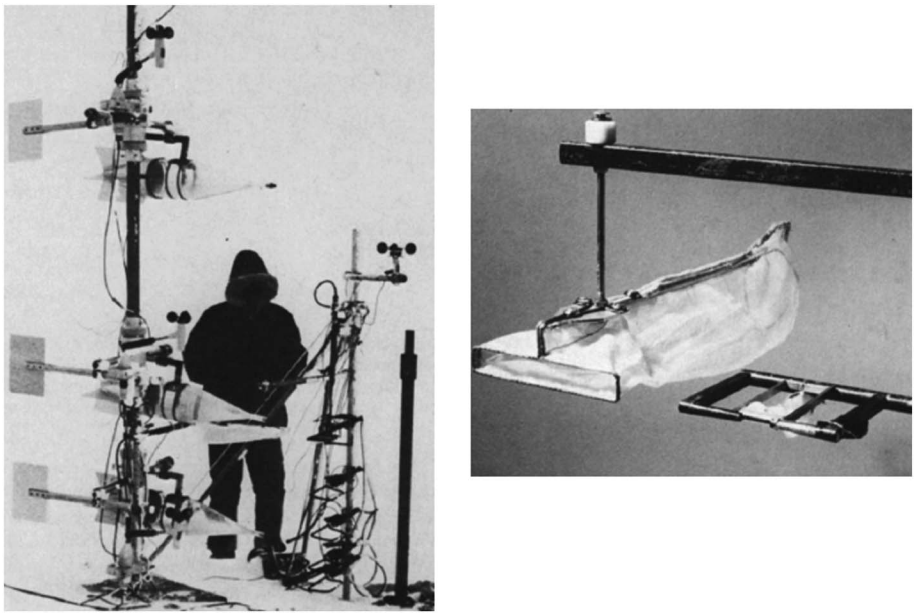

Figure 23. (left) "Rocket-type" Fohn traps and (right) sock traps. One sock trap is installed in front of an optical blowing snow device [from *Schmidt et al.*, 1984].

Using a mechanical trap, the mass flux of blowing snow is determined by measuring the mass of snow particles m_s entering a known area A_c over a time interval t_c, thereby determining the overall mass flux q_m (kg m^{-2} s^{-1}). Concomitant measurements of the mean wind speed $\bar{c}_w$ with an anemometer over the time of measurement allows for calculation of the blowing snow mass concentration (flux density) $\bar{\rho}_p$:

$$q_m = \frac{m_s}{t_c A_c} = \bar{\rho}_p \bar{c}_w.$$

Mellor [1960] describes a rocket-type trap consisting of a cylinder with fins. The fins helped to minimize local disruption of the airflow. *Budd et al.* [1966] used this trap to collect blowing snow in Antarctica along with a similar style of trap; this trap had a "distorted body" and was referred to as a "Williams special." *Fohn* [1980] modified the Mellor trap, choosing Plexiglas as the body material so that the trap could be visually checked for blowing snow particles. The center part of the gauge was elongated by 10% relative to the Mellor design and the shape changed slightly to ensure that snow could be efficiently collected. *Fohn* [1980] also used a small glass container to collect snow at distances close to the snow surface. These measurements enabled an understanding of the physics associated with blowing snow transport at different heights above the snow surface.

Takeuchi [1980] used a fabric bag trap to collect snow. The trap was mounted on a post that positioned the orifice of the trap at a fixed distance above the snow surface. *Schmidt et al.* [1984] and *Brown and Pomeroy* [1989] used similar "sock traps" to measure blowing snow along with the Fohn trap.

Jairell [1975] describes a mechanical trap gauge composed of a rocket-type turning assembly that collected blowing snow particles into a reservoir created from a weighing-type precipitation gauge installed beneath the ground surface. *Schmidt et al.* [1982] later improved the design of this device and used a plastic bucket situated on an electronic weighing scale to determine the mass m_s of blowing snow particles. This device eliminated the need for human measurements of the mass of collected snow particles. A major disadvantage of all mechanical trap gauges is the possible sublimation of trapped blowing snow after collection. This occurs for sock traps and is also briefly discussed by *Jairell* [1975].

Bolognesi [1995] describes the use of a mechanical trap referred to as the "driftometer." This device consisted of a container to which was attached a curving access tube. Blowing snow particles are admitted into the tube and fall into the container. Use of the driftometer in Switzerland is mentioned by *Chritin et al.* [1999].

2.15. Optical Blowing Snow Measurement

Optical blowing snow measurement devices ("particle detectors") consist of a light source situated at an offset distance to a detector. The light beam is interrupted by a blowing snow particle. The idea is conceptually

similar to an "electric eye" used to count objects passing over a conveyor belt or safety mechanisms installed in automatic sliding doors. Particle counter devices have used either incandescent light sources or light emitting diodes (LEDs) to produce a light beam. Unlike blowing snow measurement by mechanical trap devices (section 2.14), particle detectors do not rely on the emptying of a container and thereby permit rapid measurements of blowing snow. These measurements can be efficiently sampled by electronic circuits at a higher temporal rate than the mechanical devices, thereby permitting the mass flux of blowing snow to be measured on the same time step as a mathematical model of blowing snow.

Landon-Smith et al. [1965] indicate that particle detectors for measuring blowing snow were reported in the Russian literature by the early 1960s. *Landon-Smith et al.* [1965] used a light bulb and a photoresistor situated on opposite sides of a mounting frame to measure blowing snow flux density. Empirical calibration of the sensing system was conducted with blowing snow traps, and a theoretical procedure was also presented based on the physics of light scattering by the snow particle. The gauge output was considered to be accurate for blowing snow flux densities below 30 g m^{-3} and could be calibrated for a reference height above the snow surface. Errors in determination of flux density ranged between −20% and 30% at distances other than the calibration height.

Sommerfeld and Businger [1965] measured blowing snow flux density using a light bulb and a photoresistor situated on the same side of a mounting frame. The light beam was reflected by a prism situated on the other side of the frame. Similar to *Landon-Smith et al.* [1965], variability in light source intensity was automatically calibrated using a bridge circuit. The average drop in light intensity caused by blowing snow was recorded by a strip chart recorder and related to the density of snow particles in the air medium by an empirical calibration curve determined from falling snow particles in a cold room. Due to the sensitivity of the electronics and the shielding of the optical detector from blowing snow, the device was only usable for wind speeds between 10 m s^{-1} and 15 m s^{-1}.

Based on work by *Hollung et al.* [1966] and *Rogers* [1968], *Schmidt and Sommerfeld* [1969] presented a gauge with a single light bulb and two phototransistors situated behind slits at an offset distance from the light bulb. Calibration of the device for temperature changes in the measurement electronics as well as for measurements of particle size, particle size distribution, and speed were reported by *Schmidt*, [1971a, 1971b]. These calibration procedures utilized a spinning wire device as well as a lab setup involving particles dropped past the sensor assembly. *Schmidt* [1987] later provided a complete description of the circuit design, operation, and calibration of this particle detector.

The system was later updated by *Schmidt* [1984] to use an analog-to-digital converter (ADC) and signal processing with a microcontroller and a computer to determine snow particle size, particle size distribution, and speed. Detectors situated in two spatial planes showed that the system did not rely on preferential particle orientation. The error in measuring the size of snow particles was ±15% within each size class. The smallest resolvable snow particle size was between 0.05 mm and 0.06 mm. *Schmidt et al.* [1984] found that compared with a mechanical flux trap, the new system underestimated blowing snow mass flux by 20%. *Schmidt* [1987] deployed a number of these systems to measure snow blowing from a forest canopy. *Wendler* [1989] independently built a version of the system and deployed it in Antarctica.

Koh and Lacombe [1986] describe a snowfall gauge similar to previous optical blowing snow measurement devices. An infrared light emitting diode (LED) and a detector placed at an offset distance behind a slit were used to determine the snowfall rate.

Gubler [1981a] developed a particle detector gauge that utilized a collimated LED (as a light source) with a collimated infrared transistor (as a detector). The transistor was situated at an offset distance to the LED. The use of infrared light reduced error due to ambient light. A stabilized voltage source was used to drive the LED, but *Gubler* [1981a] notes that a constant current source would have ensured greater stability. The system was able to detect particles greater than 50 μm in diameter and was able to determine the mass flux of blowing snow between 0.1 g m^{-2} s^{-1} and 100 g m^{-2} s^{-1}. Particle size distribution was determined using five separate classes. The maximum error in a measurement was ±50%, with systematic errors ranging between −39% and +26%.

Pomeroy et al. [1987] and *Brown and Pomeroy* [1989] placed a LED at an offset distance to a fiber optic cable, on the end of which was a pinhole cap (Figure 24). Further theory on the device can be found in the report by *Pomeroy and Male* [1985]. The fiber optic cable helped to minimize the effects of the measurement

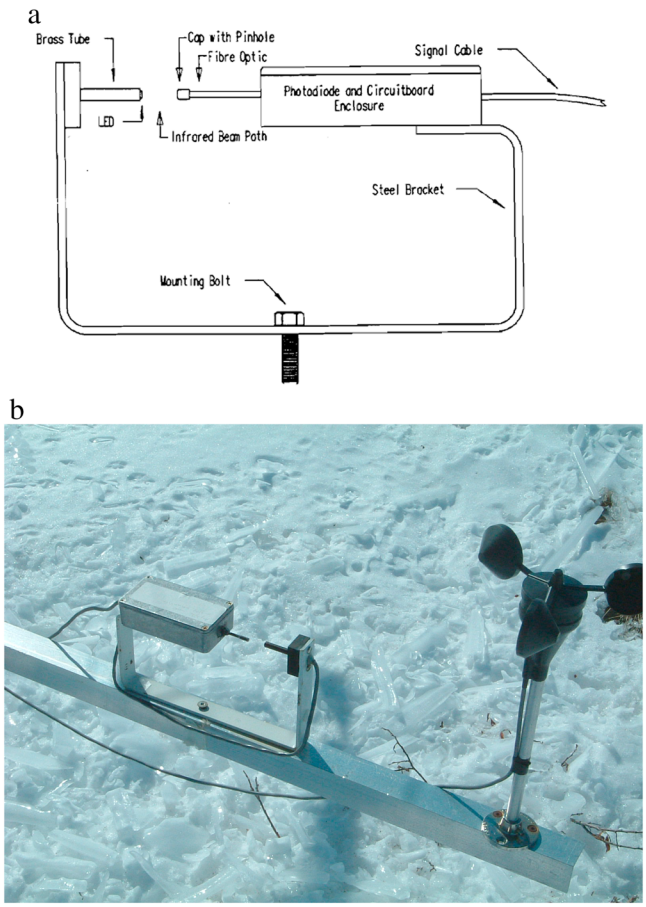

Figure 24. Blowing snow particle detector. (a) Diagram from *Brown and Pomeroy* [1989]. (b) Particle detector and anemometer deployed at a field site in northern Canada.

system on the flow of blowing snow. The fiber optic cable was attached to a phototransistor that was spectrally matched to the LED to reduce the effects of ambient light. This particle detector could detect snow particles with a minimum radius of 22.5 μm. Mie electromagnetic scattering theory was used to relate particle counts to the blowing snow mass flux. Field tests showed that the mean difference between particle detector and mechanical trap measurements of blowing snow mass flux was 2.11 g m^{-2} s^{-1}. Simple equations were derived relating particle counts to mass flux in the snow saltation and suspension layers above the snow surface. The instrument by *Brown and Pomeroy* [1989] is the only known particle detector that utilized a fiber optic cable. The device was used for validation of a blowing snow model that provided a physically accurate means of determining the mass flux of blowing snow [*Pomeroy et al.*, 1993]. *Leonard et al.* [2012] used the *Brown and Pomeroy* [1989] particle detector along with other blowing snow measurement sensors to suggest that the initiation of blowing snow transport is related to snow particle size.

Sato et al. [1993] used a laser diode and detector with a collimator lens. The rest of the system was similar to *Schmidt* [1984], with some modification to the measurement electronics. The system output was a pulse-density modulated bitstream that allowed a snow particle size distribution to be determined with 25 to 100 classes. Theory adapted from *Brown and Pomeroy* [1989] was used in the calculation of mass fluxes. The mean error in determined mass flux was approximately 20%.

Optical disdrometers have been used for measurement of blowing snow. The disdrometer consists of one or more video cameras situated so that a light source can illuminate blowing snow particles. Use of the disdrometer in this fashion is similar to the Multi-Angle Snowflake Camera device that measures falling snow (section 2.5). *Hershey and Osborne* [2006] used a disdrometer composed of multiple cameras to measure blowing snow particle size. Flood lights placed in front of each camera illuminated the camera assembly field of view. *Gordon and Taylor* [2009] utilized a video camera and lens assembly at an offset to a light source.

The measurement system geometry is conceptually similar to other systems such as used by *Brown and Pomeroy* [1989], but the detector is a video camera. The particle velocity, shape, size distribution, and number of particles could be detected by the system. *Gordon et al.* [2009] report the use of a single video camera with an illumination source situated behind the camera so that particle mass density could be measured by backscattering of light. The cameras are available commercially, but most systems have been assembled by individual investigators.

2.16. Acoustic Blowing Snow Measurement

Acoustics has been used to determine the mass flux of blowing snow. Acoustic blowing snow measurement sensors consist of a pipe into which is placed a microphone or similar pressure transducer. Snow particles in saltation and suspension above the snow surface impact the pipe, inducing acoustic waves that are detected by the microphone and digitized using an analog-to-digital converter (ADC) to create a time domain signal. An empirical relationship developed from calibration data can be used to relate signal amplitude to blowing snow mass flux.

Font et al. [1998] describe an acoustic sensor consisting of a single pipe installed vertical to the snow surface. The pipe was chosen to be a length greater than the maximum snow depth at a field site. Similar to a snow ruler, snow accumulates around the pipe. Using a pipe with a length of 2 m, *Michaeux et al.* [2000] placed the device in a wind tunnel and used artificial snowmaking equipment to create snow particles that impacted the pipe, thereby creating a signal suitable for empirical calibration. The initiation of blowing snow events could be determined by the device. Noise from wind can be removed using a low-pass filter [*Lehning et al.*, 2002].

The FlowCapt sensor [*Chritin et al.*, 1999] is available commercially from ISAW (Tannay, Switzerland) and utilizes a pipe installed vertical to the snow surface on a mounting structure. The pipe can be coated with Teflon to prevent ice accretion [*Cierco et al.*, 2007]. Multiple pipes can also be installed at different heights above the snow surface to measure the mass flux of blowing snow [*Cierco et al.*, 2007; *Naaim-Bouvet et al.*, 2010]. Wind tunnel calibration is required to relate the mass flux of blowing snow to the microphone signal.

Calibration of the FlowCapt sensor can be conducted using plastic particles [*Chritin et al.*, 1999], snow from artificial snowmaking equipment [*Lehning et al.*, 2002], or other organic particulate matter [*Cierco et al.*, 2007]. Alternately, calibration can also be accomplished using data from optical devices deployed alongside the FlowCapt [*Bellot et al.*, 2011]. *Lehning et al.* [2002] present a test apparatus utilizing a laser to increase the precision of the calibration procedure. *Cierco et al.* [2007] calibrated the FlowCapt using mass flux equations of blowing snow.

Lehning et al. [2002] and *Naaim-Bouvet et al.* [2010] have discussed the difficulties of FlowCapt calibration indicating that innovative procedures are required to increase the accuracy of this measurement instrument. This is because some measurements made with the device can have an error greater than 1 order of magnitude. If the signal from the microphone exceeds 2.5 V, clipping of the signal will occur. This limits the FlowCapt device to measure a maximum snow particle flux of 1875 g m^{-2} s^{-1} [*Cierco et al.*, 2007].

Tüg [1988] describes a sensor to perform particle counting of blowing snow. The sensor and associated measurement electronics is placed into a rotating enclosure shaped similar to an anemometer vane. The sensor is situated at the end of the vane facing the wind. Snow particles transported by blowing snow impact the sensor. The sensor assembly is composed of a piezoelectric transducer situated in the middle of two cylindrical enclosures. The impacting snow particles induce pressure waves in the enclosures, causing acoustic resonance to occur. A histogram of particle counts as a function of amplitude can be determined for an uncalibrated detector, although some empirical calibration may be utilized to correct for sensor response time. The error in determining particle count rate has been estimated to be within 5% to 10%. Errors occur due to the cross section of the detector and the hardness of snow particles. Snow particle hardness may influence the acoustic response of the impacting snow particles or cause fragmentation of the particles.

2.17. Infrared Thermometers and Cameras

Infrared (IR) thermometers and cameras measure longwave radiation emitted by a surface [*Bates and Gerard*, 1989]. These devices have been used to record snow surface temperature and temperatures in a snowpit [*Shea et al.*, 2012a], the temperature of snow and shrubs [*Pomeroy et al.*, 2006], and to measure the temperature of snow and tree trunks in a forest [*Pomeroy et al.*, 2009b; *Howard and Stull*, 2013]. Placed into a radiation shield facing the snow surface, an IR thermometer can be used to measure snow surface temperature [*Kondo and Yamazawa*, 1986]. It is crucial to realize that IR thermometry measures only the "skin" temperature of

the snow surface from layers less than a few microns and cannot measure snowpack interior temperatures. Nevertheless, the use of IR thermometers have enabled a better understanding of energy exchange processes and how these processes influence snowmelt [*Pomeroy et al.*, 2006].

The Stefan-Boltzmann law states that the temperature T (Kelvin) is related to the emitted power per area P (W m^{-2}) and the emissivity ϵ of a snow surface by

$$T = \left(\frac{P}{\epsilon\sigma}\right)^{1/4}.$$

The Stefan-Boltzmann constant is $\sigma = 5.67 \times 10^{-8}$ W m^{-2} K^{-4}. The P is measured by the IR camera, and temperature T is calculated [*Shea and Jamieson*, 2011].

The emissivity ϵ is a nondimensional number that models the difference between a blackbody emitter and a graybody emitter. For a blackbody, $\epsilon = 1.0$. The emissivity of snow varies between 0.98 and 0.99 as a function of the viewing angle [*Dozier and Warren*, 1982; *Marks and Dozier*, 1992]. Emissivity was found by *Hori et al.* [2006] to be dependent on the snow particle size, wavelength of light, and viewing angle, with most fine-, medium-, and coarse-grained snow having $\epsilon > 0.98$. The emissivity only ranged between 0.90 and 0.98 for Sun-crusted snow associated with the observation of specular reflection of thermal infrared radiation from the snow surface. Moreover, although the emissivity is dependent on the wavelength, it is normally taken as an effective constant over the operating wavelengths of an IR camera, which is nominally 7.5 μm to 13 μm [*Schirmer and Jamieson*, 2014].

Pomeroy et al. [2006] noted that for measuring the temperature of shrubs and snow, an IR camera (FlexCam®, Minneapolis, MN, USA) had an absolute measurement error of 2°C, but a measurement error of only 0.2°C between pixels in an image. The resolution of the image was 120 × 120 pixels. The experiments conducted by *Pomeroy et al.* [2006] quantified the transfer of longwave radiation from shrubs to snow. Using the same thermal camera and additional radiation balance measurement instrumentation, *Pomeroy et al.* [2009b] showed that a large amount of energy for snowmelt can be provided from longwave radiation associated with the heating of tree trunks in a forest.

Shea and Jamieson [2011] used a FLIR B300 camera (FLIR Systems, Wilsonville, Oregon, United States) with a resolution of 320 × 240 pixels and a 25° angle of view to measure spatial distributions of temperature at the snow surface and within snowpits; the camera had an accuracy of <2°C, with a 0.05°C accuracy between pixels. To obtain accurate thermal images, the camera had to be calibrated using the Stefan-Boltzmann law with an assumed emissivity. As a practical approximation, thermal images of gold and aluminum foil at the field site can be used to calibrate the image to account for the effects of atmospheric radiation on the measured thermal temperatures [*Shea and Jamieson*, 2011].

For imaging of snow at <1 m distances to the camera, the error in temperature can be <0.1°C due to the small influence of water vapor on the temperature of the surrounding air between the camera and the snowpack. This error rises to ~4°C if the camera is situated 1 km away from the snowpack due to errors introduced by a drop of light intensity associated with the inverse square law and local variations in air temperature and density. Another source of error in the measurements is the presence of a human operator holding the IR camera. The heat radiated by a nearby human body can cause rapid changes in snowpack temperature ranging between ~1°C and as high as 10°C within a time period of seconds to minutes after the snowpit has been created [*Shea and Jamieson*, 2011]. Using an IR camera, *Shea and Jamieson* [2011] were able to track changes in snow temperature only a few minutes after the occurrence of a slab avalanche.

Shea et al. [2012a] further explored the ability of an IR camera to measure snowpit temperatures. The FLIR B300 camera was used during these experiments. When used for IR measurements of snow, lens distortion of the camera was found to introduce an error of ~0.03°C over the entire image. Snowpack layers of less than 2 mm thickness could be observed in the image. *Shea et al.* [2012a] found that handheld operation of an IR camera presents a number of challenges, since the camera should be held at an angle of normal incidence to the snowpit surface and the snowpit images should be ideally taken within 90 s of exposing the pit wall to environmental and anthropogenic sources of radiation. Since the snowpit is created with a shovel, small irregularities in the snowpit wall created during digging of the snowpit introduces a source of error into the measurements. Using the IR imager, a subsurface heating layer beneath the snow surface was identified by *Shea et al.* [2012b], independently confirming the observations by *Brandt and Warren* [1997].

Shea et al. [2012b] later used a FLIR P660 camera with a resolution of 240 × 320 pixels, a 0.03°C accuracy between pixels, and a 18° × 24° angle of view. Thermal imaging of a snow pit was once again associated with errors that occur due to heating of the exposed snow surface by shortwave and longwave radiation, as well as heating due to the presence of a nearby human operating the IR camera. Using the IR camera, *Shea et al.* [2012b] were able to measure temperature gradients in the snowpack and relate these temperature gradients to snow particle size and metamorphism.

Using an IR camera, *Shea et al.* [2012c] showed that ice crust layers within the snowpack experience rapid changes in temperature over the course of a day. The temperature of the ice crust in the snowpack was observed to be warmer or colder than the temperature of the snowpit. These changes were exhibited over a time period of only a few hours.

Hori et al. [2013] used a FLIR SC660 camera with a resolution of 640 × 480 pixels to obtain images of a snow-covered field at a site near Hokkaido, Japan; the camera had an accuracy of < 2°C, with a 0.045°C accuracy between pixels. *Hori et al.* [2013] determined that the temperature of the snow surface showed low variability immediately after a fresh snowfall. During the day, higher levels of solar insolation and small differences in metamorphism and snow surface topography caused greater variability in snow surface temperatures. Snow metamorphism and localized melting of snow were also observed at the snow surface. At night, small patches of snow remained at a higher temperature than the surrounding snow surface. *Hori et al.* [2013] also presented a model of snow surface emissivity, finding that snow metamorphism can change the emissivity of snow.

Schirmer and Jamieson [2014] showed that imaging of snowpits by an IR camera is complicated by energy fluxes from longwave and shortwave radiation, as well as turbulent transfer of heat to the sides of the snowpit during windy conditions. Video was captured by an IR camera at frame rates between 1 Hz and 10 Hz. Scour marks created along the sides of the snowpit were visible in the IR image. *Schirmer and Jamieson* [2014] conducted an experiment in a cold room freezer, showing that in a localized area around these scour marks, snow temperature was modified by >1°C only 30 s after a large snow sample had been placed in the freezer. *Schirmer and Jamieson* [2014] also found that by 4 min after the sides of a snowpit were exposed in the field, up to a 2°C change in snow temperature was observed.

Experiments conducted with an IR camera have demonstrated the versatility of this technology with respect to measuring the snow surface temperature and understanding snowpack energetics. However, because of the great uncertainty in measurements of snowpit wall temperatures with IR as clearly shown by *Schirmer and Jamieson* [2014] and the destructive nature of snowpit-based measurements, there remains a need for noninvasive measurement of snow temperature beneath the surface of the snowpack.

2.18. Photogrammetry and Photography

Photogrammetry is the use of two cameras situated at a known offset distance to determine the depth of objects in a scene. This method has been applied to measure snow depth using cameras situated on airplanes and satellites and has also been used in near-surface photography. In a similar fashion to the laser ranging method, images of the landscape before and after snow accumulation are required. The cameras are situated so that there is overlap between the images. Depth in the image pair is determined using linear algebra equations that relate points on each image to the camera positions [*Smith et al.*, 1967a; *Cline*, 1993]. The resulting snow depth is used in a similar fashion to lidar applications (section 2.12). Recent research has utilized algorithms that are able to automatically extract snow depth from overlapping images taken using remote sensing platforms and represents a significant breakthrough in the measurement of snow depth at centimeter resolutions [*Nolan et al.*, 2015].

Blyth et al. [1974] took photographs at two locations facing the side of a hillslope in an upland area near Plynlimon, Wales. The camera locations were situated 30 m apart on a vertical line, and 2.5 m high markers were used to delineate the corners of a trapezoidal area spanning 4 ha. A stereoplotter normally used to measure depth from air-photo pairs was used to determine distances to the snow surface. Comparison with depth rod measurements revealed that this method could determine snow depth within 10% error.

Vallet [2001] and *Skaloud et al.* [2005] described a single-camera system used to measure snow depth. The system was mounted on the side of a helicopter for deployment near the ground and in Alpine areas. Placed near the single camera was a high-accuracy differential GPS system, inertial measurement sensors, and a laser

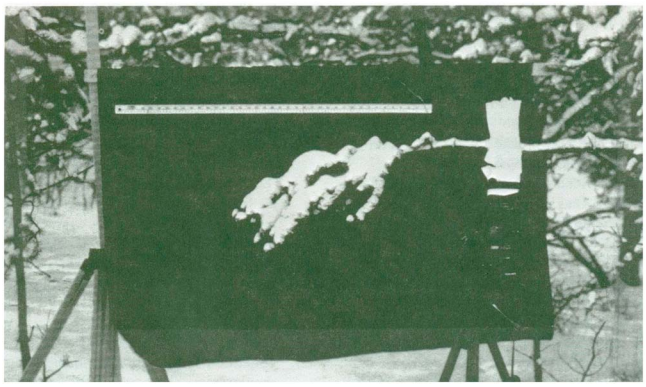

Figure 25. Setup used for the fractal analysis of snow clumps [from *Pomeroy and Schmidt*, 1993].

ranging device. The position of the camera relative to a digital elevation model (DEM) was used to obtain estimates of the volume of snow for an avalanche control application.

Photography has been used to measure canopy cover and snow-covered area. For example, *Codd* [1959] showed how hemispherical photography can be used to obtain canopy cover measurements for snow science applications. *Pomeroy and Schmidt* [1993] photographed snow clumps on branches and used image analysis to determine a fractal scaling coefficient for use in the calculation of intercepted snow sublimation, thereby increasing the accuracy of snow sublimation calculations (Figure 25). *Essery et al.* [2008a] used a digital camera fitted with a hemispherical (fisheye) lens to calculate the fraction of the sky (expressed as the "sky view factor") not obscured by a forest canopy so that longwave radiation incident on snow beneath the canopy could be calculated. *Debeer and Pomeroy* [2009] used near-surface photography to measure snow-covered area (SCA). The investigators set up a single camera facing a cirque on the side of Mount Allen in the Rocky Mountains of Alberta, Canada. Using a DEM of the area and the known position of the camera, a software tool developed by *Corripio* [2004] was used to extract SCA from the single-camera image to quickly obtain an accurate measurement so that snow ablation could be modeled.

The Photo Rectification And ClassificaTIon SoftwarE (PRACTICE) toolkit is a software package written in MATLAB that can be used for time-lapse camera applications [*Härer et al.*, 2013]. The software uses a DEM as input, and the camera position can be automatically determined from the images and from "ground control points" as known positions on the ground surface. Maps of snow-covered extent can be automatically obtained.

Construction of time-lapse camera systems suitable for deployment in cold environments have been discussed by *Banner and Van Everdingen* [1979]; this technology was developed at the National Hydrology Research Institute of Environment Canada using military surplus Kodak KB9A 16-mm strike cameras. These cameras were later deployed by *Pomeroy and Schmidt* [1993] to record snow-covered area in a forest canopy over a cold boreal winter in northern Saskatchewan.

2.19. Radioisotope Devices

Active measurements of snow often use a radioisotope such as ^{60}Co or ^{137}Ce to produce gamma radiation [*Goodison et al.*, 1981]. The advantage of using ^{60}Co over other isotopes such as ^{65}Zn is that this isotope has a greater penetration of snow [*Gerdel et al.*, 1950], thereby allowing for a larger sampling area to be sensed [*Armstrong*, 1976]. The ^{60}Co isotope also emits a narrow-wavelength spectrum of radiation that can be empirically related to snow density with less error than an isotope with a broader wavelength spectrum [*Gerdel et al.*, 1950]. The source is collimated so that the radiation escapes from a slit in a lead box. A complete design for the collimator is presented by *Gerdel* [1952].

Two common active designs exist: either the source and a detector are situated above and below the snow surface [*Gerdel et al.*, 1950], or in two parallel metal tubes installed perpendicular to the ground so that snow density can be measured by moving the source and detector vertically [*Armstrong*, 1976; *Smith and Halverson*, 1969]. Movement of the source and detector is accomplished using an electric motor and mechanical assembly [*Paulin*, 1978; *Smith et al.*, 1967a]. The disadvantage of using the above-and-below configuration is that snow profiles cannot be recorded [*Smith et al.*, 1967a]. *Davis* [1973] noted that the above-and-below configuration was used at a field site in California with a radioactive source buried under the snowpack and a detector

situated on an airplane passing over the site. Measurement of blowing snow mass flux was once attempted using radioactive sources of beta radiation, but these experiments were not successful due to the similarity of attenuation by blowing snow and changes in air density [*Landon-Smith et al.*, 1965].

Portable versions of active sampling gauges were once utilized by the Division of Hydrology at the University of Saskatchewan [*Pomeroy*, 1988], and the parallel tube device was deployed at the Bad Lake Field Site near Rosetown, Saskatchewan [*Gray et al.*, 1970b, 1970a]. Laboratory testing and calibration of the parallel tube device at the University of Saskatchewan were reported by *Olfert* [1970] and *Gray et al.* [1970b]. The spacing between the parallel tubes can range from 30.5 cm to 61 cm center to center [*Gray et al.*, 1970b, 1970a]. Figure 26 shows a mechanical apparatus setup of a parallel tube device being calibrated in a lab at the University of Saskatchewan and then deployed at the Bad Lake Field Site near Rosetown, Saskatchewan, Canada.

An increase in the SWE and density of snow results in a decrease of the number of particles per unit time transmitted through the snowpack from the radioactive isotope to the detector. Empirical equations are used to relate particle counts to SWE or snow density. *Gerdel et al.* [1950] used Beer's law with an empirically determined extinction coefficient. *Smith et al.* [1965] used a simple logarithmic relationship.

Geiger-Muller tube [*Armstrong*, 1976] and sodium iodide tube [*Smith et al.*, 1965] detectors have been used to detect the particles. The advantage of using a Geiger-Muller tube is operational stability [*Blincow and Dominey*, 1974] due to temperature shifts in sodium iodide tubes. Cosmic background radiation particle counts are required to completely correct for errors in received counts [*Gerdel*, 1952]. Empirical calibration may be necessary before each run to correct for temporal changes in the system [*Howe and Houghton*, 1968]. *Gray et al.* [1970a] found that calibration is essential at least once every five readings. An empirical calibration procedure to correct for temperature changes in the metal tubes of the active gauge was proposed by *Gray et al.* [1970a].

The accuracy of such active gauges is within 1% to 7% of SWE measured using gravimetric techniques [*Blincow and Dominey*, 1974; *Pyper*, 1962; *Smith et al.*, 1965]. Inherent difficulties in the deployment of the system arise due to temperature shifts in the electronics and snowmelt occurring around tubes buried in the snow [*Smith et al.*, 1967]. Uneven snow drifts can also form around the tubes, influencing the accuracy of the measurement and making detection of the snow surface more difficult. For an active gauge with two tubes, misalignment of the source and receiver can also occur [*Kattelmann et al.*, 1983]. Compared to snow pillows, daily estimates of SWE using active radioisotope gauges show greater variability in measurements [*Ord*, 1968].

The backscattering method is an active measurement method that uses only one tube containing a source and a receiver [*Anderson et al.*, 1965; *Morris*, 2008a]. A gauge of similar design was once available commercially as the Digiray Portable Profiling Snow Gauge PSG-1 [*Blincow and Dominey*, 1974]. Initially, a core of snow is extracted from the snowpack [*Young*, 1976]. The single-tube device is then inserted into the hole created by removal of the snow sample. A source containing ^{85}Kr [*Blincow and Dominey*, 1974], ^{185}Cs [*Anderson et al.*, 1965] or ^{241}Am [*Hawley and Morris*, 2006; *Morris and Cooper*, 2003] produces radioactive particles that escape through slits in a lead collimator into the snowpack [*Blincow and Dominey*, 1974]. The backscattered particles from the snowpack are sensed by a Geiger-Muller tube receiver. For the PSG-1, the sampling volume is a torus situated around the tube with a vertical extent of 5 cm and a horizontal extent of 30 cm [*Young*, 1976]. Insertion of the single-tube device into a provided "calibration can" containing a substance of known density allows for counts of backscattered particles to be related to snow density [*Blincow and Dominey*, 1974] or empirical calibration is performed using gravimetric samples of snow density at a field site [*Schytt et al.*, 1962]. Recently, *Morris*, [2008a, 2008b] presented a nonempirical model for determining snow density using the backscattering method. The model is based on the physics of backscattered particles from snow and does not require empirical relationships.

The backscattering method was tested in the mountains of California [*Anderson et al.*, 1965; *Gay*, 1962] and on glaciers in Sweden [*Schytt et al.*, 1962]. The investigators found that errors in snow density determination were greatest near air-snow [*Anderson et al.*, 1965; *Schytt et al.*, 1962] and ground-snow [*Anderson et al.*, 1965] interfaces. *Young* [1976] tested the PSG-1 device on Peyto Glacier in the Canadian Rockies, finding that depth-averaged densities agreed to within 5% of gravimetric measurements. The densities of individual layers in the snowpack did not necessarily coincide with gravimetric measurements due to the sampling volume of the detector and lags in particle counts associated with vertical movement of the sensing apparatus. *Gerland et al.* [1999] used the backscattering method to measure snow density in Antarctica, finding an error of 2%

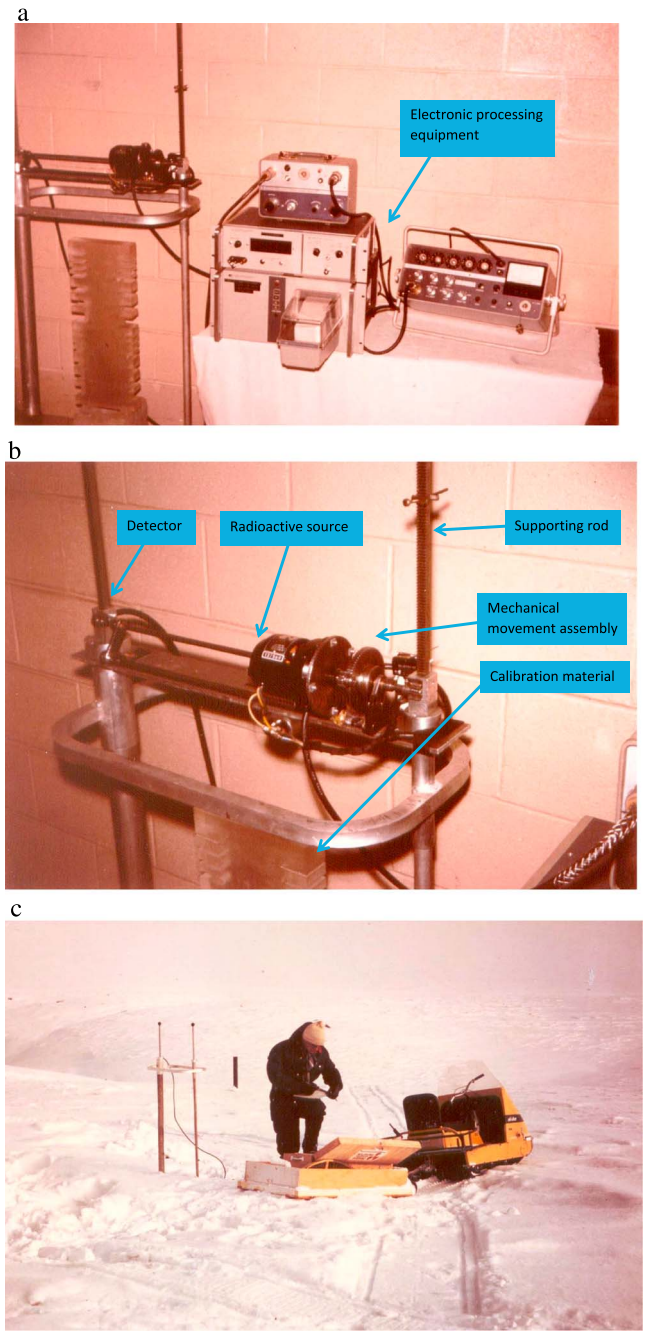

Figure 26. (a, b) Pictures of a parallel tube gamma attenuation device being calibrated in a laboratory at the University of Saskatchewan. (c) Deployment of the device at the Bad Lake Field Site [from *Olfert*, 1970].

comparison with gravimetric estimates of snow density. Measurements of snow density on the Devon Ice Cap [*Morris and Cooper*, 2003] and the Greenland ice sheet [*Hawley and Morris*, 2006] in Nunavut, Canada, showed that a disadvantage of the backscattering method was "smoothing" of the density profile due to the size of the backscattered sampling volume.

Due to environmental and human health hazards associated with radioisotopes, active gauges are presently not used in an operational context [*Pomeroy and Gray*, 1995] despite "acceptable risk" arguments once used to rationalize the deployment of such instrumentation [*Gerdel et al.*, 1950; *Morrison*, 1976]. However, active gauges are still used for research applications [*Morris and Cooper*, 2003; *Hawley and Morris*, 2006]. The devices were initially invented in the twentieth century to quickly measure SWE at a field location without the use of gravimetric instrumentation.

Figure 27. Photograph of GMON installed at a field site in the Rocky Mountains.

Passive radioactivity gauges work in a similar fashion to the active gauges but rely on the natural background radiation in the soil to provide a source of gamma radiation. The passive radioactivity gauge is situated in the air above the snow surface as a stationary device. Although this technique is very safe, background radiation counts at the same field site during the snow-free season are required and the gauge must count the number of particles accumulated over daily time periods. This does not permit "on-demand" measurements of SWE. As the SWE and snow depth increases, particle attenuation increases and the signal-to-noise ratio decreases. Care must be taken in evaluating SWE from natural soil emissions where soil moisture changes over the winter or spring as gamma emissions from soil are influenced by soil moisture content. The gamma radiation particles are often highly attenuated by the snow, thereby limiting the snow depth and SWE that can be determined by this measurement technique [*Bissell and Peck*, 1973]. Passive radioactivity gauges can also be used for measuring SWE from aircraft. For this application, the mass of the air beneath the aircraft must be taken into consideration as a variable affecting attenuation and background radiation counts are determined from flight paths over the same area during the snow-free season [*Carroll and Carroll*, 1989].

Morrison [1976] briefly describes a passive radioactivity gauge being developed for prairie hydrology applications. The gauge was able to measure snow with SWE less than 50 mm and a depth less than 150 cm. The GMON (GammaMONitor) SWE gauge (Campbell Scientific Canada, Edmonton, Alberta) is a stationary device that can measure up to 600 mm of SWE using the passive radioactivity method [*Wright et al.*, 2011]. SWE measurement by this gauge is limited by the attenuation of radioactive particles by the snow and the sensitivity of the detector. The gauge provides a method of continuously monitoring SWE for input into models of snowpack evolution. Moreover, temporal measurements of SWE can be taken at a higher frequency than snow tube sampling and are thereby better suited for snow ablation and runoff modeling for scientific or hydrological prediction applications. When suspended 3 m above the ground, the effective measurement area of the gauge is due to collimation of the detector. Aside from particle count rates during the snow-free season, the empirical equation used to determine SWE also requires measurements of soil moisture prior to winter freeze-up [*Wright et al.*, 2011]. A photograph of the GMON installed at a field site is shown in Figure 27.

2.20. Chemical Liquid Water Content Measurements

Chemical measurement of liquid water content relies on physical changes in the concentration of ions in a snow sample. These methods involve the extraction of a sample of snow from a snowpit or from the snow surface and can be used for calibration or comparison to other methods of liquid water content measurement.

Davis and Dozier [1984] added a fluorescent dye (Rhodamine WT) to a snow sample and then measured the fluorescent intensity of the mixture using a chemical fluorometer. The intensity of the sample was related to water saturation of snow using an empirical curve and chemical mixing formulas.

Perla and LaChapelle [1984] and *Davis et al.* [1985] conducted experiments in the Canadian Rockies to develop an acid dilution technique. A solution of hydrochloric acid was added to a snow sample, and an electrolytic

conductivity meter was used to measure the conductivity of the resulting solution. The conductivity was then related to snow wetness.

Because the acid dilution technique does not involve the use of empirical curves, it can be used to calibrate capacitor cells [*Perla and Banner*, 1988]. The error in dilution methods is ±1.5% liquid water content [*Davis et al.*, 1985]. Although these methods can be used to measure snow wetness in a snow pit at a field site, the preparation and mixing of chemicals at a remote location can be tedious and time consuming and is therefore not often used.

2.21. Calorimetric Measurements

Calorimetry is used to measure the liquid water content of snow. A calorimeter consists of an insulated container into which is placed a snow sample. The insulated container is fitted with a temperature sensor to measure internal temperature. The mass of the snow sample is determined before a liquid is added to the insulated container. Stirring of the sample occurs over the time of measurement to ensure that heat is evenly distributed between the liquid and the snow sample. A change in heat content due to a change in phase of the mixture is related to the liquid water content of the snow sample using a heat balance equation. Empirical calibration coefficients in the heat balance equation can correct for heat loss by the insulated container. Freezing, melting, and chemical calorimeters have been used to measure snow [*Boyne and Fisk*, 1990; *Jones et al.*, 1983]. In a similar fashion to the chemical methods of liquid water content (section 2.20), the time taken for measurement and the equipment used creates logistical problems at field sites.

Freezing calorimetry requires a liquid freezing agent that is held at a temperature between −40°C and −50°C. This is accomplished by keeping the freezing agent in a portable cooler that is packed with dry ice and taken to the field site. Toluene has been used as a freezing agent, but this is a hazardous chemical, and so silicone oil can be used instead. After addition of the freezing agent to the insulated container, the container is shaken by hand and a change in temperature is recorded in 30 s intervals for approximately 10 min. The error in determination of liquid water content using freezing calorimetry is ±1% to ±2% [*Jones et al.*, 1983], but the method can be inaccurate due to uneven transfer of heat between the snow sample and the freezing agent [*Fisk*, 1986]. Moreover, the specific heat of the silicone oil will often change between purchased bottles and must be measured before use in the calorimeter [*Boyne and Fisk*, 1990]. The presence of snow chunks in the sample can affect the measurement due to liquid water contained inside the snow chunk [*Boyne and Fisk*, 1987].

Melting calorimetry involves the addition of hot water to the snow sample. The hot water serves as a melting agent. The hot water can be directly added to the snow sample [*Halliday*, 1950; *Akitaya*, 1985; *Yosida*, 1967], or the water can be heated using an electric coil, which has an advantage of controlling the rise in temperature of the sample [*Brun*, 1989; *Halliday*, 1950]. *Brun* [1989] describes a melting calorimeter that uses a combination of calorimetry and dielectric techniques to measure liquid water content. The melting calorimetry method has better transfer of heat between the snow sample and the melting agent and is quicker than freezing calorimetry [*Fisk*, 1986]. The absolute measurement error in liquid water content ranges from ∼1% to ∼5% [*Halliday*, 1950; *Akitaya*, 1985; *Morris*, 1981].

Chemical methods involve the addition of a chemical to a snow sample. The chemical breaks intermolecular bonds holding the snow particles together and disperses ions and molecules into the solution, causing a resulting change in temperature. The use of methanol (alcohol) as a chemical agent has an absolute liquid water content measurement error of ∼1% [*Fisk*, 1986]. Because methanol is hygroscopic, a drying agent must be used to prevent water contamination during storage of the methanol solution [*Boyne and Fisk*, 1987]. *Morris* [1981] used a NaCl (salt) solution, finding that the measurement error in snow liquid water content was ±4% when the salt dissolved in solution did not exceed 5% by volume. *Bader* [1950] reported on the use of a NaOH (sodium hydroxide) solution as the chemical agent. *Boyne and Fisk* [1990] compared the alcohol and freezing calorimetry methods to dielectric techniques, finding that all methods had a maximum ±2% measurement error.

The irreducible liquid water content of a snow sample can be obtained by calorimetric measurements. The snow sample is first soaked in water, then drained in an insulated chamber, and kept at an isothermal temperature by an ice bath. The irreducible water content is then measured using a freezing calorimeter [*Coléou and Lesaffre*, 1998]. These techniques permit observations of the amount of liquid water that cannot be removed from a snow sample.

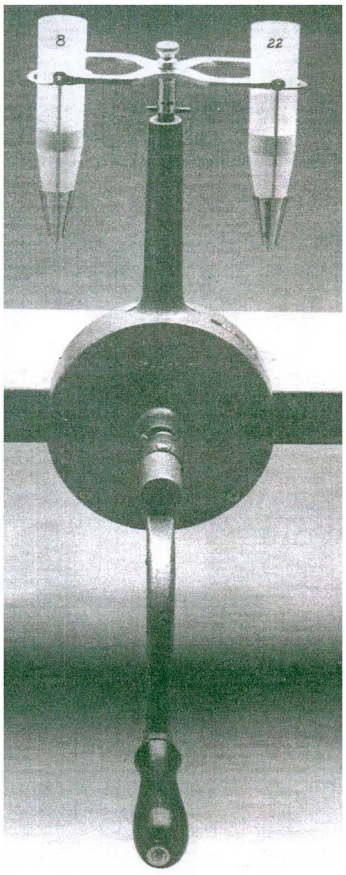

Figure 28. Centrifugal apparatus with sampler tubes [from *Jones*, 1979].

2.22. Centrifugal Measurements

Centrifugal methods (Figure 28) generally involve the spinning of a snow sample to separate out liquid water from the snow. This is accomplished by extracting a snow sample from the snowpack and placing the sample inside of a centrifuge that is often hand operated [*Carroll*, 1978]. A sieve inside of the sampler tube is used to separate the snow from the liquid water present in the sample [*Jones*, 1979]. Instead of a sieve, the sampler tube can be filled with an organic chemical that is not miscible with water [*Kuroda and Hurukawa*, 1954]. Despite possible errors associated with melting of the snow sample during handling [*Langham*, 1974], error analysis has shown a $\pm 0.7\%$ error in the determination of liquid water content [*Jones*, 1979]. The idea of using centrifugal methods is similar to blood fractionation by centrifuge used in medical lab testing and provides a means of comparison to calorimetric, chemical, or dielectric measurements.

Drawbacks of this method include melting that occurs due to friction and the incomplete extraction of all liquid water from the sample [*Colbeck*, 1978; *Jones et al.*, 1983]. This could be mitigated by repeated centrifuging [*Langham*, 1974]. Freezing calorimeter measurements of snow are considered to be more accurate than centrifugal measurements [*Jones*, 1979].

A procedure used to determine the tensile strength of a cylindrical snow sample has also been described by *Perla* [1969]. A cylindrical sample of snow is spun around an axis, and the rotational speed at snow sample failure is used to determine tensile strength for avalanche forecasting applications.

2.23. Acoustic Snow Depth Measurements

Most acoustic measurements of snow depth have been made using ultrasonic devices that determine the distance to the snow surface (Figure 29). The measurement device is fixed to a mast of known height situated above the snowpack. An ultrasonic sensor produces an inaudible (>20 kHz) acoustic pulse that is reflected from the snow surface. Measuring the time between the sent and received pulses enables calculation of snow depth using kinematics. This is a "time-of-flight" measurement. Concomitant measurements of air temperature are used to calculate the speed of sound in air. The measurement system principle is similar to pulse sonar and radar systems, and the range accuracy is limited by the pulse duration.

The acoustic snow depth sensor can be considered as an important development in snow science since this permits snow depth to be determined at a high temporal sampling rate at remote observation stations [*Goodison*, 1985]. Snow depth collected by the acoustic device can be used for climatological, hydrologic, or avalanche forecasting applications and models.

Gubler [1981b] designed a snow depth measurement system using separate sending and receiving piezoelectric transducers. The transducers were situated next to each other in a bistatic sonar configuration. The sending transducer was driven at its resonant frequency of 40 kHz. Drifting and blowing snow caused scattering of the acoustic wave due to the small signal-to-noise ratio of the pulse. *Gubler* [1981b] also observed that soft surface layers of snow would not cause strong reflections of the pulse, implying that some penetration of the snowpack by the ultrasonic wave may have occurred. This was recognized by *Caillet et al.* [1979] as occurring due to changes in the porosity and roughness of the snowpack surface, but the physics of this phenomenon is not well understood.

A prototype acoustic depth gauge was first developed in the Department of Physics and Division of Hydrology at the University of Saskatchewan in 1970 as part of the Water Resources Research Subvention Program of the Government of Canada. Informed by this prototype, *Goodison et al.* [1984] adapted an acoustic rangefinder from the Polaroid Corporation to measure the distance to the snow surface. This approach

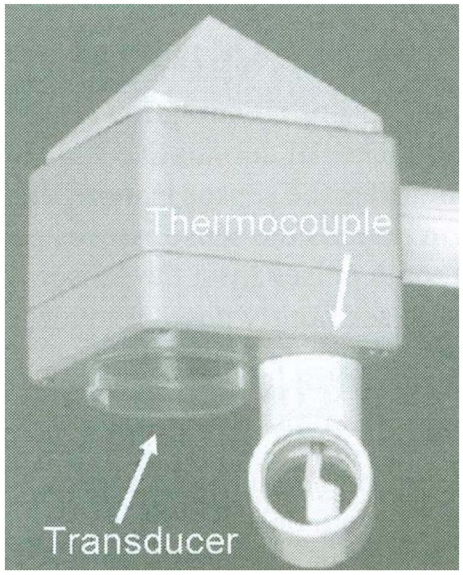

Figure 29. Example of acoustic snow depth measurement device [from *Anderson and Wirt*, 2008]. The ultrasonic transducer and air temperature measurement devices are visible in the picture.

was later followed by *Earl et al.* [1985]. An improved sensing system was later proposed by *Goodison et al.* [1988]. Only a single transducer module was used in this system. Once again, the transducer module was an acoustic ranging sensor manufactured by Polaroid. The transducer produced acoustic waves at a frequency between 50 and 60 kHz with a range of 27 cm to 10.7 m, an accuracy of ~3 mm for distances ranging up to 3 m, and an overall accuracy of ±1% [*Mims*, 2000]. Increasing the speed of the microcontroller increased the time resolution and permitted the measurement of snow depth to within 1 mm depth error [*Goodison et al.*, 1988]. The air temperature was automatically measured at the same time that the acoustic pulse was sent toward the snowpack. The ultrasonic sensor device was able to detect drifting and blowing snow events. The system was observed to underestimate snow depth by 6 cm relative to snow ruler measurements [*Goodison*, 1985]. *Goodison et al.* [1984] remarked that this bias may be due to partial penetration of the snow surface by the acoustic wave. This may occur if the snow is of relatively low density.

Acoustic scattering of the sound wave at the snow surface and temperature gradients near the air-snow interface were also considered by *Goodison et al.* [1984] to influence the accuracy of the gauge. Measurement test details of the gauge are given by *Edey* [1985] and *Metcalfe et al.* [1987]. *Osterhuber et al.* [1994] present an empirical calibration procedure for removing the influence of temperature changes on spurious fluctuations in determined snow depth.

Acoustic measurement gauges are available commercially from several companies. *Ryan et al.* [2008] tested commercially available ultrasonic snow depth gauges, finding that the maximum RMSD between ultrasonic and snow ruler measurements was less than 3 cm for 17 sites in the USA. *Anderson and Wirt* [2008] examined the factors that contribute to errors in ultrasonic snow depth measurement, finding that contamination of the transducer by dirt or insects, tears in the transducer surface, and obstruction of the transducer or snow surface under the transducer were major influences. *Bergman* [1989] found that heating of the thermocouple used to measure air temperature could affect the resolution of the depth measurement by up to ±3 cm, indicating the need to ensure adequate shielding of the thermocouple.

2.24. Acoustic Bulk Property Measurements

2.24.1. Description

Smith [1965] and *Smith* [1969] sent sound waves through cylindrical snow samples extracted from a snowpack and related the speed of the sound wave to snow density and the elastic constants of snow using semiempirical equations. *Buser* [1986] and *Buser and Good* [1986] placed snow in an impedance tube and used the Zarek porous media model [*Zarek*, 1978] to explicitly determine snow density. *Lee and Rogers* [1985] set up a loudspeaker and microphone above a snow surface. The loudspeaker was used to send a 30 ms impulse into a 2 cm snow layer that had accumulated on a roof. Selecting the parameters of the Zarek porous media model allowed for generation of a synthetic waveform. The synthetic waveform was compared with the waveform recorded by the microphone. The measurement method used by *Lee and Rogers* [1985] was not systematic and was not applied to a seasonal snowpack.

In a similar fashion to Vertical Seismic Profiling (VSP) in seismology, *Moore et al.* [1991] created a probe microphone that was inserted beneath the snow surface on a rod. A loudspeaker situated above the snow surface produced white noise. The porous media model proposed by *Attenborough* [1983] was used to predict snow porosity within <20% error.

Using a seismic array and acoustic models of snow, *Albert*, [1998, 2001] used an inversion procedure to determine snow depth and permeability. The acoustic inversion procedure was similar to *Lee and Rogers* [1985] but fully automated.

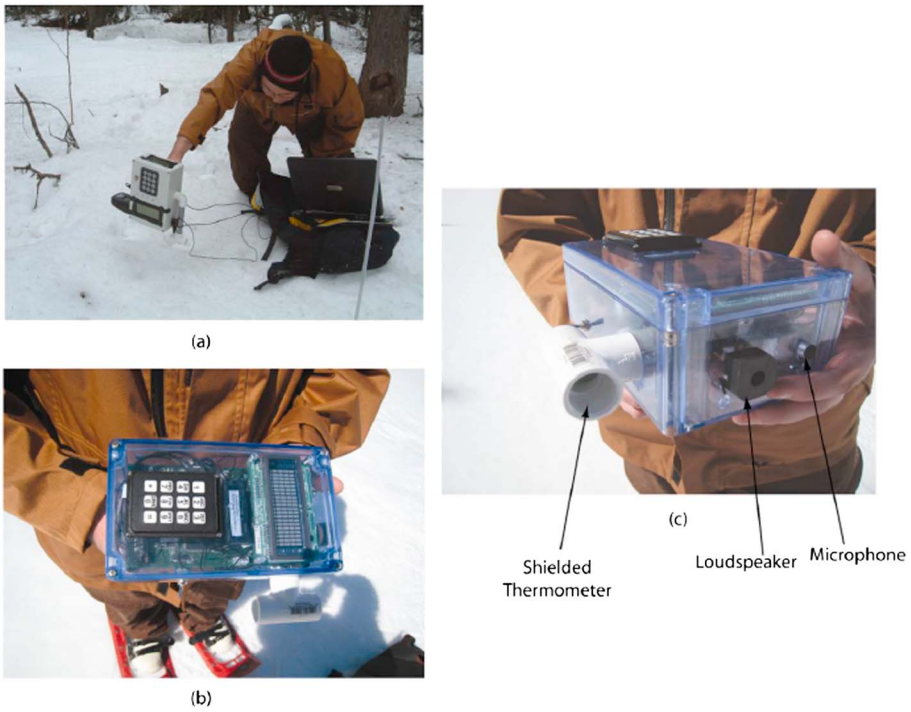

Figure 30. Picture of acoustic snow measurement devices [from *Kinar and Pomeroy*, 2008b]. (a) Side view of device, (b) top view, and (c) picture showing shielded thermometer, loudspeaker, and microphone.

SWE has been measured using a loudspeaker and microphone situated above the snow surface in a similar fashion to bistatic radar or sonar. In an analogous fashion to FMCW radar, the active and noninvasive measurement system sent a frequency-swept sound wave into snow. The frequency sweep was between 20 Hz and 20 kHz. The reflection response was related to SWE using a recursive acoustic model [*Kinar and Pomeroy*, 2007]. Later work used a Maximum Length Sequence (MLS) as the source signal and another recursive acoustic model relating geometric spreading and reflection of the sound wave beneath the snow surface. The model incorporated theory from sonar and described a complete theory of acoustic scattering from snowpack layers using fractal analysis of rough snow interfaces [*Kinar and Pomeroy*, 2008a, 2008b, 2009]. A picture of an acoustic sensing apparatus described in these papers is shown in Figure 30.

Kinar and Pomeroy [2015] used multiple microphones situated in an acoustic array at an offset distance to a loudspeaker source to noninvasively determine SWE, snow density, temperature, and liquid water content using a unified model of sound wave propagation in snow. The unified model considered changes in the bulk and thermal properties of snow to influence the speed and attenuation of sound waves sent through the snowpack. Stationary and portable versions of an acoustic sensing device were tested at field sites in the Rocky Mountains, and noninvasive images of snowpack layering were obtained using theory adapted from seismic signal processing. Acoustic scattering of sound waves was observed to occur due to the presence of buried vegetation beneath the snow surface and high levels of liquid water content filling the pore spaces of the snowpack. A stationary version of the device was able to noninvasively measure changes in the snowpack over time at a fixed location, showing a rise in snow temperature and liquid water content over the snow accumulation and ablation seasons. Further applications of this technology will provide a noninvasive and unprecedented ability to monitor the physical properties of snow. Because acoustic techniques are noninvasive, this allows for a greater number of snow measurements to be made along a transect or over an area in lieu of invasive measurements made using snow tubes (section 2.3), snowpits (section 2.4), or dielectric devices (section 2.9). Moreover, the use of acoustics allows for multiple measurements of snowpack properties to be made at the same location and temporal changes in SWE, snow density, temperature, and liquid water content to be tracked without the use of multiple devices.

Snow acoustics studies have mostly focused on the physics of sound wave propagation in snow. A review of snow acoustics was presented by *Sommerfeld* [1982]. The audibility of sound within snow has been discussed

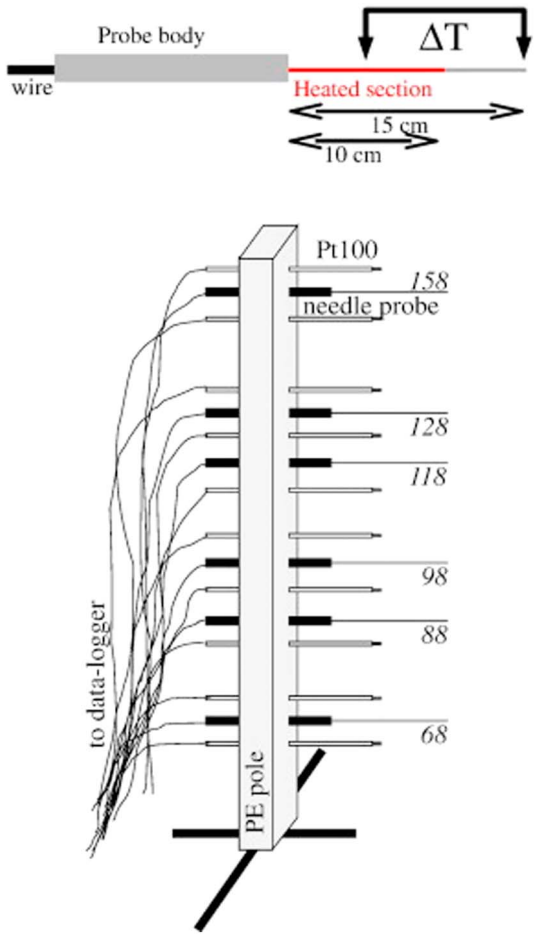

Figure 31. Picture of heat pulse probe used to measure snow thermal conductivity [from *Morin et al.*, 2010]. The change in temperature over the heated section is ΔT. Also shown is a measurement apparatus composed of multiple needles used to determine thermal conductivity of the snowpack over the winter season.

by *Johnson* [1985] to provide greater insight into rescuing buried avalanche survivors, but the acoustic impedance of snow was not calculated as a porous medium [*Kinar and Pomeroy*, 2007]. Seismic arrays composed of geophones can be used to determine the location and movement of avalanches by the use of beamforming; these passive sensing systems have been briefly reviewed by *O'Neel et al.* [2007] and *Lacroix et al.* [2012]. Passive avalanche sensing systems provide insight into the physics of avalanches and help to provide warning of avalanche activity.

2.25. Heat Pulse Probes

The heat pulse probe measurement begins by applying an electrical current to a heater wire looped inside of one of the needles. The heater needle warms up, and a rise in temperature is sensed by a thermocouple. The thermocouple is placed either inside of the heater needle (single needle) or inside another needle situated at a radial distance to the heater needle (multiple needle) [*Mori et al.*, 2003]. The change in temperature during heating or cooling of the needle is related to material properties by a mathematical model [*Kluitenberg et al.*, 1993, 2000; *Carslaw and Jaeger*, 1959; *Liu and Si*, 2008, 2010; *Mori et al.*, 2003].

Most heat pulse probes used to measure the thermal conductivity of snow utilized a single needle [*Jaafar and Picot*, 1970; *Riche and Schneebeli*, 2013; *Sturm and Johnson*, 1992; *Sturm et al.*, 1997]. *Fowler* [1974] and *Sturm et al.* [1997] measured the thermal conductivity of snow using a single-needle heat pulse probe and related this measurement to density using an empirical relationship. Single-needle probes (Figure 31) have been buried in a snowpack and used to measure effective thermal conductivity of snow over a 3 month period [*Morin et al.*, 2010]. Heating of cylinders, spheres, plates, and wires have been used since 1886 to measure the thermal conductivity of snow [*Sturm et al.*, 1997]. Because the thermal conductivity of snow governs the rate of heat transport in a snowpack, thermal conductivity is an important variable in models of snowpack evolution and is associated with the physics of snowpack metamorphism. Heat pulse probes have provided measurements of thermal conductivity of snow and thereby advanced scientific understanding of the spatial and temporal changes in this property [*Sturm et al.*, 1997; *Usowicz et al.*, 2008].

Liu and Si [2008] showed that both the density and thermal conductivity of snow could be measured using a multiple-needle heat pulse probe. Care must be taken to ensure that the strength of the heat pulse is not high enough to melt snow and that the radial distance between the heater needle and temperature-sensing needle is calibrated in a medium with a known thermal conductivity. Although the multiple-needle heat pulse probe is an invasive measurement apparatus, the investigators realized that the probe could measure snow density and thermal conductivity in a snowpit. Alternately, the probe could be buried in the snowpack to make continuous measurements [*Liu and Si*, 2008].

2.26. Discrete Temperature Sensors

The snow temperature is often related to snowpack metamorphism or snowpack evolution. The temperature sensor most often used by snow surveyors is a dial thermometer [*McGurk*, 1983; *Fierz et al.*, 1999] or

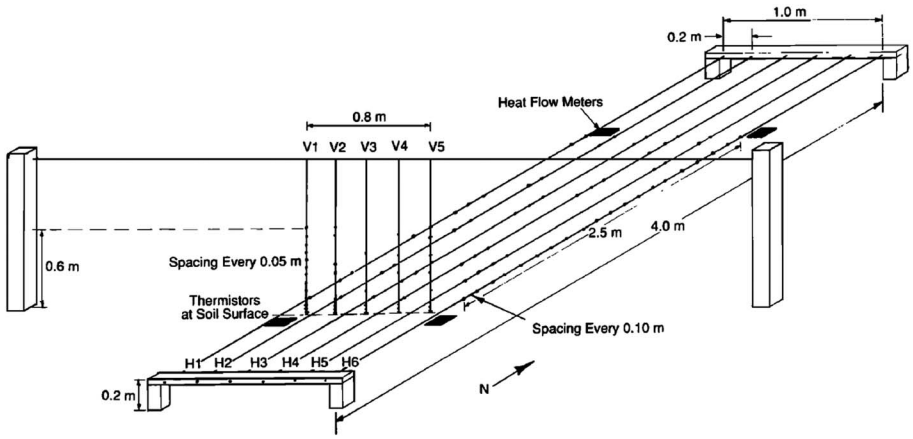

Figure 32. Thermocouple assembly suspended throughout the snowpack [from *Sturm and Johnson*, 1991].

a thermocouple with a digital readout (digital thermometer) [*Koh and Jordan*, 1995]. The thermometer is inserted into the snowpit wall at successive depths beneath the snow surface [*Crook and Freeman*, 1973]. The temperature of the thermometer sensing surface is allowed to equalize with snowpit temperature before a measurement is read from the dial.

Brandt and Warren [1997] inserted a tube with 3 mm diameter into the side of a snowpit and used the tube to extract a small core of snow. The tube was removed, and a thermocouple was placed into the hole created by the tube. Snow was then placed by hand over the thermocouple leads to retain the thermocouple in the snowpack. The process was repeated for layers at various depth in the snowpack to obtain a temperature profile. Back shoveling of snow into the snowpit allowed for thermocouples to be buried under snow and temperature profiles to be determined over an extended period of time. The measurements were used with a physical model of heat transport through snow that provided insight into the relationships between solar radiation fluxes and heating of the snowpack. Snowpit-based measurement of snow temperature is laborious, invasive, and time consuming due to the creation of a snowpit [*Sauter and Tanner*, 1992].

Thermocouple arrays have been buried in the snowpack to measure temperature distribution throughout the snow. The basic setup of this apparatus is a series of thermocouples situated over a vertical distance. Installation of the stationary version of this apparatus occurs during the snow-free season so that snow can accumulate around the thermocouples. The vertical extent is selected to be higher than the maximum depth of snow over which temperature is to be measured.

Sturm and Johnson [1991] suspended a two-dimensional network of thermocouples on strings between two posts before the snow accumulation season (Figure 32). Four rows of vertical thermocouples over an 80 cm horizontal distance were used to record temperature gradients throughout the snowpack. The vertical thermocouple spacing was every 5 cm over a 60 cm distance. The thermocouple array setup was able to detect convection plumes under the snowpack surface. *Conway and Benedict* [1994] later used a similar setup to measure temperature changes caused by meltwater propagation through snow. The network of thermistors spanned a 2 m vertical distance and a 1.5 m width. The spacing between thermocouples was 15 cm. These experiments allowed for greater insight to be gained into the physics of heat transport through the snowpack.

Albert and McGilvary [1991] progressively laid down rows of thermocouples on the snow surface before a snow deposition event. Over the winter season, this caused the thermocouples to be buried inside of the snowpack without the need for a supporting structure. Although this method would have minimized the effects associated with heat conduction apparent in application of the other methods, the thermocouples could only be buried at depths related to snow deposition events. A similar system composed of "settling disks" was reported by *Morin et al.* [2012]. The disks were suspended on a vertical wire, and successive disks were placed on the snow surface after each snowfall event. The system was also used to measure the gradual compaction of the snowpack due to gravity and metamorphic processes. A semiautomated system similar to the one used by *Morin et al.* [2012] was devised by *Swanson* [1968].

Albert and McGilvary [1992] later suspended thermocouples on nylon fishing wire between wooden dowels. Arranging thermocouple arrays in two separate directions allowed for a three-dimensional measurement

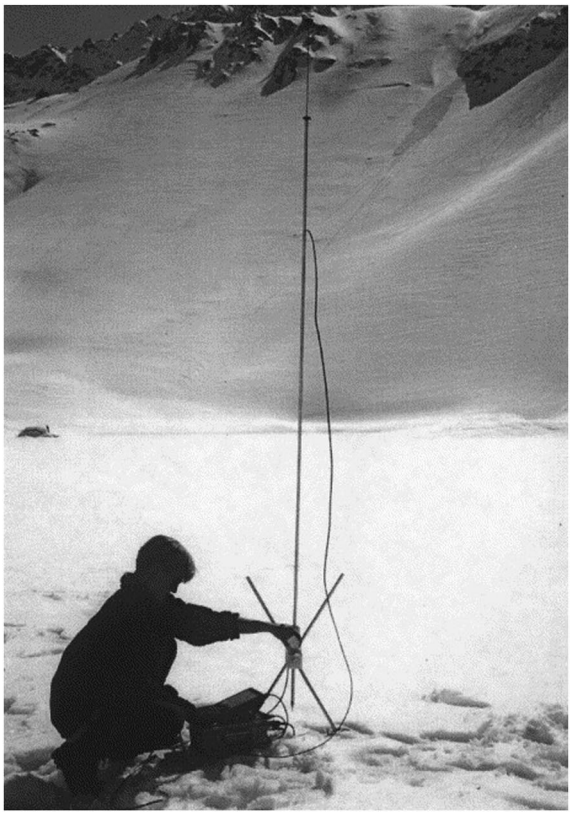

Figure 33. Image of SnowMicroPen device [from *Schneebeli et al.*, 1999].

of snowpack temperature. *Pfeffer and Humphrey* [1996] installed a network of thermocouples through the side of a snowpit. Snow was replaced in the snowpack, and the thermistor network was allowed to settle in the snowpack over the winter season. The data collected from these devices were used to better understand the physics related to heat transport by wind and water within the snowpack.

Luce and Tarboton [2001] used nylon fishing wire to place thermocouples vertically along a line at distances of 5, 12.5, 27.5, and 35 cm from the ground surface. Temperature measurements made by the thermocouples were used to test a model of heat transport through snow. *Helgason and Pomeroy* [2012a] deployed this "snow harp" design in the Canadian Prairies for a study of snowpack energetics. Further testing of this measurement device showed substantial solar heating of near-surface thermocouples which degrades measurement performance of the snow harp. The snow harp was used by *Helgason and Pomeroy* [2012a] to provide data showing that there is a missing term in the energy balance over the snowpack.

2.27. Mechanical Property Measurements

Devices used to measure the mechanical properties of snow apply compressive or shear forces to the snowpack. These devices can be used in the field to measure snow, or a sample can be extracted and subjected to measurement. A brief review on snow mechanical measurement devices is given by *Von Moos et al.* [2003]. These devices are used in avalanche forecasting applications.

A simple test often used to measure the hardness of a snowpack is the "hand hardness" test. A human observer pushes a fist, a number of fingers, a pencil, or a knife into the snowpack and records the hardness based on the element that can be inserted into the snowpack. The insertion force is approximately 50 N, and a "knife" hardness reading corresponds to the highest hardness reading. This test is qualitative, and the accuracy varies between observers [*Pielmeier and Schneebeli*, 2003a].

The Rammsonde is a device used to determine snow hardness to assess ski trafficability. Similar to a cone penetrometer used to estimate soil strength, the Rammsonde consists of a rod with a diameter of 2 cm to which is attached a drop hammer. Knowledge of the hammer height before the drop, the mass of the hammer, and the penetration depth in snow enables computation of the Ram index R_I. "Alta" and "Haefeli" penetrometers that are similar to the Rammsonde are discussed by *Perla* [1969]. The Rammsonde resolution is limited by the size of the measurement cone and exhibits a hysteresis effect with respect to depth beneath the snow surface [*Pielmeier and Schneebeli*, 2003a].

Waterhouse [1966] presents a derivation of the Rammsonde equation based on the physics of the measurement technique. Empirical compensation coefficients are often required for Ram readings corresponding to penetration depths of less than 10 cm near the surface due to discontinuities created by the conical geometry. For $R_I < 800$ the Ram index numbers are believed to be accurate indicators of snow hardness [*Adam*, 1981; *Perla and Glenne*, 1981]. The Ram index numbers can be related to snow [*Adam*, 1981] and firn [*Bull*, 1956] densities by empirical relationships.

Dowd and Brown [1986] developed an automated version of the Rammsonde with a microcontroller. *Martinelli and Ozment* [1985] developed an automated device where a spherical probe was dropped on the

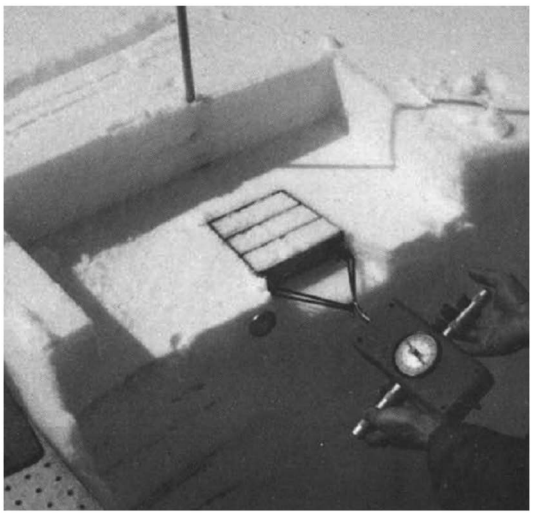

Figure 34. A shear frame being used to measure a shear strength index of snow [from *Perla et al.*, 1982].

snow surface by a microcontroller to determine the minimum force required to erode snow surface elements for blowing snow transport studies.

The SnowMicroPen is a high-resolution penetrometer that can be used to measure snow texture (Figure 33). The principle of operation is conceptually similar to the other devices described above. A conical tip with a 5 mm diameter is driven into the snowpack at a maximum speed of 2 cm s^{-1}. The resistive force exerted by the snow on the tip is recorded by a force transducer. The snow texture is related to the resistive force by an empirical relationship [*Schneebeli et al.*, 1999], or the resistive force recorded by the device can serve as a proxy for hand hardness [*Pielmeier and Schneebeli*, 2003a]. The SnowMicroPen (SMP) can be used to determine differences between layers in the snowpack and compares well with FMCW radar stratigraphy [*Marshall et al.*, 2007]. Using SMP data, *Havens et al.* [2013] identified snow particle type and layering using machine learning techniques. *Proksch et al.* [2015] used a statistical signal processing algorithm with SMP data to determine snow density, SSA, and "correlation length" as an alternative measure of snow density and particle size.

Snow stability tests are often used in snowpits to quickly determine in a semiqualitative fashion the ability for snow structural failure in avalanche terrain. The tests should have some measure of reproducibility. The "compression test" consists of a snow column created out of the side of a snowpit. An observer places a shovel on top of the snow column and taps the shovel until the snow column fails, recording the number of taps and the part of the body (wrist, arm, and shoulder) used to initiate structural failure. The "stuffblock" test is similar to the compression test but uses a bag filled with 4.5 kg of snow rather than the shovel to initiate failure. The bag is dropped from progressively higher heights above the snow column and the height of drop required to cause snow column failure is recorded [*Tremper*, 2008].

The Rutchblock test consists of an isolated snow column on a slope that is subjected to a mechanical load by a skier. The snow column is created by hand using a saw [*Ferguson and LaChapelle*, 2003]. The failure of the snow column based on actions of the skier can be recorded using a descriptive system [*Powers*, 2008]. Similar tests and variations on these tests are discussed by *Tremper* [2008], *Powers* [2008], and *Ferguson and LaChapelle* [2003]. Saw cuts into snow and induced avalanche slab fracture have been recorded using high-speed cameras [*McClung*, 2011].

The "cantilever" test for snow stability was devised by *Perla* [1969]. A 30 cm wide section is excavated out of the snowpack, and a flat aluminum plate is inserted into the section. The plate is removed from the side of the snowpit, and the depth of insertion required for structural failure is recorded.

Shear frames (Figure 34) are used to measure an index of the shear strength of snow. The shear frame consists of a metal box with a number of slanted cross bars. A force gauge is attached to a ring situated on the side of the shear frame, and a human observer pulls on the frame. The maximum force required to dislodge the frame from the snowpack is recorded as the shear strength index [*Perla*, 1969]. *Jamieson and Johnston* [1995] present a brief review of the shear frame literature.

Results from the shear frame are sensitive to the size of the frame and its area, the type of metal used for frame construction, and the pull rate of the human observer. For operational use, the area of the frame cannot be less than 0.01 m^2 nor greater than 0.05 m^2 [*Perla and Beck*, 1983], with a recommended area of 0.025 m^2 related to a precision of 10% between measurements [*Perla et al.*, 1982]. Larger frames may require more than an upper limit of 1000 N of pull force that can be exerted by a human observer. The shear strength index tends to drop with an increase in shear frame size and increase with a slower pull speed and frame mass [*Perla and Beck*, 1983]. Similar to the isolated column of the Rutchblock test, the shear frame can be isolated from the snow

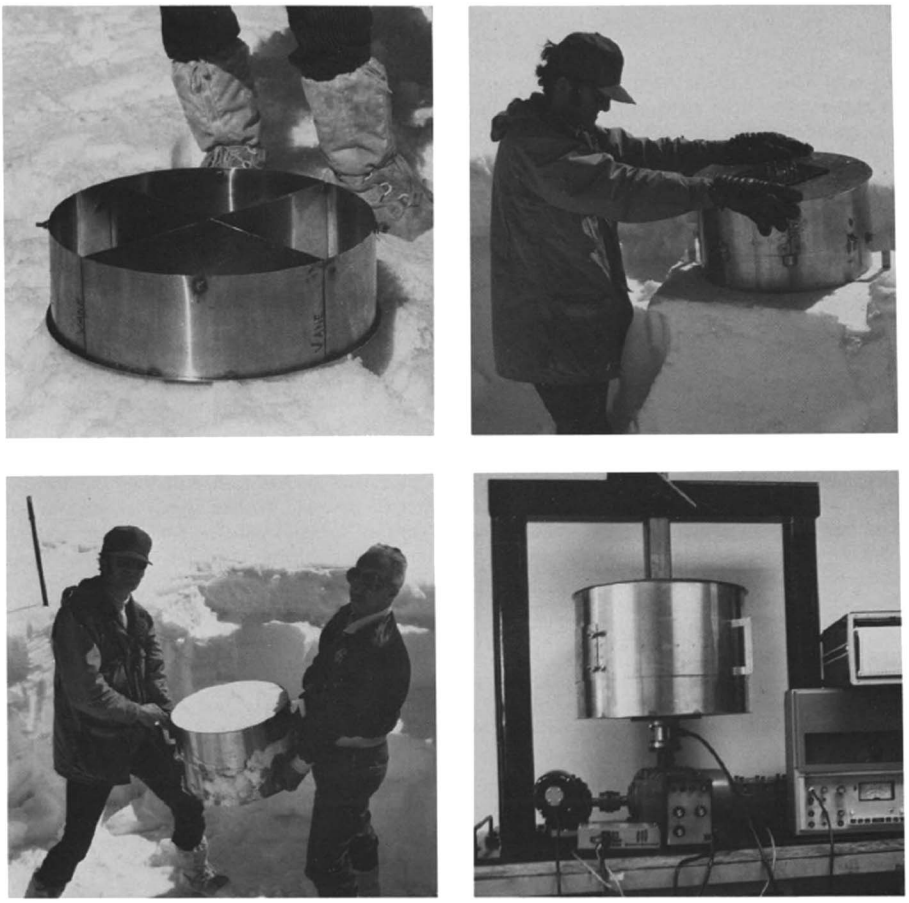

Figure 35. Rotary vane device used to measure shear strength of snow [from *Perla et al.*, 1982].

surface to minimize the effects of side shear. Correction for forces due to gravity permits the shear strength of snow to be determined [*Conway and Abrahamson*, 1984a]. A slip plate can also be inserted under the shear frame to reduce the effects of basal shearing [*Jamieson and Johnston*, 1990; *Conway and Abrahamson*, 1984a]. The use of pull frames is allowed for relationships to be determined between the mechanical properties of snow and snow density.

Rotary vane devices consist of two large crossed plates that are inserted into the snowpack (Figure 35). The torque required to cause movement of the device is measured using a manual torque wrench [*Perla*, 1969] or by strain gauges coupled to an electric motor responsible for imparting the torque [*DeMontmollin*, 1982]. Rotary vane devices can be used on large snow samples extracted from the snowpack [*Perla et al.*, 1982]. The measured torque is related to the shear strength of snow by rotational dynamics [*Perla*, 1969].

Triaxial tests to determine the mechanical properties of snow have been conducted using laboratory instruments installed in a cold room. These instruments impart shear or tensile stresses and strains to snow samples placed in a holder and are described by *Watanabe* [1980], *Lang and Harrison* [1995], *Schweizer and Camponovo* [2002], and *Von Moos et al.* [2003]. These measurement techniques are similar to established mechanical and rheological measurements [*Collyer and Clegg*, 1998], with some adaptation to accommodate snow properties [*Von Moos et al.*, 2003].

Nakamura et al. [2010] have reported a novel method that can be used to determine shear strength. A snow sample is placed on a table that is horizontally moved by a mechanical assembly. The force required to cause shear fracture of the snow sample is recorded.

2.28. Snow Permeometer

The permeometer has been used to measure the permeability of snow so that the movement of air through the snowpack can be determined [*Hardy and Albert*, 1993]. Windpumping is a physical process where air

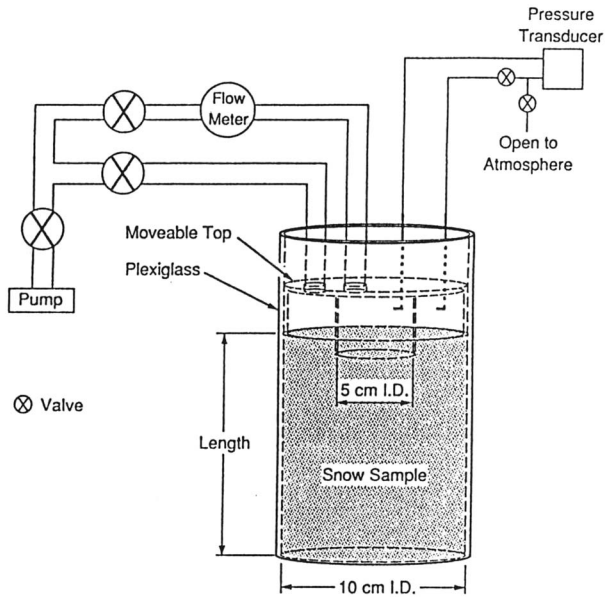

Figure 36. Schematic diagram of snow permeometer [from *Hardy and Albert*, 1993].

enters the snowpack due to changes in topography or airflow. Because windpumping transfers heat and energy to snow, it influences snowpack metamorphism [*Colbeck*, 1989b]. Permeometer measurements of permeability have indicated differences in permeability throughout layers of the snowpack with respect to vertical and lateral flow [*Luciano and Albert*, 2002]. Attempts have been made to relate permeability measured by the permeometer to snow microstructure [*Hardy and Albert*, 1993; *Albert et al.*, 2000].

Permeometer theory related to determination of the air-saturated permeability of snow k_s is given by *Shimizu* [1970]. A snow sample is placed inside of a container, and air is pumped through the sample. The speed of the air and the air pressure inside and outside of the container is recorded [*Albert et al.*, 2000]. Measurement with approximately 16 different flow rates allows for determination of when the flow is nonlinear. A regression equation is then used to determine the air-saturated permeability of snow using Darcy's law [*Hardy and Albert*, 1993].

Albert and Perron [2000] describe a design for a permeometer sample holder that can be used to determine the permeability of ice layers and snow surface crusts. Alternate permeometer designs have been presented by *Yen* [1980] and *Conway and Abrahamson* [1984b]. A diagram of a permeometer is shown in Figure 36.

3. Conclusions

Investigators have utilized numerous techniques to measure the physical properties of the seasonal snowpack. Recent developments over the past half-century have ensured that electronic systems are often used when collecting data indicative of snowpack processes.

Data collected of snowpack properties that is deemed to be worthwhile for preservation should be submitted to an online archive for historical and scientific reporting purposes. Although such archives exist, there is currently a lack of photographic images of snow measurement devices and the deployment of such devices at field sites. There is a need for online archives to also preserve photographic images and video for historical and training purposes.

There has been very little intercomparison between devices that measure similar snowpack properties. Intercomparison attempts may have been hampered by lack of commercial availability of some devices, and consequently, these systems have not been extensively tested or used. There is a need for more device intercomparison studies where the physics of each device is carefully validated and improved. Groups such as the International Association of Cryospheric Sciences MicroSnow group (http://www.cryosphericsciences.org/wg_microSnow.html) is an important step in this direction. The Global Energy and Water Exchanges Project of the World Climate Research Programme has recently launched the

International Network for Alpine Research Catchment Hydrology which will address intercomparison of snow measurement instrumentation and operating techniques in high-altitude regions with recommendations for best practices in harsh environments [*Pomeroy et al.*, 2015].

Despite the widespread use of automation technologies, many snow sampling techniques require the presence of a human observer. This does not permit temporal observations to be made without the possibility of human error and the difficulties of humans traveling to remote snow measurement locations. The techniques are often invasive, resulting in the destruction of the snowpack and the inability for multiple samples to be taken at the same location. This suggests that automation of currently available invasive devices and the development of noninvasive instrumentation are two priorities for research. Automation of noninvasive techniques would permit greater spatial coverage and spatial density of snow measurements and therefore better assess the spatial and temporal variability of snow properties much better than do current observation networks.

Some snow measurement devices such as depth measurement rods (section 2.2), snow tubes (section 2.3), dielectric sensors (section 2.9), and mechanical property measurement devices (section 2.27) have not been designed with recourse to snowpack physical processes. This is because the papers describing these devices do not fully provide justification for selection of design parameters, particularly when invasive measurement instruments must be inserted into the snowpack. This is understandable since the research is often pioneering and allows for additional research. Future designs could be optimized by mathematical modeling of device operation using finite difference time domain, finite element, or finite particle methods. This is standard practice in mechanical and electrical engineering, and such procedures should be more widely used in snowpack measurement device engineering.

Electronic devices that measure snowpack properties are often reliant on empirical equations to obtain measurements. These empirical equations are dependent on the data set used to devise the relationship and may not be applicable at all geographic locations and environmental conditions. There is a need to replace these empirical relationships with nonempirical equations developed from the physics of active and passive sensing devices. If an empirical relationship is used for calculations performed by a microcontroller embedded in a proprietary sensing system, the system outputs are dependent on the empirical relationship. If the system operation and equations used during processing are not available to the end user, the sensing system operates as a "black box" system and the user can be unaware if the device is properly functioning and cannot improve upon its estimation of physical properties. This suggests that system design should be openly documented before a device is to be used for crucial or important snow measurement applications.

Snow scientists have often been reliant on measurement instrumentation designed to collect data that is postprocessed at a location away from the field site. Although laptops and mobile computing devices can be used to achieve this goal in the field, there is often a delay between the collection of data and the measurement of a snowpack physical variable. Postprocessing of the data by the sensing system itself is a worthwhile goal since this permits a human observer, robotic observer, or the sensing system itself to decide whether another sample is required. This ensures that valid data have been collected. Although such a goal has not always been possible in the past due to limitations on processor speed, current trends in electronics related to miniaturization, an increase in processor speed, fanless computing, multicore processing, and hardware acceleration will continue to provide the impetus to achieve the goal of intelligent snow sensors. There still will be a role for the personal observation of snow, but with less destructive techniques and greater ability to obtain the results of detailed calculations in the field from such intelligent sensors—this should permit more comprehensive snow measurement designs particularly when changing environmental conditions require adaptive management of snow surveying practices. The increase in the capability of drones, robots, and autonomous vehicles also provides exciting platforms for new intelligent snow sensors and developing and deploying such sensors should be a priority for snowpack research and development.

The data collected from improved, autonomous, and physically accurate devices can be used for validation and calibration of snowpack evolution models. The physics associated with such models often treats the snowpack as a black box system, where changes in snowpack properties are calculated using mass and energy fluxes that are incident at the boundaries of a control volume. If these internal snowpack properties are measured rather than modeled, this will improve the accuracy of predictions made with such models related to drought, flooding, water availability, climate change, and avalanche prediction. Using electronic and noninvasive snowpack measurement devices, the physical properties of the snowpack can be measured on the same

time step as other environmental variables such as air temperature, relative humidity, and radiation. Such measurements are commonly taken at distances above the surface of the snowpack and are traditionally used as inputs to snowpack evolution models.

Moreover, since measurement devices used to determine snow properties have often been invasive and not completely autonomous, multiple snowpack properties cannot be measured simultaneously, and this precludes a more complete scientific understanding with respect to how the snowpack evolves and changes over time. Understanding the physics of snowpack evolution is important for developing snowpack models. With the use of better snow measurement devices, the possibility exists of a new generation of snowpack evolution models that have improved physical accuracy and predictive capabilities.

Acknowledgments

We would like to acknowledge the Natural Sciences and Engineering Research Council of Canada (NSERC), Canada Research Chair Programme (CRC), the Global Institute for Water Security, and the Canada Foundation for Innovation (CFI) for providing funding that allowed for the establishment of the Canadian Rockies Hydrological Observatory including the well-instrumented Marmot Creek Research Basin where many measurement examples and trials took place over the past decade. Special acknowledgement is also extended to those individuals who helped with fieldwork, sometimes in adverse conditions. In addition, we thank the respective journals for granting permission to reproduce some of the figures utilized in this paper. The use of any company names has been minimized. Implicit or explicit references to company names or products in this document does not imply advertisement or endorsement for the services or products provided by these companies. Data used to create this review can be accessed by contacting centre.hydrology@usask.ca. We thank the Editor and three reviewers for providing helpful comments and suggestions that have improved the presentation of this paper.

The Editor on this paper was Fabio Florindo. He thanks three anonymous reviewers for their review assistance on this manuscript.

References

Abramovich, R. (2007), Uses of natural resources conservation service snow survey data and products, paper presented at 75th Western Snow Conference, pp. 103–113.

Adam, K. (1981), Travel over snow, in *Handbook of Snow: Principles, Processes, Management and Use*, edited by D. M. Gray and D. H. Male, pp. 521–561, Pergamon Press Canada, Toronto, Canada.

Akitaya, E. (1985), A calorimeter for measuring free water content of wet snow, *Ann. Glaciol.*, *6*, 246–247.

Albert, D. (1998), Snow cover effects on impulsive noise propagation in a forest, *Noise Control Eng. J.*, *46*, 208–214.

Albert, D. (2001), Acoustic waveform inversion with application to seasonal snow, *J. Acoust. Soc. Am.*, *109*, 91–101.

Albert, M. (2002), Seasonal changes in snow surface roughness characteristics at Summit, Greenland: Implications for snow and firn ventilation, *Ann. Glaciol.*, *35*, 510–514.

Albert, M., and W. McGilvary (1991), Multidimensional observation of snow temperature on windy days, paper presented at 48th Eastern Snow Conference, pp. 189–200.

Albert, M., and W. McGilvary (1992), Induced flow channels in a natural snowpack, paper presented at 49th Eastern Snow Conference, pp. 55–60.

Albert, M., and F. Perron (2000), Ice layer and surface crust permeability in a seasonal snow pack, *Hydrol. Process.*, *14*, 3207–3214.

Albert, M., E. Shultz, and F. Perron (2000), Snow and firn permeability at Siple Dome, Antarctica, *Ann. Glaciol.*, *31*, 353–356.

Amanzio, G., D. Bertolo, M. de Maio, L. P. Lodi, L. Pitet, and E. Suozzi (2015), Global warming in the Alps: Vulnerability and climatic dependency of alpine springs in Italy, Regione Valle d'Aosta and Switzerland, Canton Valais, in *Engineering Geology for Society and Territory*, vol. 5, pp. 1375–1378, Springer, Switzerland, doi:10.1007/978-3-319-09048-1_263.

Ambach, W., and B. Mayr (1981), Ski gliding and water film, *Cold Reg. Sci. Technol.*, *5*(1), 59–65, doi:10.1016/0165-232X(81)90040-9.

Anderson, H., P. McDonald, and L. Gay (1965), *Use of Radioactive Sources in Measuring Characteristics of Snowpacks*, U.S. Forest Service Research Note PSW-11, Pacific Southwest Forest and Range Experimental Station, Berkeley, Calif.

Anderson, J., and J. Wirt (2008), Ultrasonic snow depth sensor accuracy, reliability and performance, paper presented at 76th Western Snow Conference, pp. 99–105.

Armstrong, R. (1976), The application of isotopic profiling snow gauge data to avalanche research, paper presented at 44th Western Snow Conference, pp. 606–676.

Armstrong, R. L., and E. S. Brun (Eds.) (2008), Snow and climate: Physical processes, surface energy exchange and modeling, Cambridge Univ. Press, Cambridge, U. K.

Arnaud, L., G. Picard, N. Champollion, F. Domine, J. C. Gallet, E. Lefebvre, M. Fily, and J. M. Barnola (2011), Measurement of vertical profiles of snow specific surface area with a 1 cm resolution using infrared reflectance: Instrument description and validation, *J. Glaciol.*, *57*, 17–29, doi:10.3189/002214311795306664.

Arons, E., and S. Colbeck (1995), Geometry of heat and mass transfer in dry snow: A review of theory and experiment, *Rev. Geophys.*, *33*(4), 463–493.

Attenborough, K. (1983), Acoustical characteristics of rigid fibrous absorbents and granular materials, *J. Acoust. Soc. Am.*, *73*(3), 785–799, doi:10.1121/1.389045.

Avanzi, F., M. Caruso, C. Jommi, C. De Michele, and A. Ghezzi (2014), Continuous-time monitoring of liquid water content in snowpacks using capacitance probes: A preliminary feasibility study, *Adv. Water Resour.*, *68*, 32–41, doi:10.1016/j.advwatres.2014.02.012.

Ayars, J. E. (2014), Adapting irrigated agriculture to drought in the San Joaquin Valley of California, in *Drought in Arid and Semi-Arid Regions*, edited by K. Schwabe et al., pp. 25–39, Springer, Netherlands, doi:10.1007/978-94-007-6636-5_2.

Bader, H. (1950), Note on the liquid water content of wet snow, *J. Glaciol.*, *1*(8), 466–467.

Banner, J. A., and R. O. Van Everdingen (1979), Automatic time-lapse camera systems, National Hydrology Res. Inst. Paper No. 4., Environment Canada, Inland Waters Directorate, Ottawa.

Barnaby, I. (1980), Snowmelt observations in Alberta, paper presented at 48th Western Snow Conference, pp. 128–137.

Barnett, T. P., et al. (2008), Human-induced changes in the hydrology of the western United States, *Science*, *319*(5866), 1080–1083, doi:10.1126/science.1152538.

Bartelt, P., and M. Lehning (2002), A physical SNOWPACK model for the Swiss avalanche warning. Part I: Numerical model, *Cold Reg. Sci. Technol.*, *35*, 123–145.

Bates, R., and S. Gerard (1989), Snow surface temperature analysis, paper presented at 46th Eastern Snow Conference, pp. 109–116.

Bear, J. (1972), *Dynamics of Fluids in Porous Media, Environ. Sci. Ser.*, American Elsevier Pub. Co., New York.

Beaumont, R. (1965), Mt. Hood pressure pillow snow gauge, *J. Appl. Meteorol.*, *4*, 626–631, doi:10.1175/1520-0450(1965)004<0626:MHPPSG>2.0.CO;2.

Beaumont, R. (1966), Snow accumulation, paper presented at 34th Western Snow Conference, pp. 3–6.

Bellot, H., A. Trouvilliez, F. Naaim-Bouvet, C. Genthon, and H. Gallée (2011), Present weather-sensor tests for measuring drifting snow, *Ann. Glaciol.*, *52*(58), 176–184, doi:10.3189/172756411797252356.

Bentley, W., and W. Humphries (1931), *Snow Crystals*, McGraw-Hill, New York.

Bergman, J. (1989), An evaluation of the acoustic snow depth sensor in a deep Sierra Nevada snowpack, paper presented at 57th Western Snow Conference, pp. 126–129.

Bewley, D., J. W. Pomeroy, and R. L. H. Essery (2007), Solar radiation transfer through a sub-arctic shrub canopy, *Arct. Antarct. Alp. Res.*, *39*(3), 365–374.

Bewley, D., R. Essery, J. W. Pomeroy, and C. Ménard (2010), Measurements and modelling of snowmelt and turbulent heat fluxes over shrub tundra, *Hydrol. Earth Syst. Sci.*, *14*, 1331–1340.
Bissell, V. C., and E. L. Peck (1973), Monitoring snow water equivalent by using natural soil radioactivity, *Water Resour. Res.*, *9*(4), 885–890, doi:10.1029/WR009i004p00885.
Blincow, D., and S. Dominey (1974), A portable profiling snow gauge, paper presented at 42nd Western Snow Conference, pp. 53–57.
Blyth, K., M. A. R. Cooper, N. E. Lindsey, and R. B. Painter (1974), Snow depth measurement with terrestrial photos, *Photogrammetric Eng.*, *40*(8), 937–942.
Bolognesi, R. (1995), The driftometer, paper presented at 1995 International Snow Science Workshop, pp. 144–148
Boniface, K., J. J. Braun, J. L. McCreight, and F. G. Nievinski (2014), Comparison of snow data assimilation system with GPS reflectometry snow depth in the western United States, *Hydrol. Process.*, *29*, 2425–2437, doi:10.1002/hyp.10346.
Boyne, H., and D. Fisk (1987), A comparison of snow cover liquid water measurement techniques, *Water Resour. Res.*, *23*(10), 1833–1836.
Boyne, H., and D. Fisk (1990), A laboratory comparison of field techniques for measurement of the liquid water fraction of snow, CRREL Rep. 90–3, Cold Regions Res. Eng. Lab., Hanover, N. H.
Brandt, R., and S. Warren (1997), Temperature measurements and heat transfer in near-surface snow at the South Pole, *J. Glaciol.*, *43*(144), 339–351.
Brandt, R., and S. Warren (1997), Solar-heating rates and temperature profiles in Antarctic snow and ice, *J. Glaciol.*, *39*, 99–110.
Brown, R. (1995), Spatial and temporal variability of North American snow cover, 1971–1992, paper presented at 52th Eastern Snow Conference, pp. 69–78.
Brown, R., and R. Armstrong (2008), Snow-cover data: Measurement, products and sources, in *Snow and Climate: Physical Processes, Surface Energy Exchange and Modeling*, edited by R. L. Amstrong and E. Brun, pp. 181–216, Cambridge Univ. Press, Cambridge, U. K.
Brown, T., and J. W. Pomeroy (1989), A blowing snow particle detector, *Cold Reg. Sci. Technol.*, *16*(2), 167–174.
Brun, E. (1989), Investigation on wet-snow metamorphism in respect of liquid water content, *Ann. Glaciol.*, *13*, 22–26.
Brun, E., and E. Pahut (1991), An efficient method for a delayed and accurate characterization of snow grains from natural snowpacks, *J. Glaciol.*, *37*(127), 420–422.
Brun, E., E. Martin, V. Simon, C. Gendre, and C. Coleou (1989), An energy and mass balance model of snow cover suitable for operational avalanche forcasting, *J. Glaciol.*, *35*, 333–342.
Brun, E., P. David, M. Sudul, and G. Brunot (1992), A numerical model to simulate snow-cover stratigraphy for operational avalanche forecasting, *J. Glaciol.*, *38*, 13–22.
Bryant, A., and T. Painter (2010), Radiative forcing by dust in snowmelt-dominated hydrologic systems using coupled satellite and in situ measurements, paper presented at 78th Western Snow Conference, pp. 43–47.
Brzoska, J.-B., C. Coléou, and B. Lesaffre (1998), Thin-sectioning of wet snow after flash-freezing, *J. Glaciol.*, *44*(146), 54–62.
Budd, W., W. Dingle, and U. Radok (1966), The Byrd snow drift project: Outline and basic results, in *Studies in Antarctic Meteorology*, vol. 9, edited by M. J. Rubin, pp. 71–134, AGU, Washington, D. C.
Bull, C. (1956), The use of the Rammsonde as an instrument for determining the density of firn, *J. Glaciol.*, *2*, 714–718.
Buser, O. (1986), A rigid-frame model of porous media for the acoustic impedance of snow, *J. Sound Vib.*, *111*(1), 71–92.
Buser, O., and W. Good (1986), Acoustic, geometric and mechanical parameters of snow, in *International Symposium on Avalanche Formation, Movement and Effects*, vol. 162, edited by B. Salm and H. Gubler, pp. 61–71, IAHS Publ., Davos, Switz.
Caillet, A., F. D'Aillon, and I. Zawadzki (1979), An ultrasound low-power sonar for snow thickness measurements, paper presented at 36th Eastern Snow Conference, pp. 108–116.
Callaghan, T. V., et al. (2011), Multiple effects of changes in Arctic snow cover, *AMBIO*, *40*(1), 32–45, doi:10.1007/s13280-011-0213-x.
Camp, P., and D. LaBrecque (1992), Determination of the water content of snow by dielectric measurements, CRREL report 91-18, CRREL, Hanover, N. H.
Carmagnola, C. M., S. Morin, M. Lafaysse, F. Domine, B. Lesaffre, Y. Lejeune, G. Picard, and L. Arnaud (2014), Implementation and evaluation of prognostic representations of the optical diameter of snow in the SURFEX/ISBA-Crocus detailed snowpack model, *Cryosphere*, *8*(2), 417–437, doi:10.5194/tc-8-417-2014.
Carroll, T. (1978), Liquid water distribution in a high altitude spring snowpack, in *Avalanche Control, Forecasting and Safety: Proceedings of a Workshop Held in Banff, Alberta, 1–4 November 1976*, edited by R. I. Perla, pp. 177–185, Natl. Res. Council of Canada, Ottawa.
Carroll, S. S., and T. R. Carroll (1989), Effect of uneven snow cover on airborne snow water equivalent estimates obtained by measuring terrestrial gamma radiation, *Water Resour. Res.*, *25*(7), 1505–1510, doi:10.1029/WR025i007p01505.
Carslaw, H. S., and J. C. Jaeger (1959), *Conduction of Heat in Solids*, 2nd ed., Clarendon Press, Oxford, U. K.
Castebrunet, H., N. Eckert, G. Giraud, Y. Durand, and S. Morin (2014), Projected changes of snow conditions and avalanche activity in a warming climate: The French Alps over the 2020–2050 and 2070–2100 periods, *Cryosphere*, *8*(5), 1673–1697, doi:10.5194/tc-8-1673-2014.
Charlton, M. B., and N. W. Arnell (2014), Assessing the impacts of climate change on river flows in England using the UKCP09 climate change projections, *J. Hydrol.*, *519*, 1723–1738, doi:10.1016/j.jhydrol.2014.09.008.
Chritin, V., R. Bolognesi, and H. Gubler (1999), FlowCapt: A new acoustic sensor to measure snowdrift and wind velocity for avalanche forecasting, *Cold Reg. Sci. Technol.*, *30*(1–3), 125–133, doi:10.1016/S0165-232X(99)00012-9.
Chu, V. W. (2014), Greenland ice sheet hydrology: A review, *Prog. Phys. Geogr.*, *38*(1), 19–54, doi:10.1177/0309133313507075.
Church, J. E. (1933), Snow surveying: Its principles and possibilities, *Geogr. Rev.*, *23*(4), 529–563, doi:10.2307/209242.
Church, J. E. (1948), The evolution of snow-melt by dyes and drip-pan, in *International Association of Hydrological Sciences, General Assembly of Oslo, Tome 2*, pp. 115–117, IASH Press, Oslo.
Cierco, F.-X., F. Naaim-Bouvet, and H. Bellot (2007), Acoustic sensors for snowdrift measurements: How should they be used for research purposes?, *Cold Reg. Sci. Technol.*, *49*(1), 74–87, doi:10.1016/j.coldregions.2007.01.002.
Clagett, G., and R. McClure (1994), Northern latitude snow pilow installation procedures, paper presented at 62nd Western Snow Conference, pp. 143–146.
Cline, D. (1993), Measuring alpine snow depths by digital photogrammetry: Part 1. Conjugate point identification, paper presented at 61st Western Snow Conference, pp. 265–271.
Codd, A. R. (1959), The photocanopyometer, paper presented at 27th Western Snow Conference, pp. 17–21.
Colbeck, S. (1972), A theory of water percolation in snow, *J. Glaciol.*, *11*(63), 369–385.
Colbeck, S. (1974), Water flow through snow overlying an impermeable boundary, *Water Resour. Res.*, *10*(1), 119–123.
Colbeck, S. (1975), A theory for water flow through a layered snowpack, *Water Resour. Res.*, *11*(2), 261–266.
Colbeck, S. (1976a), An analysis of water flow in dry snow, *Water Resour. Res.*, *12*, 523–527.
Colbeck, S. (1976b), On the use of tensiometers in snow hydrology, *J. Glaciol.*, *17*(75), 135–140.

Colbeck, S. (1977), Short-term forecasting of water run-off from snow and ice, *J. Glaciol.*, *19*(81), 571–588.
Colbeck, S. (1978), The difficulties of measuring the water saturation and porosity of snow, *J. Glaciol.*, *20*(82), 189–201.
Colbeck, S. (1982), An overview of seasonal snow metamorphism, *Rev. Geophys.*, *20*(1), 45–61.
Colbeck, S. (1986a), Classification of seasonal snow cover crystals, *Water Resour. Res.*, *22*(9S), 59S–70S, doi:10.1029/WR022i09Sp0059S.
Colbeck, S. (1986b), Snow metamorphism and classification, in *Seasonal Snowcovers: Physics, Chemistry, Hydrology*, edited by H. G. Jones and W. J. Orville-Thomas, pp. 1–35, D. Reidel, Netherlands.
Colbeck, S. (1989a), Snow-crystal growth with varying surface temperatures and radiation penetration, *J. Glaciol.*, *35*(119), 23–29.
Colbeck, S. C. (1989b), Air movement in snow due to windpumping, *J. Glaciol.*, *35*, 209–213.
Colbeck, S. C. (1991), The layered character of snow covers, *Rev. Geophys.*, *29*(1), 81–96.
Colbeck, S. C. (1997), A review of sintering in seasonal snow, CRREL Rep. 97-10, Cold Regions Research and Engineering Laboratory, Hanover, N. H.
Colbeck, S., and E. Anderson (1982), The permeability of a melting snow cover, *Water Resour. Res.*, *18*(4), 904–908.
Coléou, C., and B. Lesaffre (1998), Irreducible water saturation in snow: Experimental results in a cold laboratory, *Ann. Glaciol.*, *26*, 64–68.
Collyer, A., and D. Clegg (1998), *Rheological Measurement*, Springer, Dordrecht, Netherlands.
Conway, H., and J. Abrahamson (1984a), Snow stability index, *J. Glaciol.*, *30*(106), 321–327.
Conway, H., and J. Abrahamson (1984b), Air permeability as a textural indicator of snow, *J. Glaciol.*, *30*(106), 328–333.
Conway, H., and R. Benedict (1994), Infiltration of water into snow, *Water Resour. Res.*, *30*, 641–649.
Corripio, J. G. (2004), Snow surface albedo estimation using terrestrial photography, *Int. J. Remote Sens.*, *25*(24), 5705–5729, doi:10.1080/01431160410001709002.
Cousins, J. J., and J. P. Newell (2005), A political-industrial ecology of water supply infrastructure for Los Angeles, *Geoforum*, *58*, 38–50, doi:10.1016/j.geoforum.2014.10.011.
Cox, L., L. Bartree, A. Crook, P. Farnes, and J. Smith (1978), The care and feeding of snow pillows, paper presented at 46th Western Snow Conference, pp. 40–47.
Crook, A., and T. Freeman (1973), A comparison of techniques of sampling the arctic-subarctic snowpack in Alaska, paper presnted at 41st Western Snow Conference, pp. 62–68.
Dahe, Q., L. Shiyin, and L. Peiji (2006), Snow cover distribution, variability, and response to climate change in western China, *J. Clim.*, *19*(9), 1820–1833, doi:10.1175/JCLI3694.1.
Daly, S. F., R. Davis, E. Ochs, and T. Pangburn (2000), An approach to spatially distributed snow modelling of the Sacramento and San Joaquin Basins, California, *Hydrol. Process.*, *14*(18), 3257–3271, doi:10.1002/1099-1085(20001230)14:18<3257::AID-HYP199>3.0.CO;2-Z.
Davis, R. (1973), Operational snow sensors, paper presented at 30th Eastern Snow Conference, pp. 57–70.
Davis, R., and J. Dozier (1984), Snow wetness measurement by fluorescent dye dilution, *J. Glaciol.*, *30*, 362–363.
Davis, R., and J. Dozier (1987), Measurement of snow grain properties, in *Seasonal Snowcovers: Physics, Chemistry, Hydrology*, edited by H. G. Jones and W. J. Orville-Thomas, pp. 63–74, D. Reidel, Dordrecht, Netherlands.
Davis, R., J. Dozier, E. LaChapelle, and R. Perla (1985), Field and laboratory measurements of snow liquid water by dilution, *Water Resour. Res.*, *21*(9), 1415–1420.
Davis, R., T. Pangburn, S. Daly, E. Ochs, J. P. Hardy, E. Bryant, and P. Pugner (1999), Can satellite snow maps, ground measurements and modeling improve water management and control in the King's River Basin, California?: Efforts toward finding the answer, paper presented at 67th Western Snow Conference, pp. 54–61.
Debeer, C. M., and J. W. Pomeroy (2009), Modelling snow melt and snowcover depletion in a small alpine cirque, Canadian Rocky Mountains, *Hydrol. Process.*, *23*, 2584–2599, doi:10.1002/hyp.7346.
DeBeer, C. M., and J. W. Pomeroy (2010), Simulation of the snowmelt runoff contributing area in a small alpine basin, *Hydrol. Earth Syst. Sci.*, *14*(7), 1205–1219, doi:10.5194/hess-14-1205-2010.
Deems, J. S., T. H. Painter, and D. C. Finnegan (2013), Lidar measurement of snow depth: A review, *J. Glaciol.*, *59*(215), 467–479, doi:10.3189/2013JoG12J154.
DeMontmollin, V. (1982), Shear tests on snow explained by fast metamorphism, *J. Glaciol.*, *28*(98), 187–198.
Denoth, A. (1980), The pendular-funicular liquid transition in snow, *J. Glaciol.*, *25*(91), 93–97.
Denoth, A. (1982), The pendular-funicular liquid transition and snow metamorphism, *J. Glaciol.*, *28*(99), 357–364.
Denoth, A. (1989), Snow dielectric measurements, *Adv. Space Res.*, *9*(1), 233–243.
Denoth, A. (1994), An electronic device for long-term snow wetness recording, *Ann. Glaciol.*, *19*, 104–106.
Denoth, A. (1999), Wet snow pendular regime: The amount of water in ring-shaped configurations, *Cold Reg. Sci. Technol.*, *30*(1–3), 13–18, doi:10.1016/S0165-232X(99)00007-5.
Denoth, A., and I. Wilhelmy (1988), Snow dielectric devices and field applications, paper presented at International Snow Science Workshop, pp. 203–206, Whistler, 12-15 Oct.
Denoth, A., A. Foglar, P. Weiland, C. Mätzler, H. Aebischer, M. Tiuri, and A. Sihvola (1984), A comparative study of instruments for measuring the liquid water content of snow, *J. Appl. Phys.*, *56*(7), 2154–2160, doi:10.1063/1.334215.
Dingman, S. L. (2015), *Physical Hydrology*, 3rd ed., Waveland Press, Long Grove, Ill.
Domine, F., R. Salvatori, L. Legagneux, R. Salzano, M. Fily, and R. Casacchia (2006), Correlation between the specific surface area and the short wave infrared (SWIR) reflectance of snow, *Cold Reg. Sci. Technol.*, *46*(1), 60–68, doi:10.1016/j.coldregions.2006.06.002.
Dowd, T., and R. Brown (1986), A new instrument for determining strength profiles in snow cover, *J. Glaciol.*, *32*(111), 299–301.
Dozier, J., and S. G. Warren (1982), Effect of viewing angle on the infrared brightness temperature of snow, *Water Resour. Res.*, *18*(5), 1424–1434.
Dozier, J., R. Davis, and R. Perla (1987), On the objective analysis of snow microstructure, in *Avalanche Formation, Movement and Effects (Proceedings of the Davos Symposium, September 1986), IASH Publication 162*, edited by B. Salm and H. Gubler, pp. 49–58, International Association of Hydrological Sciences, Wallingford, Oxon, U. K.
Dunne, T., A. Price, and S. Colbeck (1976), The generation of runoff from subarctic snowpacks, *Water Resour. Res.*, *12*(4), 677–685.
Dutra, E., Viterbo P., Miranda P. M. A., and Balsamo G. (2012), Complexity of snow schemes in a climate model and its impact on surface energy and hydrology, *J. Hydrometeorol.*, *13*(2), 521–538, doi:10.1175/JHM-D-11-072.1.
Dvornikov, Y., A. Khomutov, D. Mullanurov, K. Ermokhina, A. Gubarkov, and M. Leibman (2015), GIS and field data based modelling of snow water equivalent in shrub tundra, *Fennia-Int. J. Geogr.*, *193*(1), 53–65, doi:10.11143/46363.
Dyck, G. (1969), *Comparison of Snow Measurements, Internal Report, Division of Hydrology, College of Engineering, University of Saskatchewan*, Univ. of Saskatchewan, Saskatoon, Canada.
Earl, W., G. Grey, H. Conway, and J. Abrahamson (1985), Remote sensing of snow accumulation, *Cold Reg. Sci. Technol.*, *11*(2), 199–202, doi:10.1016/0165-232X(85)90019-9.

Edey, S. (1985), Remote monitoring of depth of snow on ground with a micrologger, paper presented at Snow Property Measurements Workshop, pp. 207–214, 1–3 April.
Eisen, O., et al. (2008), Ground-based measurements of spatial and temporal variability of snow accumulation in East Antarctica, *Rev. Geophys.*, *46*, RG2001, doi:10.1029/2006RG000218.
Elder, K., M. Gray, P. Major, and C. Nyberg (1999), Measuring and monitoring snow depth using the Global Positioning System, paper presented at 67th Western Snow Conference, pp. 104–113.
Ellerbruch, D., and H. Boyne (1980), Snow stratigraphy and water equivalence measured with an active microwave system, *J. Glaciol.*, *26*(94), 225–233.
Ellis, C. R., J. W. Pomeroy, R. L. Essery, and T. E. Link (2011), Effects of needleleaf forest cover on radiation and snowmelt dynamics in the Canadian Rocky Mountains, *Can. J. For. Res.*, *41*(3), 608–620, doi:10.1139/X10-227.
Engman, E. T. (1966), Review of snow measuring instrumentation and evaluation of a pressure pillow snow-measuring device, paper presented at 23rd Eastern Snow Conference, pp. 1–17.
Essery, R., and J. Pomeroy (2004), Implications of spatial distributions of snow mass and melt rate for snow-cover depletion: Theoretical considerations, *Ann. Glaciol.*, *38*(1), 261–265, doi:10.3189/172756404781815275.
Essery, R., J. Pomeroy, C. Ellis, and T. Link (2008a), Modelling longwave radiation to snow beneath forest canopies using hemispherical photography or linear regression, *Hydrol. Process.*, *22*(15), 2788–2800, doi:10.1002/hyp.6930.
Essery, R., P. Bunting, A. Rowlands, N. Rutter, J. Hardy, R. Melloh, T. Link, D. Marks, and J. Pomeroy (2008b), Radiative transfer modeling of a coniferous canopy characterized by airborne remote sensing, *J. Hydrometeorol.*, *9*(2), 228–241, doi:10.1175/2007JHM870.1.
Essery, R., N. Rutter, J. Pomeroy, R. Baxter, M. Stähli, D. Gustafsson, A. Barr, P. Bartlett, and K. Elder (2009), SNOWMIP2: An evaluation of forest snow process simulations, *Bull. Am. Meteorol. Soc.*, *90*(8), 1120–1135, doi:10.1175/2009BAMS2629.1.
European Environment Agency (2009), Regional climate change and adaptation: The Alps facing the challenge of changing water resources, EEA Rep. 8/2009, Office for Official Publications of the European Communities, Luxemboug.
Fang, X., and J. W. Pomeroy (2008), Drought impacts on Canadian prairie wetland snow hydrology, *Hydrol. Process.*, *22*(15), 2858–2873.
Farnes, P. (1967), Criteria for determining mountain snow pillow sites, paper presented at 35th Western Snow Conference, pp. 59–62.
Farnes, P., and J. Rompel (1969), Montana telemetry system, paper presented at 37th Western Snow Conference, pp. 102–107.
Farnes, P., B. Goodison, N. Peterson, and R. Richards (1980), Proposed metric snow samplers, paper presented at 48th Western Snow Conference, pp. 107–119.
Farnes, P., N. Peterson, B. Goodison, and R. Richards (1982), Metrification of manual snow sampling equipment, paper presented at 50th Western Snow Conference, pp. 120–132.
Fassnacht, S., C. Heun, J. López-Moreno, and J. Latron (2010), Variability of snow density measurements in the Rio Esera Valley, Pyrenees Mountains, Spain, *Cuadernos de Investigación Geográfica*, *36*(1), 59–72.
Fassnacht, S. R., S. Helfrich, D. Lampkin, K. Dressler, R. Bales, E. Halper, D. Reigle, and B. Imam (2001), Snowpack modelling of the Salt Basin with water management implications, *Proc. Western Snow Conf.*, *69*, 65–76.
Fassnacht, S. R., J. D. Stednick, J. S. Deems, and M. V. Corrao (2009), Metrics for assessing snow surface roughness from digital imagery, *Water Resour. Res.*, *45*, W00D31, doi:10.1029/2008WR006986.
Ferguson, S. A., and E. R. LaChapelle (2003), *The ABCs of Avalanche Safety*, The Mountaineers Books, Seattle, Wash.
Fierz, C., R. Armstrong, Y. Durand, P. Etchevers, E. Greene, D. McClung, K. Nishimura, P. Satyawali, and S. A. Sokratov (1999), *The International Classification for Seasonal Snow on the Ground. IHP-VII Technical Documents in Hydrology N° 83, IACS Contribution N° 1, UNESCO-IHP, Paris*, UNESCO, Paris.
Fisk, D. (1986), Method of measuring liquid water mass fraction of snow by alcohol solution, *J. Glaciol.*, *32*(112), 538–539.
Fohn, P. M. (1980), Snow transport over mountain crests, *J. Glaciol.*, *26*(94), 469–480.
Font, D., F. Naaim-Bouvet, and M. Roussel (1998), Drifting-snow acoustic detector: Experimental tests in La Molina, Spanish Pyrenees, *Ann. Glaciol.*, *26*, 221–224.
Fortin, R., and R. Fortier (2001), Tomographic imaging of a snowpack, paper presented at 58th Annual Meeting- Eastern Snow Conference, Ottawa, Ontario, Canada.
Fortin, G., G. Jones, M. Bernier, and M. Schneebeli (2002), Changes in the structure and permeability of artificial ice layers containing florescent tracer in cold and wet snow cover, *Proc. Eastern Snow Conf.*, *59*, 257–266.
Fowler, W. (1974), Thermal conductivity-basis of a potential method for determining in situ snow density, *Proc. Western Snow Conf.*, *42*, 46–52.
Frankenstein, S., A. Sawyer, and J. Koeberle (2008), Comparison of FASST and SNTHERM in three snow accumulation regimes, *J. Hydrometeorol.*, *9*(6), 1443–1463, doi:10.1175/2008JHM865.1.
Frei, A., M. Tedesco, S. Lee, J. Foster, D. K. Hall, R. Kelly, and D. A. Robinson (2012), A review of global satellite-derived snow products, *Adv. Space Res.*, *50*(8), 1007–1029, doi:10.1016/j.asr.2011.12.021.
Gallet, J.-C., F. Domine, C. S. Zender, and G. Picard (2009), Measurement of the specific surface area of snow using infrared reflectance in an integrating sphere at 1310 and 1550 nm, *Cryosphere*, *3*(2), 167–182, doi:10.5194/tc-3-167-2009.
Garen, D. C., and D. Marks (2005), Spatially distributed energy balance snowmelt modelling in a mountainous river basin: Estimation of meteorological inputs and verification of model results, *J. Hydrol.*, *315*(1–4), 126–153, doi:10.1016/j.jhydrol.2005.03.026.
Garrett, T. J., E. H. Bair, C. J. Fallgatter, K. Shkurko, R. E. Davis, and D. Howlett (2012), The multi-angle snowflake camera, paper presented at International Snow Science Workshop, 16–21 Sept.
Gary, H. (1967), Density variation in a snowpack of northern New Mexico, *Proc. Western Snow Conf.*, *35*, 6–10.
Gay, L. (1962), Measuring snowpack properties with radioactive sources, *Proc. Western Snow Conf.*, *30*, 14–19.
Gerdel, R. W. (1952), The development of the radioactive snow gauge, *Proc. Eastern Snow Conf.*, *9*, 1–12.
Gerdel, R. (1954), The storage and transmission of water in snow, *Proc. Eastern Snow Conf.*, *10-11*, 18–21.
Gerdel, R. W., B. L. Hansen, and W. C. Cassidy (1950), The use of radioisotopes for the measurement of the water equivalent of a snow pack, *Trans. AGU*, *31*, 449–453, doi:10.1029/TR031i003p00449.
Gerland, S., H. Oerter, J. Kipfstuhl, F. Wilhelms, H. Miller, and W. Miners (1999), Density log of a 181 m long ice core from Berkner Island, Antarctica, *Ann. Glaciol.*, *29*(1), 215–219, doi:10.3189/172756499781821427.
Gluns, D., and G. Rose (1992), An improved carrying case for snow tubes, *Proc. Western Snow Conf.*, *60*, 146–149.
Gobiet, A., S. Kotlarski, M. Beniston, G. Heinrich, J. Rajczak, and M. Stoffel (2014), 21st century climate change in the European Alps—A review, *Sci. Total Environ.*, *493*, 1138–1151, doi:10.1016/j.scitotenv.2013.07.050.
Good, W. (1987), Thin sections, serial cuts and 3-D analysis of snow, in *Avalanche Formation, Movement and Effects (Proceedings of the Davos Symposium, September 1986), IASH Publication No. 162*, pp. 35–48, IAHS Press, Wallingford, Oxon, U. K.

Good, W., and G. Krusi (1992), Micro- and macro-analyses of stratigraphic snow profiles, paper presented at International Snow Science Workshop, pp. 1–9, 4–8 Oct.
Goodison, B. (1975), Standardization of snow course data: Reporting and publishing, *Proc. Eastern Snow Conf.*, *32*, 12–23.
Goodison, B. (1978), Accuracy of snow samplers for measuring shallow snowpacks: An update, *Proc. Eastern Snow Conf.*, *35*, 36–49.
Goodison, B. (1985), The impact of automation on winter precipitation measurement, in *Proceedings of the Snow Properties Measurement Workshop*, pp. 471–490, Lake Louise, Alberta.
Goodison, B., H. Ferguson, and G. McKay (1981), Measurement and data analysis, in *Handbook of Snow: Principles, Processes, Management and Use*, pp. 191–274, Pergamon Press Canada, Toronto, Canada.
Goodison, B., B. Wilson, K. Wu, and J. Metcalfe (1984), An inexpensive remote snow-depth gauge: An assessment, *Proc. Western Snow Conf.*, *52*, 188–191.
Goodison, B., R. Metcalf, R. Wilson, and K. Jones (1988), The Canadian automatic snow depth sensor: A performance update, *Proc. Western Snow Conf.*, *56*, 178–181.
Gordon, M., and P. A. Taylor (2009), Measurements of blowing snow. Part I: Particle shape, size distribution, velocity, and number flux at Churchill, Manitoba, Canada, *Cold Reg. Sci. Technol.*, *55*(1), 63–74.
Gordon, M., S. Savelyev, and P. A. Taylor (2009), Measurements of blowing snow. Part II: Mass and number density profiles and saltation height at Franklin Bay, NWT, Canada, *Cold Reg. Sci. Technol.*, *55*(1), 75–85.
Granberg, H., and C. Kingsbury (1984), Tests of new snow density samplers, *Proc. Eastern Snow Conf.*, *41*, 224–228.
Granger, R., and D. M. Gray (1990), A net radiation model for calculating daily snowmelt in open environments, *Nord. Hydrol.*, *21*, 217–234.
Granlund, N., D. Gustafson, J. Feiccabrino, and A. Lundberg (2007), Laboratory test of snow wetness influence on impulse radar amplitude damping, *Proc. Western Snow Conf.*, *75*, 151–155.
Gray, D., and P. Landine (1988), An energy-budget snowmelt model for the Canadian Prairies, *Can. J. Earth Sci.*, *25*(8), 1292–1303.
Gray, D., D. Norum, and G. Dyck (1970a), Snow measurement in the prairie environment, *Can. Agric. Eng.*, *12*(1), 38–41.
Gray, D. M., and D. H. Male (Eds.) (1981), *Handbook of Snow: Principles, Processes, Management and Use*, edited by D. M. Gray and D. H. Male, Pergamon Press Canada, Toronto, Canada.
Gray, D. M., D. Norum, and G. Dyck (1970b), *Densities of Prairie Snowpacks, Research Paper No. 2*, Division of Hydrology, Univ. of Saskatchewan, Division of Hydrology, Univ. of Saskatchewan, Saskatoon, Canada.
Greenan, H., and E. Anderson (1984), A snowmelt lysimeter for research applications, *Proc. Eastern Snow Conf.*, *41*, 209–218.
Grenfell, T. C. (1983), A visible and near-infrared scanning photometer for field measurements of spectral albedo and irradiance under polar conditions, *J. Glaciol.*, *27*(97), 476–481.
Grenfell, T. C., S. G. Warren, and P. C. Mullen (1994), Reflection of solar radiation by the Antarctic snow surface at ultraviolet, visible, and near-infrared wavelengths, *J. Geophys. Res.*, *99*(D9), 18,669–18,684, doi:10.1029/94JD01484.
Gubler, H. (1981a), An electronic remote snow-drift gauge, *J. Glaciol.*, *27*, 164–174.
Gubler, H. (1981b), An inexpensive remote snow-depth gauge based on ultrasonic wave reflection from the snow surface, *J. Glaciol.*, *27*, 157–163.
Gubler, H., and M. Hiller (1984), The use of microwave FMCW radar in snow and avalanche research, *Cold Reg. Sci. Technol.*, *9*(2), 109–119, doi:10.1016/0165-232X(84)90003-X.
Halliday, I. (1950), The liquid water content of snow measurement in the field, *J. Glaciol.*, *1*(7), 357–361.
Hallikainen, M., F. Ulaby, and M. Abdelrazik (1986), Dielectric properties of snow in the 3 to 37 GHz range, *IEEE Trans. Antennas Propag.*, *34*, 1329–1340, doi:10.1109/TAP.1986.1143757.
Halpin, M. A., and J. A. Bissonette (1988), Influence of snow depth on prey availability and habitat use by red fox, *Can. J. Zool.*, *66*(3), 587–592, doi:10.1139/z88-086.
Harding, R. J., and J. W. Pomeroy (1996), The energy balance of the winter boreal landscape, *J. Clim.*, *9*, 2778–2787.
Hardy, J., and D. Albert (1993), The permeability of temperate snow: Preliminary links to microstructure, *Proc. Eastern Snow Conf.*, *50*, 149–156.
Härer, S., M. Bernhardt, J. G. Corripio, and K. Schulz (2013), PRACTICE — Photo Rectification And ClassificaTIon SoftwarE (V.1.0), *Geosci. Model Dev.*, *6*(3), 837–848, doi:10.5194/gmd-6-837-2013.
Harper, J. T., and J. H. Bradford (2003), Snow stratigraphy over a uniform depositional surface: Spatial variability and measurement tools, *Cold Reg. Sci. Technol.*, *37*(3), 289–298, doi:10.1016/S0165-232X(03)00071-5.
Harr, R. (1981), Some characteristics and consequences of snowmelt during rainfall in western Oregon, *J. Hydrol.*, *53*, 277–304.
Harshburger, B., T. Blandford, K. Humes, V. Walden, and B. Moore (2005), Evaluation of enhancements to the snowmelt runoff model, *Proc. Western Snow Conf.*, *2005*, 57–63.
Haupt, H. F. (1969), A simple snowmelt lysimeter, *Water Resour. Res.*, *5*(3), 714–718, doi:10.1029/WR005i003p00714.
Havens, S., H. Marshall, C. Pielmeier, and K. Elder (2013), Automatic grain type classification of snow micro penetrometer signals with random forests, *IEEE Trans. Geosci. Remote Sens.*, *51*(6), 3328–3335, doi:10.1109/TGRS.2012.2220549.
Hawley, R. L., and E. M. Morris (2006), Borehole optical stratigraphy and neutron-scattering density measurements at Summit, Greenland, *J. Glaciol.*, *52*(179), 491–496, doi:10.3189/172756506781828368.
Hedstrom, N. R., and J. W. Pomeroy (1998), Measurements and modelling of snow interception in the boreal forest, *Hydrol. Process.*, *12*(10-11), 1611–1625, doi:10.1002/(SICI)1099-1085(199808/09)12:10/11<1611::AID-HYP684>3.0.CO;2-4.
Heggli, M., B. Köchle, M. Matzl, B. Pinzer, F. Riche, S. Steiner, D. Steinfeld, and M. Schneebeli (2011), Measuring snow in 3-D using x-ray tomography: Assessment of visualization techniques, *Ann. Glaciol.*, *52*(58), 231–236, doi:10.3189/172756411797252202.
Helgason, W., and J. Pomeroy (2012a), Problems closing the energy balance over a homogeneous snow cover during midwinter, *J. Hydrometeorol.*, *13*(2), 557–572, doi:10.1175/JHM-D-11-0135.1.
Helgason, W., and J. W. Pomeroy (2012b), Characteristics of the near-surface boundary layer within a mountain valley during winter, *J. Appl. Meteorol. Climatol.*, *51*(3), 583–597, doi:10.1175/JAMC-D-11-058.1.
Henderson, T. (1953), The use of aerial photographs of snow depth markers in water supply forecasting, *Proc. Western Snow Conf.*, *21*, 44–47.
Hermann, A. (1978), A recording snow lysimeter, *J. Glaciol.*, *20*(82), 209–213.
Hershey, B., and L. F. Osborne (2006), Disdrometer data use in analyzing blowing snow characteristics within the roadway environment. paper presented at AMS Extended Abstract, 22nd International Conference on Interactive Information Processing Systems for Meteorology, Oceanography, and Hydrology.
Hodge, A. J., H. Huxley, and D. Spiro (1954), A simple new microtome for ultrathin sectioning, *J. Histochem. Cytochem.*, *2*, 54–61.
Hollung, W., W. Rogers, and J. A. Businger (1966), Development of a system to measure the density of drifting snow, Tech. Rep., Dep. of Electrical Eng. and Atmos. Sci., Washington, D. C.

Holmgren, J., M. Sturm, N. E. Yankielun, and G. Koh (1998), Extensive measurements of snow depth using FM-CW radar, *Cold Reg. Sci. Technol.*, *27*(1), 17–30, doi:10.1016/S0165-232X(97)00020-7.
Hood, J. L., and M. Hayashi (2010), Assessing the application of a laser rangefinder for determining snow depth in inaccessible alpine terrain, *Hydrol. Earth Syst. Sci.*, *14*(6), 901–910, doi:10.5194/hess-14-901-2010.
Hopkinson, C., L. Chasmer, S. Munro, and M. N. Demuth (2010), The influence of DEM resolution on simulated solar radiation-induced glacier melt, *Hydrol. Process.*, *24*(6), 775–788, doi:10.1002/hyp.7531.
Hori, M., et al. (2006), In-situ measured spectral directional emissivity of snow and ice in the 8–14 μm atmospheric window, *Remote Sens. Environ.*, *100*(4), 486–502.
Hori, M., T. Aoki, T. Tanikawa, A. Hachikubo, K. Sugiura, K. Kuchiki, and M. Niwano (2013), Modeling angular-dependent spectral emissivity of snow and ice in the thermal infrared atmospheric window, *Appl. Opt.*, *52*(30), 7243–7255, doi:10.1364/AO.52.007243.
Howard, R., and R. Stull (2013), IR radiation from trees to a ski run: A case study, *J. Appl. Meteorol. Climatol.*, *52*(7), 1525–1539, doi:10.1175/JAMC-D-12-0222.1.
Howe, C., and R. Houghton (1968), The twin-probe snow density gage, *Proc. Eastern Snow Conf.*, *25*, 61–72.
Hubbard, B., and N. F. Glasser (2005), *Field Techniques in Glaciology and Glacial Geomorphology*, Wiley, Chichester, U. K.
Ishizaka, M. (1993), An accurate measurement of densities of snowflakes using 3-D microphotographs, *Ann. Glaciol.*, *18*, 92–96.
Jaafar, H., and J. Picot (1970), Thermal conductivity of snow by a transient state probe method, *Water Resour. Res.*, *6*(1), 333–335.
Jacobson, M. D. (2010), Inferring snow water equivalent for a snow-covered ground reflector using GPS multipath signals, *Remote Sens.*, *2*(10), 2426–2441, doi:10.3390/rs2102426.
Jairell, R. L. (1975), An improved recording gage for blowing snow, *Water Resour. Res.*, *11*(5), 674–680, doi:10.1029/WR011i005p00674.
Jamieson, B., and C. Johnston (1990), In-situ tensile tests of snow-pack layers, *J. Glaciol.*, *36*(122), 102–106.
Jamieson, J., and C. Johnston (1995), Shear frame stability parameters for large-scale avalanche forecasting, *Ann. Glaciol.*, *18*, 268–273.
Johnson, J., and G. Schaefer (2002), The influence of thermal, hydrologic, and snow deformation mechanisms on snow water equivalent pressure sensor accuracy, *Proc. Western Snow Conf.*, *70*, 111–121.
Johnson, J. B. (1985), Audibility within and outside deposited snow, *J. Glaciol.*, *31*, 136–142.
Johnson, J. B. (2004), A theory of pressure sensor performance in snow, *Hydrol. Process.*, *18*(1), 53–64, doi:10.1002/hyp.1310.
Johnson, J. B., and D. Marks (2004), The detection and correction of snow water equivalent pressure sensor errors, *Hydrol. Process.*, *18*(18), 3513–3525, doi:10.1002/hyp.5795.
Johnson, J. B., A. Gelvin, and G. Schaefer (2007), An engineering design study of electronic snow water equivalent sensor performance, *Proc. Western Snow Conf.*, *75*, 23–30.
Jones, E., A. Rango, and S. Howell (1983), Snowpack liquid water determinations using freezing calorimetry, *Nord. Hydrol.*, *14*(3), 113–126.
Jones, H. G., J. W. Pomeroy, T. D. Davies, M. Tranter, and P. Marsh (1999), CO_2 in arctic snow cover: Landscape form, in-pack gas concentration gradients, and the implications for the estimation of gaseous fluxes, *Hydrol. Process.*, *13*(18), 2977–2989.
Jones, R. (1979), *A Comparison of Centrifuge and Freezing Calorimeter Methods for Measuring Free Water in Snow*, U.S. Dep. of Commerce, National Bureau of Standards, Washington, D. C.
Jones, S. B., J. M. Wraith, and D. Or (2002), Time domain reflectometry measurement principles and applications, *Hydrol. Process.*, *16*(1), 141–153, doi:10.1002/hyp.513.
Jordan, P. (1983), Meltwater movement in a deep snowpack. 1. Field observations, *Water Resour. Res.*, *19*(4), 971–978.
Jordan, R. (1991), *A One-Dimensional Temperature Model for a Snow Cover: Technical Documentation for SNTHERM*, Cold Regions Res. and Eng. Lab., Hanover, N. H.
Jordan, R. E., J. P. Hardy, F. E. Perron, and D. J. Fisk (1999), Air permeability and capillary rise as measures of the pore structure of snow: An experimental and theoretical study, *Hydrol. Process.*, *13*(12–13), 1733–1753, doi:10.1002/(SICI)1099-1085(199909)13:12/13<1733::AID-HYP863>3.0.CO;2-2.
Judson, A., and N. Doesken (2000), Density of freshly fallen snow in the central Rocky Mountains, *Bull. Am. Meteorol. Soc.*, *81*(7), 1577–1587, doi:10.1175/1520-0477(2000)081<1577:DOFFSI>2.3.CO;2.
Julander, R. (2007), Soil surface temperature differences between steel and hypalon pillows, *Proc. Western Snow Conf.*, *75*, 165–169.
Kaempfer, T. U., M. Schneebeli, and S. A. Sokratov (2005), A microstructural approach to model heat transfer in snow, *Geophys. Res. Lett.*, *32*, L21503, doi:10.1029/2005GL023873.
Karpilo, R. (2009), Glacier monitoring techniques, in *Geological Monitoring*, edited by R. Young and L. Norby, pp. 141–162, Geol. Soc. of Am., Boulder, Colo.
Kasurak, A., R. Kelly, and J. King (2012), A simple in-situ sensor for snow grain measurement, *Proc. Eastern Snow Conf.*, *69*, 41–56.
Kattelmann, R. (1984), Snow melt lysimeters: Design and use, *Proc. Western Snow Conf.*, *52*, 68–79.
Kattelmann, R. (2000), Snowmelt lysimeters in the evaluation of snowmelt models, *Ann. Glaciol.*, *31*, 406–410.
Kattelmann, R., B. McGurk, and N. Berg (1983), The isotope profiling snow gauge: Twenty years of experience, *Proc. Western Snow Conf.*, *1983*, 1–8.
Kay, A. L., and S. M. Crooks (2014), An investigation of the effect of transient climate change on snowmelt, flood frequency and timing in northern Britain, *Int. J. Climatol.*, *34*(12), 3368–3381, doi:10.1002/joc.3913.
Kendra, J., F. T. Ulaby, and K. Sarabandi (1994), Snow probe for in-situ determination of wetness and density, *IEEE J. Geosci. Remote Sens.*, *32*(6), 1152–1159.
Kerbrat, M., B. Pinzer, T. Huthwelker, H. W. Gäggeler, M. Ammann, and M. Schneebeli (2008), Measuring the specific surface area of snow with X-ray tomography and gas adsorption: Comparison and implications for surface smoothness, *Atmos. Chem. Phys.*, *8*(5), 1261–1275, doi:10.5194/acp-8-1261-2008.
Kerr, T., M. Clark, J. Hendrikx, and B. Anderson (2013), Snow distribution in a steep mid-latitude alpine catchment, *Adv. Water Resour.*, *55*, 17–24, doi:10.1016/j.advwatres.2012.12.010.
Kinar, N. J., and J. W. Pomeroy (2007), Determining snow water equivalent by acoustic sounding, *Hydrol. Process.*, *21*(19), 2623–2640, doi:10.1002/hyp.6793.
Kinar, N., and J. W. Pomeroy (2008a), Operational techniques for determining SWE by sound propagation through snow: I. General theory, *Proc. Eastern Snow Conf.*, *65*, 309–323.
Kinar, N. J., and J. W. Pomeroy (2008b), Operational techniques for determining SWE by sound propagation through snow: II. Instrumentation and testing, *Proc. Eastern Snow Conf.*, *65*, 19–33.
Kinar, N. J., and J. W. Pomeroy (2009), Automated determination of snow water equivalent by acoustic reflectometry, *IEEE Trans. Geosci. Remote Sens.*, *47*(9), 3161–3167, doi:10.1109/TGRS.2009.2019730.
Kinar, N. J., and J. W. Pomeroy (2015), SAS2: The system for acoustic sensing of snow, *Hydrol. Processes*, doi:10.1002/hyp.10535, in press.

Kitahara, T., M. Shirakashi, and Y. Kajio (1993), Development of a snow fraction meter based on the conductometric method, *Ann. Glaciol.*, *18*, 60–64.
Klauder, J., A. Price, S. Darlington, and W. Albersheim (1960), The theory and design of chirp radars, *Bell Syst. Tech. J.*, *39*(4), 745–808.
Kluitenberg, G. J., R. Horton, and T. Ren (2000), Determining soil water flux and pore water velocity by a heat pulse technique, *Soil Sci. Soc. Am. J.*, *64*(2), 552–560.
Kluitenberg, G. J., J. M. Ham, and K. L. Bristow (1993), Error analysis of the heat pulse method for measuring soil volumetric heat capacity, *Soil Sci. Soc. Am. J.*, *57*, 1444–1451.
Koch, R., and A. Fisher (2000), Effects of inter-annual and decadal-scale climate variability on winter and spring streamflow in western Oregon and Washington, *Proc. Western Snow Conf.*, *68*, 1–11.
Koch, F., M. Prasch, L. Schmid, J. Schweizer, and W. Mauser (2014), Measuring snow liquid water content with low-cost GPS receivers, *Sensors*, *14*(11), 20975–20999, doi:10.3390/s141120975.
Koh, G., and R. Jordan (1995), Sub-surface melting in a seasonal snow cover, *J. Glaciol.*, *41*(139), 474–482.
Koh, G., and J. Lacombe (1986), Optical snow precipitation gauge, *Proc. Eastern Snow Conf.*, *43*, 26–31.
Koh, G., N. Mulherin, J. P. Hardy, R. E. Davis, and A. Twombly (2002), Microwave interaction with snowpack observed at the Cold Land Processes Field Experiment, *Proc. Eastern Snow Conf.*, *59*, 251–254.
Koivusalo, H., and M. Heikinheimo (1999), Surface energy exchange over a boreal snowpack: Comparison of two snow energy balance models, *Hydrol. Process.*, *13*, 14–15, doi:10.1002/(SICI)1099-1085(199910)13:14/15<2395::AID-HYP864>3.0.CO;2-G.
Kondo, J., and H. Yamazawa (1986), Measurement of snow surface emissivity, *Boundary Layer Meteorol.*, *34*(4), 415–416, doi:10.1007/BF00120992.
König, M., J.-G. Winther, and E. Isaksson (2001), Measuring snow and glacier ice properties from satellite, *Rev. Geophys.*, *39*(1), 1–27, doi:10.1029/1999RG000076.
Kovacs, A. (1993), Dyeing of snow surfaces to observe snow structure, *J. Glaciol.*, *39*, 709–711.
Kulessa, B., D. Chandler, A. Revil, and R. Essery (2012), Theory and numerical modeling of electrical self-potential signatures of unsaturated flow in melting snow, *Water Resour. Res.*, *48*, W09511, doi:10.1029/2012WR012048.
Kuroda, M., and I. Hurukawa (1954), Measurement of water content of snow, *IASH Assemblee Generale de Rome*, *39*(IV), 38–41.
LaChapelle, E. R. (1977), *Field Guide to Snow Crystals*, J. J. Douglas, Vancouver, Canada.
Lacroix, P., J.-R. Grasso, J. Roulle, G. Giraud, D. Goetz, S. Morin, and A. Helmstetter (2012), Monitoring of snow avalanches using a seismic array: Location, speed estimation and relationships to meteorological variables, *J. Geophys. Res.*, *117*, F01034, doi:10.1029/2011JF002106.
Lalumiere, L. (2006), Ground penetrating radar for helicopter snow and ice surveys, Canadian Tech. Rep. of Hydrography and Ocean Sci. 248, Bedford Inst. of Oceanogr., Dartmouth, Nova Scotia, Canada.
Landon-Smith, I., B. Woodberry, and E. Wishart (1965), The photoelectric metering of wind-blown snow and a new photoelectric drift snow gauge, Anare interim reports, Series A (IV) Glaciology, Publication No. 79, Melbourne, Australia.
Landry, M. (2012), Water as white coal, in *On Water: Perceptions, Politics, Perils*, edited by A. Kneitz and M. Landry, pp. 7–11, RCC Perspectives, Rachel Carson Center, Munich, Germany.
Lang, R., and W. Harrison (1995), Triaxial tests on dry, naturally occurring snow, *Cold Reg. Sci. Technol.*, *23*, 191–199.
Langham, E. (1973), The occurrence and movement of liquid water in the snowpack, in *Advanced Concepts and Techniques in the Study of Snow and Ice*, edited by H. S. Santeford and J. L. Smith, pp. 67–75, Natl. Acad. of Sci., Washington, D. C.
Langham, E. (1974), Problems of measuring meltwater in the snowpack, *Proc. Eastern Snow Conf.*, *31*, 60–71.
Langham, E. (1981) edited by D. M. Gray and D. H. Male, Physics and properties of snowcover, in *Hanbook of Snow: Principles, Processes, Management and Use*, pp. 275–337, Pergamon Press, Toronto, Canada.
Langlois, A., A. Royer, B. Montpetit, G. Picard, L. Brucker, L. Arnaud, P. Harvey-Collard, M. Fily, and K. Goïta (2010), On the relationship between snow grain morphology and in-situ near infrared calibrated reflectance photographs, *Cold Reg. Sci. Technol.*, *61*(1), 34–42, doi:10.1016/j.coldregions.2010.01.004.
Larson, K. M., E. D. Gutmann, V. U. Zavorotny, J. J. Braun, M. W. Williams, and F. G. Nievinski (2009), Can we measure snow depth with GPS receivers?, *Geophys. Res. Lett.*, *36*(17), L17502, doi:10.1029/2009GL039430.
Lee, S., and J. Rogers (1985), Characterization of snow by acoustic sounding: A feasibility study, *J. Sound Vib.*, *99*(2), 247–266.
Lehning, M., P. Bartelt, B. Brown, T. Russi, U. Stökli, and M. Zimmerli (1999), SNOWPACK model calculations for avalanche warning based upon a new network of weather and snow stations, *Cold Reg. Sci. Technol.*, *30*, 145–157.
Lehning, M., F. Naaim, M. Naaim, B. Brabec, J. Doorschot, Y. Durand, G. Guyomarc'h, J.-L. Michaux, and M. Zimmerli (2002), Snow drift: Acoustic sensors for avalanche warning and research, *Nat. Hazards Earth Syst. Sci.*, *2*(3/4), 121–128, doi:10.5194/nhess-2-121-2002.
Leonard, K. C., L.-B. Tremblay, J. E. Thom, and D. R. MacAyeal (2012), Drifting snow threshold measurements near McMurdo station, Antarctica: A sensor comparison study, *Cold Reg. Sci. Technol.*, *70*, 71–80, doi:10.1016/j.coldregions.2011.08.001.
Libbrecht, K. G. (2005), The physics of snow crystals, *Rep. Prog. Phys.*, *68*(4), 855–895, doi:10.1088/0034-4885/68/4/R03.
Libbrecht, K. G. (2006), *Ken Libbrecht's Field Guide to Snowflakes*, MBI Pub., St. Paul, Minn.
Libbrecht, K. G., and V. M. Tanusheva (1998), Electrically induced morphological instabilities in free dendrite growth, *Phys. Rev. Lett.*, *81*(1), 176–179, doi:10.1103/PhysRevLett.81.176.
Link, T. E., and D. Marks (1999), Point simulation of seasonal snow cover dynamics beneath boreal forest canopies, *J. Geophys. Res.*, *104*(D22), 27,841–27,857, doi:10.1029/1998JD200121.
Liston, G. E., and K. Elder (2006), A distributed snow-evolution modeling system (SnowModel), *J. Hydrometeorol.*, *7*(6), 1259–1276, doi:10.1175/JHM548.1.
Liston, G. E., R. B. Haehnel, M. Sturm, C. A. Hiemstra, S. Berezovskaya, and R. D. Tabler (2007), Simulating complex snow distributions in windy environments using SnowTran-3D, *J. Glaciol.*, *53*, 241–256, doi:10.3189/172756507782202865.
Liu, G., and B. Si (2008), Dual-probe heat pulse method for snow density and thermal properties measurement, *Geophys. Res. Lett.*, *35*, L16404, doi:10.1029/2008GL034897.
Liu, G., and B. Si (2010), Errors analysis of heat pulse probe methods: Experiments and simulations, *Soil Sci. Soc. Am. J.*, *74*(3), 797–803.
Louge, M. Y., R. Foster, N. Jensen, and R. Patterson (1998), A portable capacitance snow sounding instrument, *Cold Reg. Sci. Technol.*, *28*, 73–81.
Lucas, R., and A. Harrison (1990), Snow observation by satellite: A review, *Remote Sens. Rev.*, *4*(2), 285–348, doi:10.1080/02757259009532109.
Luce, C., and D. Tarboton (2001), A modified force-restore approach to modelling snow-surface heat fluxes, *Proc. Western Snow Conf.*, *69*, 103–114.
Luciano, G. L., and M. R. Albert (2002), Bidirectional permeability measurements of polar firn, *Ann. Glaciol.*, *35*, 63–66.

Lundberg, A., C. Richardson-Näslund, and C. Andersson (2006), Snow density variations: Consequences for ground-penetrating radar, *Hydrol. Processes*, *20*(7), 1483–1495, doi:10.1002/hyp.5944.
Lundy, C., and E. Adams (1998), Non-destructive collection of natural snow samples for use with CT scan analysis, paper presented at International Snow Science Workshop, Sun River, Oregon September 1998, vol. 11, pp. 208–213.
Lundy, C., M. Edens, and R. Brown (2002), Measurement of snow density and microstructure using computed microtomography, *J. Glaciol.*, *48*(161), 312–316.
Male, D. (1980), The seasonal snowcover, in *Dynamics of Snow and Ice Masses*, edited by S. Colbeck, pp. 305–395, Academic Press, New York.
Male, D., and D. Gray (1981), Snowcover ablation and runoff, in *Handbook of Snow: Principles, Processes, Management and Use*, edited by D. M. Gray and D. H. Male, pp. 360–436, Pergamon Press Canada, Toronto.
Mann, M. E., and P. H. Gleick (2015), Climate change and California drought in the 21st century, *Proc. Natl. Acad. Sci.*, *112*, 3858–3859, doi:10.1073/pnas.1503667112.
Marks, D., and J. Dozier (1992), Climate and energy exchange at the snow surface in the alpine region of the Sierra Nevada: 2. Snow cover energy balance, *Water Resour. Res.*, *28*(11), 3043–3054.
Marks, D., J. Kimball, D. Tingey, and T. Link (1998), The sensitivity of snowmelt processes to climate conditions and forest cover during rain-on-snow: A case study of the 1996 Pacific Northwest flood, *Hydrol. Processes*, *12*(10–11), 1569–1587, doi:10.1002/(SICI)1099-1085(199808/09)12:10/11<1569::AID-HYP682>3.0.CO;2-L.
Marks, D., K. Cooley, D. Robertson, and A. Winstral (2001), Long-term snow database, Reynolds Creek Experimental Watershed, Idaho, United States, *Water Resour. Res.*, *37*(11), 2835–2838, doi:10.1029/2001WR000416.
Marks, D., and A. Winstral (2001), Comparison of snow deposition, the snow cover energy balance, and snowmelt at two sites in a semiarid mountain basin, *J. Hydrometeorol.*, *2*(3), 213–227, doi:10.1175/1525-7541(2001)002<0213:COSDTS>2.0.CO;2.
Marks, D., A. Winstral, and M. Seyfried (2002), Simulation of terrain and forest shelter effects on patterns of snow deposition, snowmelt and runoff over a semi-arid mountain catchment, *Hydrol. Processes*, *16*(18), 3605–3626, doi:10.1002/hyp.1237.
Marsh, P. (1990), Snow hydrology, in *Northern Hydrology: Canadian Perspectives, NHRI Science Rep. 1*, edited by T. D. Prowse and C. S. L. Ommanney, pp. 37–61, Natl. Water Res. Inst., Saskatoon, Canada.
Marsh, P. (1991), Water flux in melting snow covers, in *Advances in Porous Media*, vol. 1, edited by M. Y. Corapcioglu, pp. 61–124, Elsevier Science Publ., Amsterdam.
Marsh, P., and M.-K. Woo (1985), Meltwater movement in natural heterogeneous snow covers, *Water Resour. Res.*, *21*(11), 1710–1716.
Marsh, P., and M.-K. Woo (1984a), Wetting front advance and freezing of meltwater within a snow cover: 1. Observations in the Canadian Arctic, *Water Resour. Res.*, *20*(12), 1853–1864.
Marsh, P., and M.-K. Woo (1984b), Wetting front advance and freezing of meltwater within a snow cover: 2. A simulation model, *Water Resour. Res.*, *20*(12), 1865–1874.
Marsh, T., A. Black, M. Acreman, and C. Elliot (2000), River flows, in *The Hydrology of the UK: A Study of Change*, edited by M. Acreman, pp. 101–133, Routledge, London.
Marshall, H.-P., and G. Koh (2008), FMCW radars for snow research, *Cold Reg. Sci. Technol.*, *52*(2), 118–131, doi:10.1016/j.coldregions.2007.04.008.
Marshall, H.-P., G. Koh, and R. R. Forster (2004), Ground-based frequency-modulated continuous wave radar measurements in wet and dry snowpacks, Colorado, USA: An analysis and summary of the 2002–03 NASA CLPX data, *Hydrol. Processes*, *18*(18), 3609–3622, doi:10.1002/hyp.5804.
Marshall, H.-P., G. Koh, and R. R. Forster (2005), Estimating alpine snowpack properties using FMCW radar, *Ann. Glaciol.*, *40*, 157–162, doi:10.3189/172756405781813500.
Marshall, H.-P., M. Schneebeli, and G. Koh (2007), Snow stratigraphy measurements with high-frequency FMCW radar: Comparison with snow micro-penetrometer, *Cold Reg. Sci. Technol.*, *47*(1–2), 108–117, doi:10.1016/j.coldregions.2006.08.008.
Martinelli, M., Jr., and A. Ozment (1985), Some strength features of natural snow surfaces that affect snow drifting, *Cold Reg. Sci. Technol.*, *11*(3), 267–283, doi:10.1016/0165-232X(85)90051-5.
Masiokas, M. H., R. Villalba, B. H. Luckman, C. Le Quesne, and J. C. Aravena (2006), Snowpack variations in the central Andes of Argentina and Chile, 1951–2005: Large-scale atmospheric influences and implications for water resources in the region, *J. Clim.*, *19*(24), 6334–6352, doi:10.1175/JCLI3969.1.
Matonse, A., D. Pierson, A. Frei, M. Zion, E. Schneiderman, A. Anandhi, R. Mukundan, and S. Pradhanang (2010), Effects of changes in snow pattern and the timing of runoff on NYC water supply, *Proc. Eastern Snow Conf.*, *67*, 61–71.
Matzl, M., and M. Schneebeli (2006), Measuring specific surface area of snow by near-infrared photography, *J. Glaciol.*, *52*(179), 558–564.
McClung, D. (2011), Analysis of critical length measurements for dry snow slab weak-layer shear fracture, *J. Glaciol.*, *57*(203), 557–566.
McClung, D., and P. Schaerer (2006), *The Avalanche Handbook*, 3rd ed., Mountaineers Books, Seattle, Wash.
McCreight, J. L., E. E. Small, and K. M. Larson (2014a), Snow depth, density, and SWE estimates derived from GPS reflection data: Validation in the western U.S., *Water Resour. Res.*, *50*, 6892–6909, doi:10.1002/2014WR015561.
McCreight, J. L., and E. E. Small (2014b), Modeling bulk density and snow water equivalent using daily snow depth observations, *Cryosphere*, *8*(2), 521–536, doi:10.5194/tc-8-521-2014.
McGurk, B. (1983), Snow temperature profiles in the central Sierra Nevada, paper presented at 51st Western Snow Conference, Colorado Stae Univ., pp. 9–81, Fort Collins, Colo.
McGurk, B. (1992), Propylene glycol and ethanol as a replacement antifreeze for precipitation gauges: Dilution, disposal and safety. paper presented at 60th Western Snow Conference, Jackson, Wyoming, pp. 56–65.
McGurk, B., and R. Kattelmann (1988), Evidence of liquid water flow through snow from thick-section photography, paper presented at 1988 International Snow Science Workshop, Canadian Avalanche Association, pp. 137–139.
McGurk, B., and P. Marsh (1995), Flow-finger continuity in serial thick-sections in a melting Sierran snowpack, in *Biogeochemistry of Seasonally Snow-Covered Catchments, IAHS Publ. No. 228*, edited by K. A. Tonnessen, M. W. Williams, and M. Tranter, pp. 81–88, IAHS Press, Wallingford, Oxfordshire, U. K.
McKay, G., and S. Blackwell (1961), Plains snowpack water equivalent from climatological records. paper presented at 29th Annual Western Snow Conference, April 1961, Spokane, Washington, pp. 27–43.
McKay, G., and B. Findlay (1971), Variation of snow resources with climate and vegetation in Canada. paper presented at 39th Western Snow Conference, Billings, Mont., 20–22 April 1971, pp. 17–26.
Meier, W. N., et al. (2014), Arctic sea ice in transformation: A review of recent observed changes and impacts on biology and human activity, *Rev. Geophys.*, *52*(3), 185–217, doi:10.1002/2013RG000431.
Meikle, H. (2008), *Modern Radar Systems*, Artech House, Boston.

Mellor, M. (1960), Gauging Antarctic drift snow, in *Antarctic Meteorology*, edited by Australian Bureau of Meteorology, 347–354, Pergamon Press, Oxford, U. K.
Metcalfe, R., R. Wilson, and B. Goodison (1987), The use of acoustic ranging devices as snow depth sensors: An assessment. paper presented at 44th Eastern Snow Conference, pp. 203–207.
Michaeux, J., F. Naaim-Bouvet, M. Naaim, and G. Guyomarc'h (2000), The acoustic snowdrift sensor: Interests, calibration and results. paper presented at 2000 International Snow Science Workshop, pp. 390–395.
Miller, R. (1962), Aerial snow depth marker configuration and installation considerations. paper presented at 30th Western Snow Conference, Chayenne, Wyoming, 16–18 April, 1962, pp. 1–15.
Mims, F. M. (2000), *Mims Circuit Scrapbook*, Newnes, Wobourn, Mass.
Mitterer, C., A. Heilig, J. Schweizer, and O. Eisen (2011), Upward-looking ground-penetrating radar for measuring wet-snow properties, *Cold Reg. Sci. Technol.*, *69*(2–3), 129–138, doi:10.1016/j.coldregions.2011.06.003.
Moffitt, J. (1995), Snow plates: Preliminary results, paper presented at 63rd Annual Western Snow Conference, April 1995, Sparks, Nevada, pp. 156–159.
Moldestad, D. A. (2005), Characteristics of liquid water content and snow density in a cross-country race ski track, *Bull. Glaciol. Res.*, *22*, 39–49.
Molnau, M. (1971), Comparison of runoff from a catchment snow pillow and a small forested watershed, *Proc. Western Snow Conf.*, *39*, 39–43.
Molotch, N. P., and R. C. Bales (2006), SNOTEL representativeness in the Rio Grande headwaters on the basis of physiographics and remotely sensed snow cover persistence, *Hydrol. Processes*, *20*(4), 723–739, doi:10.1002/hyp.6128.
Montpetit, B., A. Royer, A. Langlois, M. Chum, P. Cliche, A. Roy, N. Champollion, G. Picard, F. Domine, and R. Obbard (2011), In-situ measurements for snow grain size and shape characterization using optical methods, *Proc. Eastern Snow Conf.*, *68*, 173–188.
Moore, H., K. Attenborough, J. Rogers, and S. Lee (1991), In-situ acoustical investigations of deep snow, *Appl. Acoust.*, *33*(4), 281–301.
Mori, Y., J. W. Hopmans, A. P. Mortensen, and G. J. Kluitenberg (2003), Multi-functional heat pulse probe for the simultaneous measurement of soil water content, solute concentration, and heat transport parameters, *Vadose Zone J.*, *2*(4), 561–571, doi:10.2113/2.4.561.
Morin, S., F. Domine, L. Arnaud, and G. Picard (2010), In-situ monitoring of the time evolution of the effective thermal conductivity of snow, *Cold Reg. Sci. Technol.*, *64*(2), 73–80, doi:10.1016/j.coldregions.2010.02.008.
Morin, S., Y. Lejeune, B. Lesaffre, J.-M. Panel, D. Poncet, P. David, and M. Sudul (2012), An 18-yr long (1993–2011) snow and meteorological dataset from a mid-altitude mountain site (Col de Porte, France, 1325 m alt.) for driving and evaluating snowpack models, *Earth Syst. Sci. Data*, *4*(1), 13–21, doi:10.5194/essd-4-13-2012.
Morris, E. (1981), Field measurement of the liquid water content of snow, *J. Glaciol.*, *27*(95), 175–178.
Morris, E. M. (2008a), A theoretical analysis of the neutron scattering method of measuring snow and ice density, *J. Geophys. Res.*, *113*, F0319, doi:10.1029/2007JF000962.
Morris, E. M. (2008b), Correction to "a theoretical analysis of the neutron scattering method of measuring snow and ice density", *J. Geophys. Res.*, *113*, F4099, doi:10.1029/2008JF001155.
Morris, E. M., and J. D. Cooper (2003), Density measurements in ice boreholes using neutron scattering, *J. Glaciol.*, *49*(167), 599–604, doi:10.3189/172756503781830403.
Morrison, R. (1976), Nuclear techniques applied to hydrology, *Proc. Western Snow Conf.*, *44*, 1–6.
Mount, J. F. (1995), *California Rivers and Streams: The Conflict Between Fluvial Process and Land Use*, Univ. of Calif. Press, Berkeley.
Musselman, K. N., J. W. Pomeroy, and T. E. Link (2015), Variability in shortwave irradiance caused by forest gaps: Measurements, modelling, and implications for snow energetics, *Agric. For. Meteorol.*, *207*, 69–82, doi:10.1016/j.agrformet.2015.03.014.
Naaim-Bouvet, F., H. Bellot, and M. Naaim (2010), Back analysis of drifting-snow measurements over an instrumented mountainous site, *Ann. Glaciol.*, *51*(54), 207–217, doi:10.3189/172756410791386661.
Nakamura, T., O. Abe, R. Hashimoto, and T. Ohta (2010), A dynamic method to measure the shear strength of snow, *J. Glaciol.*, *56*(196), 333–338, doi:10.3189/002214310791968502.
Nakaya, U. (1954), *Snow Crystals: Natural and Artificial*, Harvard Univ. Press, Cambridge, U. K.
Nolan, M., C. F. Larsen, and M. Sturm (2015), Mapping snow-depth from manned-aircraft on landscape scales at centimeter resolution using structure-from-motion photogrammetry, *Cryosphere Discuss.*, *9*(1), 333–381, doi:10.5194/tcd-9-333-2015.
Niang, M., M. Bernier, Y. Gauthier, G. Fortin, E. Van Bochove, M. Stacheder, and A. Brandelik (2003), On the validation of snow densities derived from SNOWPOWER probes in a temperate snow cover in eastern Canada: First results, *Proc. Eastern Snow Conf.*, *60*, 175–187.
O'Brien, H. (1977), Observations of the ultraviolet spectral reflectance of snow, CRREL Rep. 77-27, Cold Regions Res. and Eng. Lab., Hanover, N. H.
O'Brien, H., and G. Koh (1981), Near-infrared reflectance of snow-covered substrates, CRREL Report 81-21, Cold Regions Res. and Eng. Lab., Hanover, N. H.
Oke, T. R. (1992), *Boundary Layer Climates*, 2nd ed., Routledge, London.
Olfert, E. (1970), Modification of a gamma attenuation snow density gauge, Internal Rep., Div. of Hydrology, College of Eng., Univ. of Saskatchewan, Saskatoon, Canada.
O'Neel, S., H. Marshall, D. McNamara, and W. Pfeffer (2007), Seismic detection and analysis of icequakes at Columbia Glacier, Alaska, *J. Geophys. Res.*, *112*, F03S23, doi:10.1029/2006JF000595.
O'Neill, A., and D. M. Gray (1973), Solar radiation penetration through snow, paper presented at UNESCO-WMO-IAHS Symposium on the Role of Snow and Ice in Hydrology, vol. 1, pp. 229–249.
Ord, M. (1968), Some comparisons from the use of radio reporting isotope snow gauges and the snow pressure pillows, paper presented at 36th Western Snow Conference, pp. 89–94.
Osterhuber, R., T. Edens, and B. McGurk (1994), Snow depth measurement using ultrasonic sensors and temperature correction, paper presented at 62nd Western Snow Conference, pp. 159–162.
Osterhuber, R., J. Howle, and G. Bawden (2008), Snow measurement using ground-based tripod laser, paper presented at 2008 Western Snow Conference, pp. 135–135.
Ozeki, T., K. Kose, T. Haishi, S.-I. Nakatsubo, K. Nishimura, and A. Hochikubo (2003), Three-dimensional MR microscopy of snowpack structures, *Cold Reg. Sci. Technol.*, *37*(3), 385–391, doi:10.1016/S0165-232X(03)00078-8.
Painter, T., N. Molotch, M. Cassidy, M. Flanner, and K. Steffen (2007), Contact spectroscopy for determination of stratigraphy of snow optical grain size, *J. Glaciol.*, *53*(180), 121–127.
Painter, T. H., and J. Dozier (2004), Measurements of the hemispherical-directional reflectance of snow at fine spectral and angular resolution, *J. Geophys. Res.*, *109*, D18115, doi:10.1029/2003JD004458.

Painter, T. H., B. Paden, and J. Dozier (2003), Automated spectro-goniometer: A spherical robot for the field measurement of the directional reflectance of snow, *Rev. Sci. Instrum.*, *74*(12), 5179–5188, doi:10.1063/1.1626011.
Palmer, C. L., N. M. Weber, and M. H. Cragin (2011), The analytic potential of scientific data: Understanding re-use value, *Proc. Am. Soc. Inform. Sci. Technol.*, *48*(1), 1–10, doi:10.1002/meet.2011.14504801174.
Pangburn, T., and H. Kim (1984), USACRREL's snow, ice, and frozen ground research at the Sleepers River Research Watershed, *Proc. Eastern Snow Conf.*, *41*, 229–240.
Pangburn, T., and B. Pratt (1980), Measurement of snow water equivalent using a load cell triangle sensor, Tech. Note, U.S. Army Cold Regions Research and Engineering Library, CRREL, Hanover, N. H.
Paulin, G. (1978), Developments in snow measurements with gamma radiation, *Proc. Eastern Snow Conf.*, *35*, 56–62.
Peitzsch, E., K. W. Birkeland, and K. Hansen (2008), Water movement and capillary barriers in a stratified and inclined snowpack, paper presented at 2008 International Snow Science Workshop, pp. 179–187.
Pelto, M. (2004), Temperature-ablation relationships on glaciers and in alpine areas, North Cascades, Washington, *Proc. Eastern Snow Conf.*, *61*, 135–145.
Perla, R. (1969), Strength tests on newly fallen snow, *J. Glaciol.*, *8*, *54*, 427–440.
Perla, R. (1978), *Snow Crystals = Les Cristaux De Neige*, National Hydrology Research Institute Paper, NHRI, Ottawa, Canada.
Perla, R. (1982), Preparation of section planes in snow specimens, *J. Glaciol.*, *28*(98), 199–210.
Perla, R. (1985), Snow in strong or weak temperature gradients. Part II: Section-plane analysis, *Cold Reg. Sci. Technol.*, *11*(2), 181–186, doi:10.1016/0165-232X(85)90016-3.
Perla, R. (1991), Real permittivity of snow at 1 MHz and 0°C, *Cold Reg. Sci. Technol.*, *19*, 215–219.
Perla, R., and J. Banner (1988), Calibration of capacitive cells for measuring water in snow, *Cold Reg. Sci. Technol.*, *15*, 225–231.
Perla, R., and T. Beck (1983), Experience with shear frames, *J. Glaciol.*, *29*(103), 485–491.
Perla, R., and B. Glenne (1981), Skiing, in *Handbook of Snow: Principles, Processes, Management and Use*, edited by D. M. Gray and D. H. Male, pp. 709–740, Pergamon Press, Toronto, Canada.
Perla, R., and E. LaChapelle (1984), Dilution method for measuring liquid water in snow, *Proc. Western Snow Conf.*, *52*, 80–85.
Perla, R., T. Beck, and T. Cheng (1982), The shear strength index of alpine snow, *Cold Reg. Sci. Technol.*, *6*, 11–20.
Perovich, D. (2007), Light reflection and transmission by a temperate snow cover, *J. Glaciol.*, *53*(181), 201–210.
Peterson, N., and A. Brown (1975), Accuracy of snow measurements, *Proc. Western Snow Conf.*, *43*, 1–9.
Petty, G. W. (2006), *A First Course in Atmospheric Radiation*, Sundog, Madison, Wis.
Pfeffer, W., and N. Humphrey (1996), Determination of timing and location of water movement and ice-layer formation by temperature measurements in sub-freezing snow, *J. Glaciol.*, *42*(141), 292–305.
Pielmeier, C., and M. Schneebeli (2003a), Stratigraphy and changes in hardness of snow measured by hand, ramsonde and snow micro penetrometer: A comparison with planar sections, *Cold Reg. Sci. Technol.*, *37*(3), 393–405, doi:10.1016/S0165-232X(03)00079-X.
Pielmeier, C., and M. Schneebeli (2003b), Developments in the stratigraphy of snow, *Surv. Geophys.*, *24*(5–6), 389–416, doi:10.1023/B:GEOP.0000006073.25155.b0.
Pomeroy, J., and E. Brun (2001), Physical properties of snow, in *Snow Ecology: An Interdisciplinary Examination of Snow-Covered Ecosystems*, edited by H. G. Jones et al., pp. 45–126, Cambridge Univ. Press, Cambridge, U. K.
Pomeroy, J., and K. Dion (1996), Winter radiation extinction and reflection in a boreal pine canopy: Measurements and modelling, *Hydrol. Processes*, *10*, 1591–1608.
Pomeroy, J., and B. Goodison (1997), Winter and snow, in *The Surface Climates of Canada*, edited by W. G. Bailey, T. R. Oke, and W. R. Rouse, pp. 68–100, McGill-Queen's University Press, Montreal, Kingston, London, Buffalo, New York.
Pomeroy, J., and D. Gray (1995), Snowcover accumulation, relocation, and management, National Hydrology Research Institute Science Rep. No. 7, Natl. Water Res. Inst., Saskatoon, Canada.
Pomeroy, J., and D. Male (1985), Optical properties and the detection of blowing snow, Division of Hydrology Report for the Symposium on Remote Sensing and Electromagnetic Properties of Snow and Ice, American Geophysical Union Division of Hydrology, Univ. of Saskatchewan, Saskatchewan, Canada.
Pomeroy, J., and R. Schmidt (1993), The use of fractal geometry in modelling intercepted snow accumulation and sublimation. paper presented at 50th Eastern Snow Conference, pp. 1–10.
Pomeroy, J., B. Toth, R. Granger, N. Hedstrom, and R. Essery (2003), Variation in surface energetics during snowmelt in a subarctic mountain catchment, *J. Hydrometeorol.*, *4*, 702–719.
Pomeroy, J., C. Ellis, A. Rowlands, R. Essery, J. Hardy, T. Link, D. Marks, and J. E. Sicart (2008), Spatial variability of shortwave irradiance for snowmelt in forests, *J. Hydrometeorol.*, *9*(6), 1482–1490, doi:10.1175/2008JHM867.1.
Pomeroy, J. W. (1988), Wind transport of snow, PhD thesis, Univ. of Saskatchewan, Division of Hydrology, Department of Agricultural Engineering, Saskatoon, Canada.
Pomeroy, J. W., and R. L. H. Essery (1999), Turbulent fluxes during blowing snow: Field tests of model sublimation predictions, *Hydrol. Processes*, *13*, 2963–2975.
Pomeroy, J. W., and L. Li (2000), Prairie and arctic areal snow cover mass balance using a blowing snow model, *J. Geophys. Res.*, *105*, 26,619–26,634, doi:10.1029/2000JD900149.
Pomeroy, J. W., T. Brown, and D. Male (1987), Measurement of blowing snow properties using optical attenuation devices, in *Proceedings of the Snow Property Measurement Workshop, Lake Louise, Alberta*, edited by P. R. Kry, *Tech. Mem.*, *140*, pp. 347–388, National Research Council of Canada, Ottawa, 1–3 April.
Pomeroy, J. W., Gray D. M., and Landine P. G. (1993), The prairie blowing snow model: Characteristics, validation, operation, *J. Hydrol.*, *144*, 165–192.
Pomeroy, J. W., D. S. Bewley, R. L. H. Essery, N. R. Hedstrom, T. Link, R. J. Granger, J. E. Sicart, C. R. Ellis, and J. R. Janowicz (2006), Shrub tundra snowmelt, *Hydrol. Processes*, *20*(4), 923–941, doi:10.1002/hyp.6124.
Pomeroy, J. W., D. M. Gray, T. Brown, N. R. Hedstrom, W. L. Quinton, R. J. Granger, and S. K. Carey (2007a), The cold regions hydrological model: A platform for basing process representation and model structure on physical evidence, *Hydrol. Processes*, *21*(19), 2650–2667.
Pomeroy, J., D. de Boer, and L. W. Martz (2007b), Hydrology and water resources, in *Saskatchewan: Geographic Perspectives*, edited by B. Thraves et al., pp. 63–80, Canadian Plains Res. Cent., Regina, Canada.
Pomeroy, J. W., M. McDonald, C. DeBeer, and T. Brown (2009a), Modeling alpine snow hydrology in the Canadian Rocky Mountains, paper presented at 77th Annual Meeting of the Western Snow Conference, pp. 3–11.
Pomeroy, J. W., D. Marks, T. Link, C. Ellis, J. Hardy, A. Rowlands, and R. Granger (2009b), The impact of coniferous forest temperature on incoming longwave radiation to melting snow, *Hydrol. Process.*, *23*(17), 2513–2525, doi:10.1002/hyp.7325.

Pomeroy, J. W., M. Bernhardt, and D. Marks (2015), Water resources: Research network to track alpine water, *Nature*, *521*(7550), 156–157, doi:10.1038/521032c.
Porter, J., and G. Horton (2010), Application of snow core and automated remote data collection to monitor SWE in NYC's water supply watershed, paper presented at 67th Annual Eastern Snow Conference, Hancock, Mass., June 8–10, 2010, pp. 87, 91.
Powell, D. (1987), Observations on consistency and reliability of field data in snow survey measurements, paper presented at 55th Annual Meeting Western Snow Conference, Vancouver, B. C., 1987, pp. 69–77.
Powers, D., K. O'Neill, and S. C. Colbeck (1985), Theory of natural convection in snow, *J. Geophys. Res.*, *90*, 10,641–10,649, doi:10.1029/JD090iD06p10641.
Powers, P. (2008), *NOLS Wilderness Mountaineering*, Stackpole Books, Mechanicsburg, Pa.
Price, A., and T. Dunne (1976), Energy balance computations of snowmelt in a subarctic area, *Water Resour. Res.*, *4*(12), 686–694.
Proksch, M., H. Löwe, and M. Schneebeli (2015), Density, specific surface area, and correlation length of snow measured by high-resolution penetrometry, *J. Geophys. Res. Earth Surface*, *120*, 346–362, doi:10.1002/2014JF003266.
Protiva, P., J. Mrkvica, and J. Machac (2009), Sub-nanosecond pulse generator for through-the-wall radar application, paper presented at European Wireless Technology Conference (EuWIT 2009), pp. 230–233.
Pyper, G. (1962), A progress report on radioactive snow gage use, paper presented at 18–19th Eastern Snow Conference, pp. 52–66.
Radionov, V. F., N. N. Bryazgin, E. I. Alexandrov, I. Solovyova, T. C. Grenfell, and University of Washington (1997), The snow cover of the Arctic Basin, No. TR 9701 in Tech. Rep. APL-UW, Appl. Phys. Lab., Univ. Washington, Seattle, Washington.
Rango, A., C. Steele, and L. DeMouche (2010), Infrastructure improvements for snowmelt runoff assessments of climate change impacts on water supplies in the Rio Grande Basin, paper presented at 78th Western Snow Conference, pp. 83–90.
Rees, G. (2006), *Remote Sensing of Snow and Ice*, Taylor and Francis, Boca Raton.
Rees, W. G. (1998), A rapid method for measuring snow surface profiles, *J. Glaciol.*, *44*, 674–675.
Rice, R., T. Painter, and J. Dozier (2007), Snowcover along elevation gradients in the Upper Merced and Tuolumne river basins of the Sierra Nevada of California from MODIS and blended ground data, paper presented at 75th Western Snow Conference, pp. 3–12.
Richardson, S., and F. Salisbury (1977), Plant responses to the light penetrating snow, *Ecology*, *58*, 1152–1158.
Riche, F., and M. Schneebeli (2013), Thermal conductivity of snow measured by three independent methods and anisotropy considerations, *Cryosphere*, *7*, 217–227.
Rittger, K., A. Kahl, and J. Dozier (2011), Topographic distribution of snow water equivalent in the Sierra Nevada. paper presented at 79th Western Snow Conference, pp. 37–46.
Rogers, W. (1968), A photoelectric snow particle counter, *Eos Trans. AGU*, *49*(4), 690.
Roos, M. (1991), A trend of decreasing snowmelt runoff in Northern California, *Proc. Western Snow Conf.*, *59*, 29–36.
Rosenthal, W., and J. Dozier (1996), Automated mapping of Montane snow cover at subpixel resolution from the Landsat Thematic Mapper, *Water Resour. Res.*, *32*, 115–130.
Roulet, R. R., G. A. Maykut, and T. C. Grenfell (1974), Spectrophotometers for the measurement of light in polar ice and snow, *Appl. Opt.*, *13*(7), 1652–1659, doi:10.1364/AO.13.001652.
Ryan, W. A., N. J. Doesken, and S. R. Fassnacht (2008), Preliminary results of ultrasonic snow depth sensor testing for National Weather Service (NWS) snow measurements in the US, *Hydrol. Processes*, *22*(15), 2748–2757, doi:10.1002/hyp.7065.
Sato, T., T. Kimura, T. Ishimaru, and T. Maruyama (1993), Field test of a new snow-particle counter (SPC) system, *Ann. Glaciol.*, *18*, 149–154.
Sauter, K., and B. Tanner (1992), Minimizing measurement errors in automated snowpack profile temperature measurements. paper presented at 60th Western Snow Conference, pp. 36–45.
Sellers, P. J., et al. (1997), BOREAS in 1997: Experiment overview, scientific results, and future directions, *J. Geophys. Res.*, *102*(D24), 28,731–28,769, doi:10.1029/97JD03300.
Schaefer, V. J. (1964), Preparation of permanent replicas of snow, frost, and ice, *Weatherwise*, *17*(6), 278–287, doi:10.1080/00431672.1964.9927022.
Schirmer, M., and B. Jamieson (2014), Limitations of using a thermal imager for snow pit temperatures, *Cryosphere*, *8*(2), 387–394, doi:10.5194/tc-8-387-2014.
Schmidt, R., and R. A. Sommerfeld (1969), A photoelectric snow particle counter, paper presented at 37th Western Snow Conference, pp. 88–91.
Schmidt, R., R. Tabler, and R. L. Jairell (1982), A new device for sampling mass flux of blowing snow, paper presented at 39th Eastern Snow Conference, pp. 102–111.
Schmidt, R., R. Jairell, and J. Pomeroy (1988), Measuring snow interception and loss from an artificial conifer, paper presented at 56th Western Snow Conference, Kalispell, MT., pp. 166–169.
Schmidt, R. A. (1971a), *Calibrating the Snow Particle Counter for Particle Size and Speed*, Rocky Mountain Forest and Range Experiment Station, Fort Collins, Colo.
Schmidt, R. A. (1971b), *Processing Size, Frequency, and Speed Data From Snow Particle Counters*, Rocky Mountain Forest and Range Experiment Station, Fort Collins, Colo.
Schmidt, R. A. (1984), Measuring particle size and snowfall intensity in drifting snow, *Cold Reg. Sci. Technol.*, *9*(2), 121–129, doi:10.1016/0165-232X(84)90004-1.
Schmidt, R. A. (1987), *A System That Monitors Blowing Snow in Forest Canopies*, Rocky Mountain Forest and Range Experiment Station, Forest Service, U.S. Dept. of Agriculture, Fort Collins, Colo.
Schmidt, R. A., R. Meister, and H. Gubler (1984), Comparison of snow drifting measurements at an alpine ridge crest, *Cold Reg. Sci. Technol.*, *9*(2), 131–141, doi:10.1016/0165-232X(84)90005-3.
Schneebeli, M., C. Pielmeier, and J. B. Johnson (1999), Measuring snow microstructure and hardness using a high resolution penetrometer, *Cold Reg. Sci. Technol.*, *30*(1–3), 101–114, doi:10.1016/S0165-232X(99)00030-0.
Schwab, F. E., and M. D. Pitt (1991), Moose selection of canopy cover types related to operative temperature, forage, and snow depth, *Can. J. Zool.*, *69*(12), 3071–3077, doi:10.1139/z91-431.
Schweizer, J., and C. Camponovo (2002), The temperature dependence of the effective elastic shear modulus of snow, *Cold Reg. Sci. Technol.*, *35*(1), 55–64, doi:10.1016/S0165-232X(02)00030-7.
Schytt, V., E. Danfors, and Å. Fleetwood (1962), Notes on glaciological activities in Kebnekajse, Sweden. 1962, *Geogr. Ann.*, *44*(3–4), 407–412, doi:10.2307/520323.
Seligman, G. (1936), *Snow Structure and Ski Fields: Being an Account of Snow and Ice Forms Met With in Nature, and a Study on Avalanches and Snowcraft*, Macmillan and Co., London.
Shannon, W. (1968), Snow surveying by electonic telemetry, paper presented at 36th Western Snow Conference, pp. 568–98.

Shea, C., and B. Jamieson (2011), Some fundamentals of handheld snow surface thermography, *Cryosphere*, *5*(11), 55–66, doi:10.5194/tc-5-55-2011.
Shea, C., B. Jamieson, and K. W. Birkeland (2012a), Use of a thermal imager for snow pit temperatures, *Cryosphere*, *6*(2), 287–299, doi:10.5194/tc-6-287-2012.
Shea, C., B. Jamieson, and K. W. Birkeland (2012b), Using a thermal imager to quantify buried thermal structure in natural snow, paper presented at 2012 International Snow Science Workshop, pp. 269–279.
Shea, C., B. Jamieson, and K. W. Birkeland (2012c), Hot crust, cold crust, *Avalanche Rev.*, *30*, 28.
Shimizu, H. (1970), Air permeability of deposited snow, *Contrib. Inst. Low Temp. Sci. A*, *22*, 1–32.
Shook, K., and J. Pomeroy (2011), Synthesis of incoming shortwave radiation for hydrological simulation, *Hydrol. Res.*, *42*, 433–446.
Shrestha, K. L. (2015), Investigating impacts of global change on the dynamics of snow, glaciers and run-off over the Himalayan mountains, in *Dynamics of Climate Change and Water Resources of Northwestern Himalaya*, edited by R. Joshi, pp. 23–34, Springer Int., Switzerland.
Sihvola, A., and M. Tiuri (1986), Snow fork for field determination of the density and wetness profiles of a snow pack, *IEEE Trans. Geosci. Remote Sens.*, *24*(5), 717–721.
Skaloud, J., J. Vallet, G. Veyssière, O. Kölbl, and K. Keller (2005), HELIMAP: Rapid large scale mapping using handheld LiDAR/CCD/GPS/INS sensors on helicopters, paper presented at ION GNSS Conference, Long Beach, Calif., Sept. 12–13, 2005.
Smith, F., and H. Boyne (1981), Snow pillow behavior under controlled laboratory conditions. paper presented at 49th Western Snow Conference, pp. 13–22.
Smith, F., C. Cooper, and E. Chapman (1967a), Measuring snow depth by aerial photogrammetry. paper presented at 35th Western Snow Conference, pp. 66–72.
Smith, J. (1965), The elastic constants, strength and density of Greenland snow as determined from measurements of sonic wave velocity, CRREL Tech. Rep. 167, Cold Regions Research and Engineering Laboratory, Hanover, New Hampshire.
Smith, J., and H. Halverson (1969), Hydrology of snow profiles obtained with the profiling snow gauge. paper presented at 37th Western Snow Conference, pp. 41–48.
Smith, J., D. Willen, and M. Owens (1965), Measurement of snowpack profiles with radioactive isotopes, *Weatherwise*, *18*, 246–251.
Smith, J., D. Willen, and M. Owens (1967), Isotope snow gages for determining hydrologic characteristics of snowpacks, in *Isotope Techniques in the Hydrologic Cycle: Papers Presented at a Symposium at the University of Illinois, Nov. 10–12, 1965*, edited by G. E. Stout, pp. 11–21, AGU, Washington, D. C.
Smith, N. (1969), Determining the dynamic properties of snow and ice by forced vibration, CRREL Tech. Rep. 216, Cold Regions Res. Engin. Lab., Hanover, N. H.
Sommerfeld, R., and J. A. Businger (1965), The density profile of blown snow, *J. Geophys. Res.*, *70*(14), 3303–3306, doi:10.1029/JZ070i014p03303.
Sommerfeld, R. A. (1982), A review of snow acoustics, *Rev. Geophys.*, *20*(1), 62–66, doi:10.1029/RG020i001p00062.
Stähli, M., D. Bayard, H. Wydler, and H. Flühler (2004), Snowmelt infiltration into alpine soils visualized by dye tracer technique, *Arctic Arct. Alp. Res.*, *36*(1), 128–135.
Stewart, R., J. Pomeroy, and R. Lawford (2011), The drought research initiative: A comprehensive examination of drought over the Canadian Prairies, *Atmos. Ocean*, *49*(4), 298–302.
Stoll, R. (1989), *Sediment Acoustics*, Springer, New York, Berlin, Heidelberg.
Storck, P., D. P. Lettenmaier, and S. M. Bolton (2002), Measurement of snow interception and canopy effects on snow accumulation and melt in a mountainous maritime climate, Oregon, United States, *Water Resour. Res.*, *38*(11), 5–1–5-16, doi:10.1029/2002WR001281.
Stove, A. (1992), Linear FMCW radar techniques, *IEE Proc. F*, *139*(5), 343–350.
Sturm, M. (1999), *Self-Recording Snow Depth Probe*, CRREL Factsheet, Cold Regions Res. Eng. Lab., Hanover, N. H.
Sturm, M., and J. Johnson (1992), Thermal conductivity measurements of depth hoar, *J. Geophys. Res.*, *97*(B2), 2129–2139.
Sturm, M., and J. B. Johnson (1991), Natural convection in the subarctic snow cover, *J. Geophys. Res.*, *96*(B7), 11,657–11,671.
Sturm, M., J. Holmgren, M. König, and K. Morris (1997), The thermal conductivity of seasonal snow, *J. Glaciol.*, *43*(143), 26–41.
Sundström, N., D. Gustafsson, A. Kruglyak, and A. Lundberg (2013), Field evaluation of a new method for estimation of liquid water content and snow water equivalent of wet snowpacks with GPR, *Hydrol. Res.*, *44*(4), 600, doi:10.2166/nh.2012.182.
Swanson, R. (1968), A system for making remote and undisturbed measurements of snow settlement and temperature, paper presented at 36th Western Snow Conference, pp. 1–5.
Tabler, R. (1982), Frequency distribution of annual peak water-equivalent on Wyoming snow courses, paper presented at 50th Western Snow Conference, pp. 139–148.
Takeuchi, M. (1980), Study on visibility in blowing snow, *Sapporo*, *74*, 1–31.
Tape, K. D., N. Rutter, H.-P. Marshall, R. Essery, and M. Sturm (2010), Recording microscale variations in snowpack layering using near-infrared photography, *J. Glaciol.*, *56*, 75–80, doi:10.3189/002214310791190938.
Techel, F., and C. Pielmeier (2011), Point observations of liquid water content in wet snow—Investigating methodical, spatial and temporal aspects, *Cryosphere*, *5*(2), 405–418, doi:10.5194/tc-5-405-2011.
Tekeli, A., A. Sorman, A. Sensoy, and A. Sorman (2003), Design, installation of a snowmelt lysimeter and analysis for energy mass balance model studies in Turkey, paper presented at 60th Eastern Snow Conference, pp. 43–57.
Tekeli, A., A. Sorman, A. Sensoy, A. Sorman, J. Bonta, and G. Schaefer (2005), Snowmelt lysimeters for real-time snowmelt studies in Turkey, *Turk. J. Eng. Environ. Sci.*, *29*, 29–40.
Thompson, K., J. DeVries, and J. Amorocho (1975), Snowmelt lysimeter, paper presented at 43rd Western Snow Conference, pp. 35–40.
Tiuri, M., and A. Sihvola (1986), Snow fork for field determination of the density and wetness profiles of a snow pack, in *Hydrologic Applications of Space Technology, Proceedings of the Cocoa Beach Workshop, Florida, August 1985, IASH 160*, edited by A. I. Johnson, pp. 225–230, IAHS Press, Oxfordshire, U. K.
Tiuri, M. E., A. Sihvola, E. Nyfors, and M. Hallikaiken (1984), The complex dielectric constant of snow at microwave frequencies, *IEEE J. Oceanic Eng.*, *9*(5), 377–382, doi:10.1109/JOE.1984.1145645.
Toikka, M. (1992), Field tests with the snow fork in determining the density and wetness profiles of a snow pack. Microwave Signature-92 Conference Proceedings, Deutsche Forschungsanstalt fur Luft- und Raumfahrt, D-8031 Oberpfaffenhofen.
Tremper, B. (2008), *Staying Alive in Avalanche Terrain*, Mountaineers Books, Seattle.
Tüg, H. (1988), A pulse-counting technique for the measurement of drifting snow, *Ann. Glaciol.*, *11*, 184–186.
Turčan, J., and H. Loijens (1975), Accuracy of snow survey data and errors in snow sampler measurements, paper presented at 32nd Eastern Snow Conference, pp. 2–11.
U.S. Army Corps of Engineers (1956), *Snow Hydrology: Summary Report of the Snow Investigations*, North Pacific Div., Corps of Eng., U.S. Army, Portland, Oregon.

Usowicz, B., J. Lipiec, and J. Usowicz (2008), Thermal conductivity in relation to porosity and hardness of terrestrial porous media, *Planet. Space Sci.*, *56*, 438–447.
Vallet, J. (2001), *Handheld mobile mapping system for helicopter-based avalanche monitoring*, paper presented at OEEPE workshop "Integrated Sensor Orientation" 17-18 Sept. 2001, vol. 1, pp. 1–12.
Von Moos, M., P. Bartelt, A. Zweidler, and E. Bleiker (2003), Triaxial tests on snow at low strain rate: Part I. Experimental device, *J. Glaciol.*, *49*(164), 81–90, doi:10.3189/172756503781830881.
Waldner, P. A., M. Schneebeli, U. Schultze-Zimmermann, and H. Flühler (2004), Effect of snow structure on water flow and solute transport, *Hydrol. Processes*, *18*(7), 1271–1290, doi:10.1002/hyp.1401.
Wankiewicz, A. (1978a), Hydraulic characteristics of snow lysimeters, paper presented at 35th Eastern Snow Conference, pp. 105–116.
Wankiewicz, A. (1978b), Water pressure in ripe snowpacks, *Water Resour. Res.*, *14*(4), 593–600.
Warren, S. (1982), Optical properties of snow, *Rev. Geophys. Space Physics*, *20*(1), 67–89.
Warren, S., and W. Wiscombe (1981), A model for the spectral albedo of snow. II: Snow containing atmospheric aerosols, *J. Atmos. Sci.*, *37*, 2737–2745.
Watanabe, Z. (1980), Tensile strain and fracture of snow, *J. Glaciol.*, *26*(94), 255–262.
Watanabe, T. (1988), Studies of snow accumulation and ablation on perennial snow patches in the mountains of Japan, *Prog. Phys. Geogr.*, *12*(4), 560–581, doi:10.1177/030913338801200404.
Waterhouse, R. W. (1966), Re-evaluation of the rammsonde hardness equation, *J. Glaciol.*, *6*, 425–430.
Wendler, G. (1989), Measuring blowing snow with a photo-electric particle counter at Pole Station, Antarctica, *Polarforschung*, *59*(1–2), 9–16.
Whetton, P. H., M. R. Haylock, and R. Galloway (1996), Climate change and snow-cover duration in the Australian Alps, *Clim. Change*, *32*(4), 447–479, doi:10.1007/BF00140356.
Williams, M., and M. Knoll (2002), Measuring material properties of a wet and draining snowpack using crosshole radar tomography, paper presented at 70th Western Snow Conference, pp. 49–57.
Williams, M., R. Sommerfeld, S. Massman, and M. Rikkers (1999), Correlation lengths of meltwater flow through ripe snowpacks, Colorado Front Range, U.S.A., *Hydrol. Process.*, *13*, 1807–1826.
Williams, M., T. Erickson, and J. Petrzelka (2010), Visualizing meltwater propagation through snow at the centimeter-to-meter scale using a snow guillotine, *Hydrol. Process.*, *24*(15), 2098–2110.
Willis, N. J. (1991), *Bistatic Radar, The Artech House Radar Library*, Artech House, Boston.
Wiscombe, W., and S. Warren (1981), A model for the spectral albedo of snow. I: Pure snow, *J. Atmos. Sci.*, *37*, 2712–2733.
Woo, M.-K. (1980), Hydrology of a small lake in the Canadian High Arctic, *Arct. Alp. Res.*, *12*(2), 227–235, doi:10.2307/1550519.
Woo, M.-K. (1982), Snow hydrology of the High Arctic, paper presented at 50th Western Snow Conference, pp. 63–74.
Woo, M.-K. (1997), *A Guide for Ground Based Measurement of the Arctic Snow Cover*, Clim. Res. Branch, Atmos. Environ. Service, Downsview, Canada.
Wright, M., J. Kavanaugh, and C. Labine (2011), Performance analysis of GMON3 snow water equivalency sensor. paper presented at 79th Annual Western Snow Conference, April 2011, Stateline, Nev., pp. 105–108.
Xia, X., L. Liu, S. Ye, H. Guan, and G. Fang (2014), A novel subnanosecond monocycle pulse generator for UWB radar applications, *J. Sens.*, *2014*, 150549, doi:10.1155/2014/150549.
Xu, G. (2007), *GPS Theory, Algorithms, and Applications*, 2nd ed., Springer, Berlin, New York.
Yankielun, N., W. Rosenthal, and R. E. Davis (2004), Alpine snow depth measurements from aerial FMCW radar, *Cold Reg. Sci. Technol.*, *40*(1–2), 123–134, doi:10.1016/j.coldregions.2004.06.005.
Yen, Y.-C. (1980), Friction loss through a uniform snow layer, *Cold Reg. Sci. Technol.*, *18*, 83–90.
Yi, H., and S. Hong (2008), Design of L-band high speed pulsed power amplifier using LDMOS FET, *Prog. Electromagnet. Res. M*, *2*, 153–165.
Yosida, Z. (1967), Free water content of wet snow, *Proc. Int. Conf. Low Temp. Sci.*, *1*(2), 773–784.
Young, G. (1976), A portable profiling snow gauge results of field tests on glaciers. paper presented at 44th Western Snow Conference, pp. 7–11.
Young, G. J., and C. S. L. Ommanney (1984), Canadian glacier hydrology and mass balance studies; a history of accomplishments and recommendations for future work, *Geogr. Ann. A*, *66*(3), 169–182.
Zarek, J. (1978), Sound absorption in flexible porous materials, *J. Sound Vib.*, *61*(2), 205–234, doi:10.1016/0022-460X(78)90004-4.
Zotov, L. V., C. K. Shum, and N. L. Frolova (2015), Gravity changes over Russian river basins from GRACE, in *Planetary Exploration and Science: Recent Results and Advances*, pp. 45–59, Springer, Berlin.